Grid integration and smart grid implementation of emerging technologies in electric power systems through approximate dynamic programming

Xiao, Jingjie

Purdue University

13 August 2013

GRID INTEGRATION AND SMART GRID IMPLEMENTATION OF EMERGING TECHNOLOGIES IN ELECTRIC POWER SYSTEMS THROUGH APPROXIMATE DYNAMIC PROGRAMMING

A Dissertation

Submitted to the Faculty

of

Purdue University

by

Jingjie Xiao

In Partial Fulfillment of the

Requirements for the Degree

of

Doctor of Philosophy

December 2013

Purdue University

West Lafayette, Indiana

ACKNOWLEDGMENTS

I would like to thank my advisors, Dr. Joseph Pekny and Dr. Andrew Liu, for their guidance, insight, patience, and trust, and for always being inspiring and supportive. I would also like to thank them for the freedom they gave me to pursue my own interests.

I would also like to thank my committee members, Dr. James Dietz and Dr. Omid Nohadani for sharing their expertise, and giving me advice and encouragement. To Dr. Gintaras Reklaitis for sharing his knowledge and being supportive.

I could never have finished without the help of my group-mates and collaborators: Dr. Bri-Mathias Hodge, Dr. Shisheng Huang, Xiaohui Liu, and Hameed Safiullah. I were lucky to work with them and have them as good friends. To my office-mates and good friends: Dr. Ye Chen, Manasa Ganoothula, Elcin Icten, Harikrishnan Sreekumaran, Emrah Ozkaya, Anshu Gupta, and Aviral Shukla who made the office a productive and entertaining place.

Finally, I would like to thank my family and friends for their love.

TABLE OF CONTENTS

Page

LIST OF TABLES

LIST OF FIGURES

Figure Page

ABSTRACT

Xiao, Jingjie Ph.D., Purdue University, December 2013. Grid Integration and Smart Grid Implementation of Emerging Technologies in Electric Power Systems Through Approximate Dynamic Programming. Major Professor: Joseph F. Pekny and Andrew L. Liu.

A key hurdle for implementing real-time pricing of electricity is a lack of consumers' responses. Solutions to overcome the hurdle include the energy management system that automatically optimizes household appliance usage such as plug-in hybrid electric vehicle charging (and discharging with vehicle-to-grid) via a two-way communication with the grid. Real-time pricing, combined with household automation devices, has a potential to accommodate an increasing penetration of plug-in hybrid electric vehicles. In addition, the intelligent energy controller on the consumer-side can help increase the utilization rate of the intermittent renewable resource, as the demand can be managed to match the output profile of renewables, thus making the intermittent resource such as wind and solar more economically competitive in the long run.

One of the main goals of this dissertation is to present how real-time retail pricing, aided by control automation devices, can be integrated into the wholesale electricity market under various uncertainties through approximate dynamic programming. What distinguishes this study from the existing work in the literature is that wholesale electricity prices are endogenously determined as we solve a system operator's economic dispatch problem on an hourly basis over the entire optimization horizon. This modeling and algorithm framework will allow a feedback loop between electricity prices and electricity consumption to be fully captured. While we are interested in a near-optimal solution using approximate dynamic programming; deterministic linear programming benchmarks are use to demonstrate the quality of our solutions.

The other goal of the dissertation is to use this framework to provide numerical evidence to the debate on whether real-time pricing is superior than the current flat rate structure in terms of both economic and environmental impacts. For this purpose, the modeling and algorithm framework is tested on a large-scale test case with hundreds of power plants based on data available for California, making our findings useful for policy makers, system operators and utility companies to gain a concrete understanding on the scale of the impact with real-time pricing.

1. INTRODUCTION

1.1 Motivation and Literature Review

The retail electricity rate has been kept flat for the past century, mainly due to technological limitations and regulatory policies. On the other hand, wholesale electricity prices vary constantly (e.g. hourly, or even minute-by-minute) to reflect changes in costs of producing electricity at different time. It has long been understood that the current flat retail rate structure is inefficient [1–5]. It prevents consumers from benefitting from a lower electricity bill by reducing their electricity consumption when the wholesale electricity price is high and increasing their consumption during time periods when the electricity price is low. An inelastic short-term demand, combined with extremely high costs of blackouts [6–8], also means that sufficient generating capacity must be installed to satisfy some extreme realizations of demand shocks. This leads to an electricity system that is overly built with capital intensive assets, solely to maintain system reliability.

Aware of potential benefits of demand-side participation, the U.S. Department of Energy (DOE) envisions a future electricity system, referred to as Smart Grid [9–13], where consumers are fully integrated into wholesale power markets. The Federal Energy Regulatory Commission (FERC) also encourages a wholesale market where demand and supply are treated symmetrically. How are the visions of smart grid to be implemented, however, is still a subject of a great deal of debate [14–18]. Programs intended to promote demand-side participation can be divided into two major categories: incentive-based demand response (DR) programs, and time-varying retail prices [19] including time-of-use tariffs (TOU), critical-peak pricing (CPP), and real-time pricing (RTP).

Incentive-based demand response programs pay customers to reduce their consumption relative to an admistratively set baseline level of consumption. Studies including Aalami et al. 2010 [20], Caron and Kesidis 2010 [21], and Parvania and Fotuhi 2010 [22] focus on efficiently integrate such programs in wholesale electricity markets to provide reserves. Time-varying prices can be static or dynamic. Static time-varying prices, generally called time-of-use prices, are preset for pre-determined hours and days; while dynamic prices are allowed to change on short notice, often within a day or less. Important dynamic pricing schemes include real-time pricing and critical peak pricing. Real-time pricing is characterized by passing on a price, which best reflects changes in wholesale electricity prices and supply/demand balance, to consumers. Critical peak pricing allows for a retailer to occasionally declare an unusually high retail price for a limited number of hours.

Economists have long recognized that dynamic pricing, reflecting varying system conditions over locations as well as time, is the path to realizing full benefits of active demand participation in the wholesale electricity market. For example, Borenstein et al. 2002 [3] conclude that real-time pricing delivers the most benefits in terms of reducing peak demand. Their conclusion is drawn based on a comprehensive theoretical and practical analysis of possible approaches to integrate an active demand side into the wholesale electricity market. Hogan 2010 [5] also concludes in favor of real-time pricing, but from a perspective of price signal development. He argues that a straightforward way to implement real-time pricing is to use full wholesale electricity prices, with a fixed customer charge for transmission and distribution, metering and billing costs. However, to apply incentive-based demand response and critical peak pricing, sophisticated calculations are required to achieve principles laid out by FERC. Bushnell et al. 2009 [4] pinpoint an important drawback of using incentive-based demand response. That is, individual customers will always know more about their true baseline than the administrator of a demand response program. Therefore, it is possible for customers to profit from that knowledge.

Despite its potential benefits, real-time pricing was not possible to implement in the past because the meter that most consumers had can record only the sum of consumption over each month, not in each minute or hour. However, these technological limitations have been greatly reduced. For example, millions of smart meters that record electricity consumption on frequent intervals have been installed. Development of advanced metering infrastructure (AMI) has been increasingly encouraged by federal and state incentives. AMI can enable a two-way communication between consumers and electricity retailers (even a system operator[1]) in terms of electricity usages and prices [11, 24, 25].

Technologies such as AMI help pave an efficient path to universal deployment of real-time pricing and active consumer participation. However, advanced infrastructures alone are not enough. There are at least two important barriers to a widespread adoption of real-time pricing. The first barrier is a lack of knowledge among consumers about how to respond to real-time updated prices. As most consumers have long been accustomed to a flat rate of electricity, it would take a long time for them to learn to track and respond to dynamic electricity rates, if they decide to do so at all. Allcott 2011 [1] has observed, based on the first real-time pricing program operated in Chicago since 2003, that households rarely actively checked hourly prices provided (via telephone or the Internet), as it was difficult for them to constantly monitor the prices and respond properly. Andersen 2011 [26] also argues that business cases for Smart Grid should work with or without consumers' behavior change. Therefore, without automation technologies, it would be difficult for consumers to respond to real-time prices that change frequently.

To overcome this hurdle, enabling technologies that allow residential customers to respond automatically to pricing signals without adding significant burden to consumers' lifestyle have emerged. Such metering and control systems, referred to as household energy management controllers (EMCs) or energy management system

[1]A system operator is responsible for the operation of the electric grid to match demand and generation, and dealing with transmission companies to maintain system reliability [23].

(EMS), can be programmed to automatically optimize home appliances energy usage in response to real-time price signals. Existing products include GE Nucleus®, Control4®, etc. Some energy scheduling algorithms that can be embedded into EMCs of a household or small business to maximize its utility (or minimize its energy cost) have been desiged (Ibars et al. 2010 [27], Mohsenian-Rad et al. 2010 [28], etc).

The second barrier to a universal deployment of real-time pricing is political resistance because of costs and risks associated with RTP. FERC 2009 [14] pinpoints the disagreement on cost-benefit analysis of real-time pricing as one of regulatory barriers. From a customer's perspective, there are two main costs associated with time-varying rates [19]. The first is the metering cost, which would be the cost of a smart meter net of its operational benefit such as the avoided meter reading cost. The second cost is the loss of welfare associated with reducing or shifting usage. There is no consensus among the literature on the debate about whether real-time pricing would have positive net welfare effects. For example, Allcott 2012 [2] estimates that moving from 10 percent of consumers on real-time pricing to 20 percent would increase welfare in the PJM electricity market by $120 million per year in the long run. In another study [1] based on a real-time pricing program in Chicago, the same author concludes that households were not sufficiently price elastic to generate gains that substantially outweigh the estimated cost of the advanced electricity meter required to observe hourly consumption.

Another valid regulatory concern regarding real-time pricing of electricity is that RTP could increase instability of the electric grid. For example, Allcott 2012 [2] observes based on simulations that real-time pricing could cause peak energy prices to increase, assuming that the reserve margin[2] is a fixed percentage of peak demand. He discovers that the reason behind this counter-intuitive observation is that the required excess capacity is less with more consumers on RTP since the peak demand with RTP is lower.

[2]Reserve margin must be imposed on the electric system to deal with some extreme realizations of system demand and maintain system reliability [2].

To address these regulatory concerns, we must show that real-time pricing could yield tangible benefits to end consumers without facing significant volatility on their monthly electric bills. One potential benefit from real-time pricing, aided with household automation devices, is that it can facilitate an increasing adoption of electric vehicles (EVs) and/or plug-in hybrid electric vehicles (PHEVs). Interests in developing EV/PHEVs are driven by environmental concerns, and high and volatile fuel prices [29]. While electric vehicles have a limited range and thus suffering from "range anxiety" [30]; plug-in hybrid electric vehicles eliminate this problem as it has an internal combustion engine that works as a backup when its battery is depleted. In this study, we use only PHEVs as an illustrative example. Adapting the modeling framework to include EVs and other household appliances such as air conditioners would be a straightforward extension.

The electricity consumed for charging PHEVs (e.g. 0.4 kW per mile driven for a Chevy Volt) will present a significant new load on the existing electric system [31]. An increased penetration of PHEVs will, if no additional measures are taken, increase the system peak, since there is usually a natural coincidence between the normal system peak and charging pattern. Thus, the uncoordinated new load associated with charging will reduce the load factor[3] and capacity utilization, increase peaking generating unit usage, and raise electricity rates. It will also increase power losses and voltage deviation [32], and reduce transformers' life [33].

The impact of PHEVs on the electric grid depends on when they are charged. From a PHEV owner's point of view, their PHEV has to be charged overnight so the driver can drive off in the morning with a fully-charged battery. This gives opportunities to strategically shift PHEV charging loads without causing inconvenience to consumers. There is extensive literature on assessment of potential benefits of coordinated charging on reducing the system demand peak, power losses, electricity generation costs and emissions. In studies including Clement et al. 2009, 2010 [34,35],

[3]The load factor is defined as the average load divided by the peak load over a specified time period [23].

Denholm and Short 2006 [36], and Sortomme et al. 2011 [37], a system operator is assumed to be able to directly control PHEV charging and to coordinate it with power system operations. It is, however, unlikely for this scenario to be implemented in the real world since it requires the system operator to track every PHEV in the system. Besides the technological difficulty associated with such a centralized charging scenario, drivers' privacy can also be a barrier in implementing this scheme [38]. Although the centralized charging controlled by a system operator is not practical, it can nonetheless serve as a benchmark case to which other more realistic charging schemes can be compared. Thus, in this study the centralized charging scheme is considered along with various other charging scenarios.

Some studies on PHEV charging argue that charging decisions should be left to individual consumers, and time-varying tariffs can be provided as incentives for consumers to shift their charging demand to late night hours when the electricity price is low. A time-of-use tariff is used in Axsen et al. 2011 [39], Huang et al. 2011 [40], and Parks et al. 2007 [41]. These studies are usually done through simulations (with a detailed modeling of PHEV driving patterns) since it is trivial to determine the start time of charging.

In this study, we are interested in using real-time pricing tariffs as signals to coordinate PHEV charging. As we discussed early on, with the help of EMCs, residential consumers will have the capability to effectively react to hourly-updated price signals and optimize their charging start time. Studies including Conejo et al. 2010 [42], Han et al. 2010 [43], Kishore and Snyder 2010 [44], and Valentine et al. 2011 [45] discuss PHEV charging with a real-time pricing tariff. However, they treat price signals as exogenous information and use historical wholesale electricity prices (or statistical models based on historical data). By doing this, they assume that PHEV charging demand does not affect the cost of generating electricity. This assumption does not hold when the real-time price of electricity changes every hour or less. Real-time pricing creates a closed feedback loop between electricity supply and demand, and as a result, the realization of random events and the reaction of PHEV owners with

respect to the price in previous hours will influence the price in the upcoming operation periods. Algorithms designed without considering this closed feedback loop may not fully realize the benefit of deployment of real-time pricing. Mohsenian-Rad and Leon-Garcia 2010 [46] argue that any residential energy management strategy in hourly-updated real-time pricing requires price prediction capabilities. A few studies share this view and examine decentralized charging, in which charging decisions are made on residential level in response to real-time pricing, based on convex optimization (Samadi et al. 2010 [47]), mixed integer linear programming (Sioshansi 2012 [48]), dynamic programming (Livengood and Larson 2009 [49]), reinforcement learning (O'Neill et al. 2010 [50]), game theory (Chen et al. 2011 [51], Mohsenian-Rad and Leon-Garcia 2010 [46]). Our work is distinguish from these studies because we demonstrate that the proposed approximate dynamic programming-based modeling and algorithm framework can be extended to solve resource planning problems and assess long-term effects of real-time pricing. In the decentralized charging scenario examined in this dissertation, we assume real-time price signals are updated hourly to reflect the real-time interaction between electricity demand and supply, and charging decisions are made by EMCs for PHEV owners in response to price signals.

PHEVs could play an even bigger role in future electric systems if we consider vehicle-to-grid (V2G) acting as storage resources. The electric grid suffers from a lack of affordable storage resources, and as a result, system generation will need to exactly match fluctuating load at any time. V2G allows a PHEV to charge when the electricity price is low and discharge to send energy back to the electric grid when the electricity price is high, thus acting as a storage resource [52, 53]. PHEV owners can potentially gain revenue, which could make PHEVs more economically competitive. Many believe that a large number of PHEVs with V2G aggregated together have the potential to participate in energy markets, from bulk energy to ancillary services including spinning reserves and frequency regulation [43, 54–56]. In this study, we consider a decentralized charging scenario in which V2G is included, and charging and discharging decisions are both optimized by EMCs.

Another benefit of a universal deployment of real-time pricing and active consumer participation enabled by EMCs is that more variable energy resources (VERs) such as wind can be incorporated into power systems. Increasing amount of wind energy has been installed in the United States, driven by policy factors such as Renewable Portfolio Standards (RPS), and by market factors such as the demand for green power, and the natural gas price volatility. For example, California's RPS program requires investor-owned utilities, electric service providers, and community choice aggregators to increase procurement from eligible renewable energy resources to 33% of total procurement by 2020 [57]. It is well known that it is difficult to accurately predict wind availability even in the short term [58–60]. The variable and unpredictable nature of wind energy imposes great challenges for system operators in balancing electricity supply and demand in the short run, and planning wind capacity investment in the long run. A number of studies, including [61–66], examine wind power generation integration into short-term power operations and quantify system reserves (back-up energy) required to maintain system reliability when wind penetration is high.

The volatility of wind resources and a possible asynchronous effect between wind and normal system demand profiles can be mitigated with real-time pricing, since RTP can signal load profile to adapt to short-term wind variations. Real-time pricing provides customers with hourly-updated price signals that reflect changing market conditions including the availability of wind resources. Residential consumers equipped with EMCs will be able to charge their vehicle when wind energy is abundant. Borenstein 2005 [67] and De Jonghe et al. 2011 [68] argue that the demand elasticity to price should be considered when we optimize long-term generation investments.

There are, however, very few resource planning models to guide investment and policy decisions on intermittent resources with or without real-time pricing. Current planning models (for example, NEMS [69] used by the Energy Information Administration (EIA) and the U.S. DOE, and MARKAL [70] used by the International Energy Agency) are based on deterministic linear or non-linear programming. They do not

perform economic dispatch[4] on a chronologically hourly basis, and use load duration curves[5] and wind capacity factor[6] for intermittent energy. To accurately represent the economics of wind resources under real-time pricing, a planning model has to capture hourly fluctuations of wind power production and consumers' reactions to price signals. Powell et al. 2012 [74] propose an approximate dynamic programming (ADP) framework for planning energy resources in the long run. This framework can handle different levels of decision granularity, link different time periods together, and handle different sources of uncertainty.

1.2 Research Objectives and Contributions

One of the main purposes of this dissertation is to present an approximate dynamic programming-based modeling and algorithm framework that optimizes PHEV charging and discharging decisions, while capturing the feedback loop between wholesale electricity prices and consumer electricity usages. While we are interested in near-optimal policies since the algorithm is based on approximations; we use deterministic linear programming solutions as benchmarks to demonstrate the high quality of our solutions. The modeling and algorithm framework is extended to solve a resource planning model to guide long-term investment decisions on wind resources. The other purpose of the dissertation is to use the framework to provide numerical evidence to the debate about whether real-time pricing is superior than the current flat rate structure in terms of both economic and environmental considerations. In the numerical analysis, we attampt to answer the following questions. First, what are the effects of increasing PHEV penetration on daily electricity system demands and wholesale electricity prices under real-time pricing, compared with the business-as-

[4]Economic dispatch is the short-term determination of the optimal output of power plants to meet the system load at the lowest possible cost. It is performed by the system operator at every hour (or less) [71].

[5]A load duration curve is similar to a load curve, but the demand data is ordered in descending order of magnitude, rather than chronologically [72].

[6]The wind capacity factor of a wind farm is defined as wind power production over certain time period divided by its nameplate capacity over the same time period [73].

usual flat tarrif? Second, to what extent will real-time pricing reduce daily electricity generation costs and emissions? Third, what are the impacts of real-time pricing on generating capacity investment decisions in the long term? Especially, will real-time pricing, coupled with an intelligent demand participation, increase the economic competitiveness of intermittent wind resources?

This dissertation contributes toward the understandings of real-time pricing in three aspects. First, distinguished from most of the existing work in the literature, real-time pricing signals are hourly-updated and endogenously determined, as we solve the system operator's economic dispatch problem on an hourly basis over the entire optimization horizon. This allows our model to capture the feedback loop between electricity demand and supply, thus representing full benefits of real-time pricing. Second, to our knowledge, this work is the first to incorporate endogenous real-time pricing in a long-term resource planning model. Our modeling framework considers hourly variations of wind resources and consumers' reactions (automated by EMCs) to real-time price signals. These price signals reflect energy market conditions including wind availability. This enables us to fully represent the economics of wind energy under real-time pricing. Third, the proposed modeling and computational framework is applied to a real-world case (with hundreds of generators and high wind penetration) based on the data available for California, thus making the findings more useful for policy makers, system operators and utilities to gain a concrete understanding of the system-level impacts of real-time pricing and its potentials to facilitate the integration of plug-in hybrid electric vehicles and wind resources into the future electric grid.

The dissertation proceeds as follows. In the remainder of this chapter, technical backgrounds on dynamic programming and approximate dynamic programming will be provided. Chapter 2 presents a centralized charging scenario based on a short-term energy model, in which a system operator is assumed to make charging decisions for PHEV owners over a 24-hour horizon. At the end of the chapter, details on the California test system are provided, based on which the ADP solutions are benchmarked

against the optimal solution. Chapter 3 extends the modeling framework to consider two decentralized charging scenarios (with and without V2G, respectively), in which EMCs are assumed to make decisions for consumers in response to price signals. At the end of the chapter, comparison analysis among various charging policies will be discussed. In Chapter 4, the modeling and algorithm framework is further extended to make resource investment decisions over a long planning horizon. Chapter 5 discusses conclusions and future works.

1.3 Technical Background

In this section, we will provide technical details on dynamic programming and approximate dynamic programming. Note that we are only interested in finite horizon problems, since both power operation and resource planning problems, studied in this dissertation, have a specific horizon. Dynamic programming (Bellman 1956 [75]) has been used to solve many optimization problems that involve a sequence of decisions over multiple time periods. It is natural for us to use dynamic programming to formulate energy system problems, since it is common for these problems to have elements that link different time periods together. It is, however, generally known that dynamic programming suffers from the curses of dimensionality. To overcome the computational difficulties of dynamic programming, approximate dynamic programming (ADP) [76] has been implemented to solve large-scale, dynamic and stochastic problems in areas such as energy resource allocation (Powell et al. 2012 [74]), network revenue management (Zhang and Adelman 2009 [77]), large-scale fleet management (Simão et al. 2009 [78]). For this reason, our computational framework is developed based on approximate dynamic programing.

1.3.1 Dynamic programming

We describe a dynamic program by defining its decision variables, state variables, random variables for exogenous information, transition functions, cost functions, and

policies to make a decision. We use $h \in \{1, 2, \ldots, H\}$ to denote a finite number of time periods. Let x_h present the vector of all decision variables at time h. Decisions at time h are made depending on state variables at time h, denoted as S_t. S_h are designed to include only the information available at time h, and as a result decisions are not allowed to anticipate events in the future. Once a decision is made, the system then evolves over time, with new information arriving that also changes the state of the system. New information at time h is captured by random variables. Let ω_h denote the vector of random variables that represent all sources of randomness at time h. Note that the realization of ω_h will not become known to the system until time $h+1$. When we make decisions, they are governed by two sets of constraints. The first set of constraints only affects decisions made at one point in time. The other set of constraints is in the form of the transition function that describes how a state evolves from one point in time to another, linking activities over time. The transition function that governs the system evolution from a state at time h to the next state at time $h+1$ is defined as

$$S_{h+1} = S^M\left(S_h,\, x_h,\, \omega_h\right), \qquad 1 \le h \le H-1. \tag{1.1}$$

Note that S_1 is the initial state, which is given as data. A cost function (for a minimization problem) at time h measures the system costs incurred at time h. Let $C_h\left(S_h,\, x_h\right)$ denote the cost function at time h. If the exogenous information is deterministic, the objective function is written as

$$\min_{x_h} \sum_{h=1}^{H} C_h\left(S_h,\, x_h\right). \tag{1.2}$$

For a stochastic problem in which the exogenous information is random, we are in a position of finding the best policy (or decision rule) for choosing decisions, since the state S_h is also random. Let $X_h^\pi(S_h)$ denote a decision rule, and let Π be a set of decision rules. The problem of finding the best policy would be written as

$$\min_{\pi\in\Pi} \mathbf{E}\left\{\sum_{h=1}^{H} C_h\left(S_h, X_h^\pi(S_h)\right)\right\}. \tag{1.3}$$

Assume that the state space is discrete, dynamic programming can be used to break down a large, finite-horizon problem into a series of simpler and more tractable subproblems. This is done by defining the value function of every state S_h, denoted as $V_h(S_h)$, to represent the sum of expected contributions from state S_h until the end of the time horizon. Bellman's Equation [75] is used to recursively compute the value associated with each state, written as:

$$V_h(S_h) = \max_{x_h} \{-C_h(S_h, x_h) + \mathbf{E}\left[V_{h+1}(S_{h+1})|S_h\right]\}, \qquad 1 \leq h \leq H-1, \tag{1.4}$$

where $S_{h+1} = S^M(S_h, x_h, \omega_h)$. A transition matrix that gives the probability that if we are in a state S_h and make a decision x_h, then we will be in state S_{h+1}, is assumed to be known. Note that the terminal value $V_H(S_H)$ is assumed to be given as data. Often we simply use $V_H(S_H) = 0$. By working backwards from the last time period, and using Bellman Equation (1.4) recursively, the optimal value V_h associated with each state can be found. Note that at time period h, we have already computed V_{h+1}. A dynamic programing algorithm is presented as follows:

Step 1 Initialization. Set the terminal value $V_H(S_H) = 0$.

Step 2 For $h = H-1, \ldots, 1$:

Step 2.1 For each S_h:

Step 2.1.1 Compute $V_h(S_h)$ using

$$V_h(S_h) = \max_{x_h} \{-C_h(S_h, x_h) + \mathbf{E}\left[V_{h+1}(S_{h+1})|S_h\right]\}.$$

Step 3 Return the optimal objective value V_1.

Note that solving the dynamic program using Bellman Equation requires to enumerate all states S_h (assuming the state space is discrete) and compute the value V_h associated with each state. Therefore, dynamic programming suffers from the "three curses of dimensionality" arising from the state space, action space, and random exogenous information space.

1.3.2 Approximate dynamic programming

To overcome the computational difficulties of dynamic programming, approximate dynamic programming has been implemented to solve large-scale, stochastic, dynamic problems. Approximate dynamic programming uses the concept of the post-decision state variable to avoid complex calculations of the expectation in Bellman Equation (1.4). The post-decision state at time h, denoted as S_h^x, is the state of the system immediately after making a decision at time h, but before any new information at time h arrives. With the use of the post-decision state variable, we can break the original transition function (1.1) into the following two steps:

$$S_h^x = S^{M,x}\left(S_h,\, x_h\right), \qquad 1 \le h \le H; \tag{1.5}$$

$$S_{h+1} = S^{M,\omega}\left(S_h^x,\, \omega_h\right), \qquad 1 \le h \le H-1, \tag{1.6}$$

where $S^{M,x}\left(S_h,\, x_h\right)$ represents the pre-transition function used to obtain the post-decision state variable at time h, and $S^{M,\omega}\left(S_h^x,\, \omega_h\right)$ represents the post-transition function used to step forward to the next pre-decision state variable (known as the state variable in the dynamic programming setting) at time $h{+}1$. Figure 1.1 illustrates a generic decision tree with decision nodes (squares) and outcome nodes (circles). The information available at a decision node is the pre-decision state S_h, at which a decision x_h needs to be made. The information available at an outcome node is the post-decision state S_h^x, right after which new information ω_h reveals. The pre-transition function $S^{M,x}\left(S_h,\, x_h\right)$ takes us from a decision node (pre-decision state at time h: S_h) to an outcome node (post-decision state at time h: S_h^x). The post-transition function $S^{M,\omega}\left(S_h^x,\, \omega_h\right)$ takes us from the outcome node to a next decision node (pre-decision state at time h: S_{h+1}).

The value function of the post-decision state S_h^x, denoted as $V_h^x(S_h^x)$, would be written as follows

$$V_h^x(S_h^x) = \mathbf{E}\left[V_{h+1}(S_{h+1})|S_h^x\right], \qquad 1 \le h \le H-1. \tag{1.7}$$

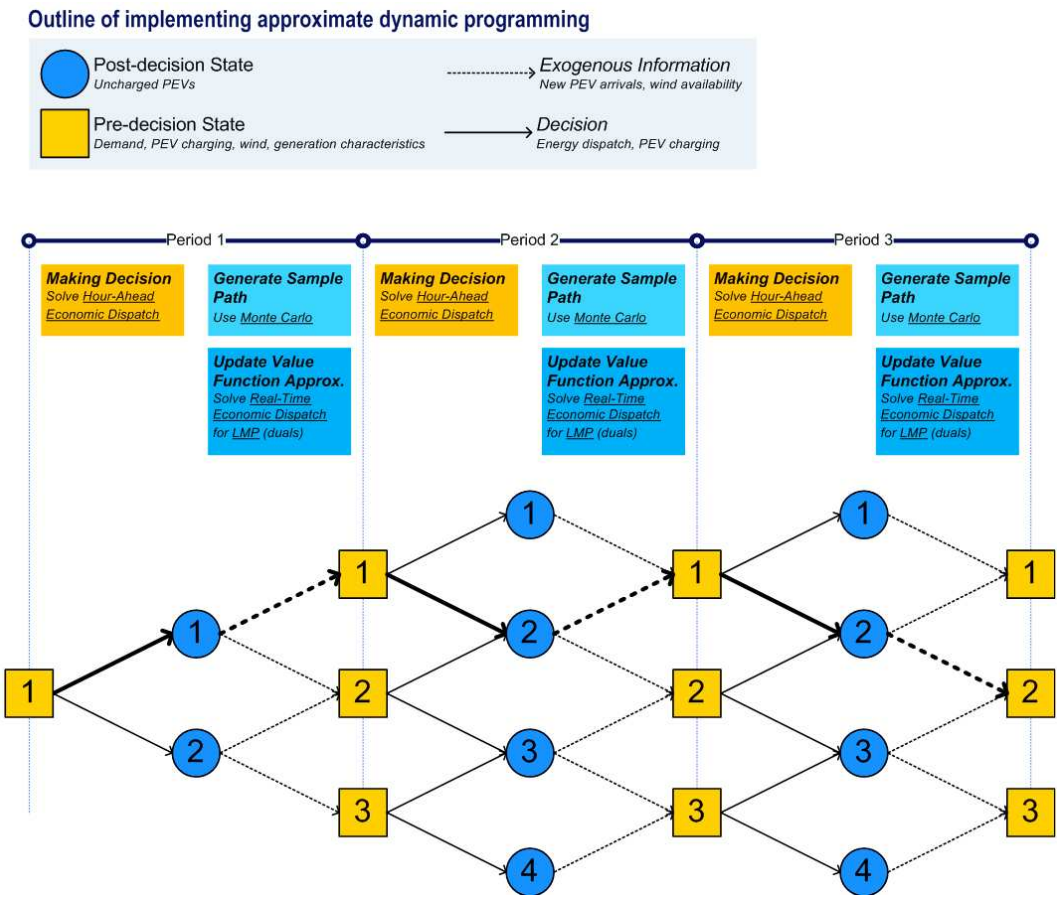

Fig. 1.1. Overview of implementing approximate dynamic programming

The value function around the post-decision state (ranther than the value function around the pre-decision state as for dynamic programming) is used in the approximate dynamic programming setting to take advantage of the fact that $V_h^x(S_h^x)$ is a deterministic function of x_h. Using $V_h^x(S_h^x)$, Bellman Equation (1.4) can be rewritten as

$$V_h(S_h) = \max_{x_h} \left\{ -C_h(S_h, x_h) + V_h^x\left(S_h^x\right) \right\}, \qquad 1 \leq h \leq H. \tag{1.8}$$

This allows us to avoid computing an expectation within the optimization formulation in Bellman Equation (1.4). Instead of calculating the exact value function associated with each post-decision state, $V_h^x(S_h^x)$ in (1.8), approximate dynamic programming

approximates the value function of the post-decision state. We use $\bar{V}_h^x\left(S_h^x\right)$ to denote an approximation of the value function around the post-decision state S_h^x, which depends only on S_h^x.

For obtaining the value function approximation $\bar{V}_h^x\left(S_h^x\right)$, approximate dynamic programming performs an iterative operation. Let $n \in \{1, \ldots, N\}$ denote the iteration counter, where N is a preset finite number. To describe the iterative operation, we add the iteration counter n to the decision variables, state variables, random variables, and value function approximations. For example, the pre-decision state at time h for iteration n is referred to as S_h^n. The initial value function approximations are assumed to be 0. Starting from iteration $n = 2$, at each time h, given a pre-decision state S_h^n, we make a decision, using the value function approximation computed in the previous iteration $n-1$, $\bar{V}_h^{n-1}(S_h^x)$. The optimizaiton problem that is solved to make an optimal decision at time h is presented as follows

$$v_h^n = \max_{x_h} \left\{-C_h(S_h^n,\, x_h) + \bar{V}_h^{n-1}\left(S_h^x\right)\right\}, \qquad 2 \le n \le N,\ 1 \le h \le H, \tag{1.9}$$

where $S_h^x = S^{M,x}\left(S_h^n,\, x_h\right)$. Let x_h^n denote an optimal solution of (1.9), and v_h^n represent the objective value associated with the optimal solution. v_h^n is a new estimate of the value of being in post-decision state $S_h^{x,n}$. We now use v_h^n to update value function approximation $\bar{V}_h^{n-1}$ according to the following equation

$$\bar{V}_h^n = (1 - \alpha_{n-1}) \times \bar{V}_h^{n-1} + \alpha_{n-1} \times v_h^n, \quad 2 \le n \le N,\ 1 \le h \le H, \tag{1.10}$$

where α_{n-1} is a step-size between 0 and 1; and, the common practice is to use a constant step-size or a declining rule such as $\alpha_{n-1} = 1/(n-1)$.

The post-decision state at time h is determined by the following pre-transition function

$$S_h^{x,n} = S^{M,x}\left(S_h^n,\, x_h^n\right), \qquad 2 \le n \le N,\ 1 \le h \le H. \tag{1.11}$$

After x_h^n is determined in (1.9), and a particular realization of new information, ω_h^n, becomes known to the system, the system evolves to the next pre-decision state at time $h+1$ using the following transition function:

$$S_{h+1}^n = S^M\left(S_h^n,\, x_h^n,\, \omega_h^n\right), \qquad 2 \le n \le N,\ 1 \le h \le H-1. \tag{1.12}$$

The realization of new information can be generated by Monte Carlo sampling. We proceed to make decisions till the end of the horizon to complete iteration n. The same procedure is repeated for a number of iterations. A generic algorithm for approximate dynamic programming is presented as follows

Step 1 Initialization. Set $\bar{V}_h^1(S_h^x) = 0$, $h \in \mathcal{H}$. Set $n = 2$.

Step 2 Generate a particular realization of new information ω_h^n, $h \in \mathcal{H}$.

Step 3 For $1 \le h \le H$:

Step 3.1 Solve the following optimization problem:

$$v_h^n = \max_{x_h} \left\{-C_h(S_h^n, x_h) + \bar{V}_h^{n-1}\left(S_h^x\right)\right\},$$

and let x_h^n denote an optimal decision of the above optimization problem.

Step 3.2 Update $\bar{V}_h^{n-1}$ using the following equation

$$\bar{V}_h^n = (1-\alpha_{n-1}) \times \bar{V}_h^{n-1} + \alpha_{n-1} \times v_h^n.$$

Step 3.3 Find the next pre-decision state using the following function

$$S_{h+1}^n = S^M\left(S_h^n,\, x_h^n,\, \omega_h^n\right).$$

Step 4 $n = n+1$. If $n \le N$, go to **Step 2**.

Step 5 Return the value function approximation $\bar{V}_h^N$, $h \in \mathcal{H}$.

Exactly how to construct and update the value function approximation in order to find a good decision rule is very problem specific. When we present our approximate dynamic programming-based modeling and algorithm framework for solving a specific energy system problem, important details such as how the value functions are approximated and updated, how to select a proper step size α_{n-1}, and how to design performance measures used to evaluate the quality of the ADP solutions, will be discussed.

2. CENTRALIZED PLUG-IN HYBRID ELECTRIC VEHICLE CHARGING

To quantify the potential benefits of real-time pricing in integrating plug-in hybrid electric vehicles into the electric grid, we will compare various PHEV charging schemes under different electricity tariffs. In this chapter, we will focus on a centralized charging scenario in which an independent system operator (ISO) controls the timing of PHEV charging. In the electric power system, a system operator is responsible for power operations to make sure electricity demand is satisfied by generation at any time. While unrealistic to be implemented in the real world, the centralized charging case can be used as a benchmark for evaluating other charging policies.

The chapter proceeds as follows. Section 2.1 provides an outline of the ISO's short-term energy system model, followed by a deterministic linear programming formulation in Section 2.2, and a stochastic optimization formulation based on approximate dynamic programming in Section 2.3. Section 2.4 provides details of the test case used in the numerical analysis, which is based on data available for California's electricity and transportation sectors. Finally, in Section 2.5, the approximate dynamic programming solutions are evaluated to show how closely they match with the optimal solution.

2.1 Outline of the Short-Term Energy System Model

A system operator solves a multi-period economic dispatch problem to determine the optimal output of each power plant at each time. Let $h \in \{1, 2, \ldots, H\}$ denote the hours within a day, and $j \in \{1, 2, \ldots, J\}$ represent individual power plants. We will describe the economic dispatch problem using the language of dynamic programming by defining the decision variable vector x_h, state variable vector S_h, random variable

vector ω_h, transition function, and cost function associated with each time h. The economic dispatch problem determines at each point in time how much energy to be produced from each power plant g_{hj} [MW], and from renewable resources such as wind energy w_h [MW] to satisfy the system demand. When the electricity demand cannot be met, electric service interruptions will occur, resulting in expensive outage costs measured by value of lost load (VOLL) [$/MWh] [79]. Note that using a variable for the quantity of lost load at each hour q_h [MW], the optimization problem is always feasible. The centralized PHEV charging scenario is modeled by assuming that a system operator has control over power system variables as well as charging decisions (how many vehicles to charge at each hour) z_h^+ [thousand]. The superscript '+' is used throughout this study to indicate the variables associated with PHEV charging. In later chapters, we will introduce the superscript '−' to represent PHEV discharging when vehicle-to-grid is modeled. The decision variables at time h, captured by a vector x_h, are presented as follows

g_{hj}	[MW]	power dispatched from power plant j at time h;
w_h	[MW]	wind power production at time h;
q_h	[MW]	lost load (unsatisfied electricity demand) at time h;
z_h^+	[thousand]	number of PHEVs to charge at time h.

The state variables consist of the PHEV charging state, system demand state, wind energy state, and system generation state. The state variables at time h, represented by a vector S_h, are described as follows

Y_h^+	[thousand]	number of PHEVs plugged in and waiting to be charged at hour h;
$\overline{\lambda}_h$	[thousand]	expected number of new PHEVs plugged in at hour h;
D_h	[MW]	system electricity demand at hour h;
CP	[kW]	PHEV battery charging power (e.g. 3.3 kW using a Level II charger);
$\overline{\beta}_h$	[100%]	expected wind availability factor (output/capacity ratio) at hour h;
W	[MW]	installed wind capacity;

NGP	[$/MMBtu]	natural gas price (e.g. 5 $/MMBtu);
G_j	[MW]	maximum power output from power plant j;
ER_j	[lb/MWh]	emission rate of power plant j;
HR_j	[MMBtu/MWh]	heat rate of power plant j;
$FUEL_j$	[$/MWh]	variable fuel cost of power plant j; and, $FUEL_j = NGP \times HR_j$;
$VOLL$	[$/MWh]	value of lost load (e.g. 2000 $/MWh).

The number of new PHEVs plugged in λ_h [thousand] and wind availability β_h [100%] are assumed to be random. The random variables for exogenous information at time h, denoted by a vector ω_h, are presented as follows

λ_h	[thousand]	number of new PHEVs plugged in at hour h,
β_h	[100%]	wind availability factor at hour h.

In the system operator's economic dispatch model, the one element that links all the time periods together is the PHEV charging state, namely the number of empty batteries plugged in and waiting to be charged at time h, Y_h^+. The system operator can strategically delay vehicles' charging to take advantage of low electricity prices and excess wind power in late night hours. The transition functions used to move the PHEV backlog at time h to the next time $h+1$ would be written as

$$Y_h^+ = 0, \qquad h = 1; \tag{2.1}$$

$$Y_{h+1}^+ = Y_h^+ - z_h^+ + \lambda_h, \qquad 1 \leq h \leq H-1. \tag{2.2}$$

Equation (2.1) states that the initial number of the PHEV backlog at the beginning of a day is assumed to be zero. Note that in general for a dynamic program the initial state S_1 is given as known. Equation (2.2) says that the new backlog at time $h+1$ depends on the backlog at previous time h, the number of vehicles to be charged at time h, z_h^+, and the number of new vehicles plugged in at time h, λ_h.

The costs incurred at time h in the system include costs of dispatching power generation to meet the system demand at time h, and costs paid for any unsatisfied demand at time h, q_h. The cost function at time h, denoted as $C_h^{disp}(S_h,\, x_h)$, is given by

$$C_h^{disp}(S_h,\, x_h) = \sum_{j=1}^{J} FUEL_j \times g_{hj} + VOLL \times q_h, \qquad 1 \le h \le H. \tag{2.3}$$

2.2 A Deterministic Linear Programming Formulation

If we assume the exogenous information is deterministic, the short-term economic dispatch problem can be formulated as a simple linear program, which can be solved using commercial packages such as GAMS® [80] and CPLEX® [81]. In this section, we will describe the deterministic linear programming formulation in which random variables of exogenous information are replaced by their expected values $\overline{\omega}_h = \left(\overline{\lambda}_h,\, \overline{\beta}_h\right)$, $1 \le h \le H$, where

$$\overline{\lambda}_h = \mathbf{E}\left(\lambda_h\right);$$
$$\overline{\beta}_h = \mathbf{E}\left(\beta_h\right).$$

The objective of the deterministic linear program for the short-term economic dispatch problem (in which charging decisions are made by a system operator) is to minimize the costs of satisfying system demand over a 24-hour horizon, written as

$$\min_{g_{hj},\, w_h,\, q_h,\, z_h^+,\, Y_h^+} \sum_{h=1}^{H} C_h^{disp}(S_h,\, x_h), \tag{2.4}$$

subject to the following constraints

$$\sum_{j=1}^{J} g_{hj} + w_h + q_h = D_h + D_h^0 + \sum_{l=1}^{L} CP \times z^+_{\{h-l+1\}_{>0}}, \quad 1 \le h \le H; \tag{2.5}$$

$$Y_h^+ = 0, \qquad h = 1; \tag{2.6}$$

$$Y_{h+1}^+ = Y_h^+ - z_h^+ + \overline{\lambda}_h, \qquad 1 \le h \le H - L + 1; \tag{2.7}$$

$$z_h^+ = Y_h^+ + \overline{\lambda}_h, \qquad H - L + 1 \le h \le H; \tag{2.8}$$

$$0 \le\ g_{hj} \le G_j, \qquad 1 \le h \le H,\ 1 \le j \le J; \tag{2.9}$$

$$0 \le\ w_h \le \overline{\beta}_h \times W, \qquad 1 \le h \le H; \tag{2.10}$$

$$q_h,\ z_h^+,\ Y_h^+ \ge\ 0, \qquad 1 \le h \le H. \tag{2.11}$$

Note that the PHEV backlog state variables Y_h^+, which link different time periods together, are treated as decisions in the above formulation, since linear programming optimizes decisions at all time periods together.

Equation (2.5) is the power balance constraint. At any point of time, the total electricity supply should match the total system demand, which includes the electricity demand associated with PHEV charging. We will explain in the following paragraphs how the electricity consumed for charging PHEVs at each hour is calculated. There is a penalty measured by value of lost load (VOLL) [$/MWh] for any unsatisfied demand q_h.

Our 24-hour daily cycle starts at 7 AM ($h = 1$). Let $1 \le l \le L$ represent the hours within a complete PHEV charging cycle, e.g. $L = 4$ for charging a Chevy Volt using a Level II charger. Once it is started, the charging is assumed to continue for L hours till it is complete and the battery is fully charged. For example, if we start charging a PHEV at hour $h = 21$ (3 AM), the PHEV will remain being charged during hour 21, 22, 23, and 24 (from 3 AM to 6 AM).

Figure 2.1 illustrates a PHEV's charging due time (by which its charging cycle needs to be completed), depending on when it is plugged in. For vehicles plugged in at and before hour $h = 20$, its charging due time is assumed to be the end of a day, i.e. 7 AM. This assumption makes sense since from a typical PHEV owner's perspective, their vehicle needs to be charged overnight so that they can drive off in the morning. This gives opportunities for a system operator to strategically shift charging demand to increase system efficiency. The PHEVs plugged in at and after hour $h = 21$ are assumed to be charged immediately without any delay, and as a result the charging decisions for vehicles that arrive at home at and after 3 AM are fixed. The electricity

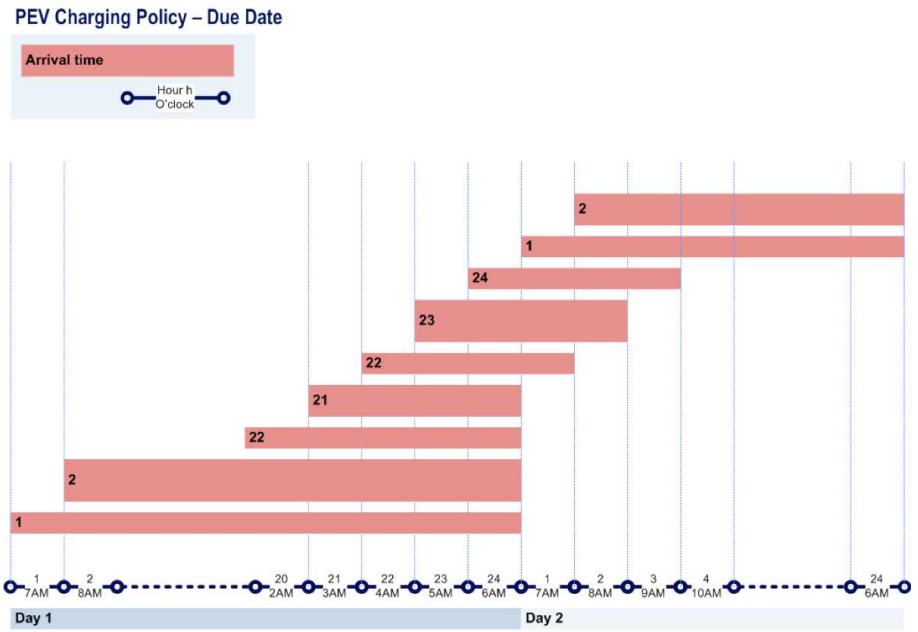

Fig. 2.1. Illustrating a PHEVs' charging due time given its arrival time

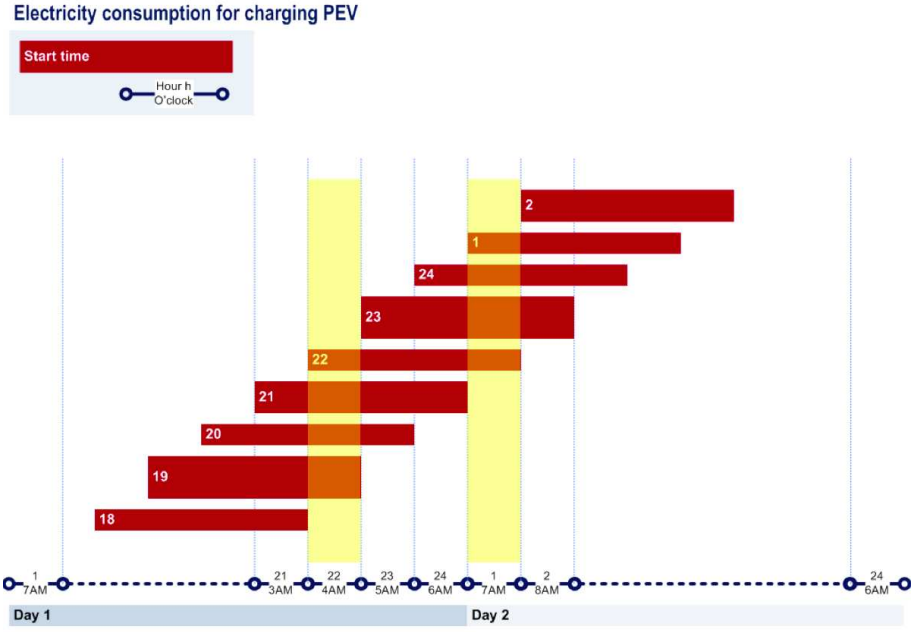

Fig. 2.2. Computing the electricity consumed for charging PHEVs at each hour in a day

consumption associated with these vehicles, represented by D_h^0 in Equation (2.5), is known to the system at time $h = 1$ and included as the initial state; that is, $D_h^0 \in S_1$.

We now explain the subscript of z^+ in Equation (2.5) with two examples. At hour $h = 22$ (4 AM), highlighted in Figure 2.2, PHEVs being charged are those dispatched between 1 AM to 4 AM (hour 19, 20, 21, and 22). Vehicles dispatched at hour 22 are in the first hour of its charging cycle; while vehicles dispatched at hour 19 are in its last charging hour. Hence, the electricity consumed due to PHEV charging at hour 22 is equal to $CP \times \left(z_{22}^+ + z_{21}^+ + z_{20}^+ + z_{19}^+\right)$, where CP is battery charging power [kW], and z_h^+ is the number of batteries to charge at time h. Consider another hour $h = 1$ (7 AM). PHEVs being charged are those dispatched between 4 AM to 7 AM (hour 22, 23, 24, and 1). As discussed earlier, the electricity consumption associated with vehicles dispatched at hour 22, 23, and 24 is treated as given data, and included in the initial state D_h^0. Thus, the PHEV charging demand to be determined at hour 1 is equal to $CP \times z_1^+$, which only depends on the charging decision at hour 1, z_1^+.

Equations (2.6) and (2.7) are the transition functions for PHEV backlog Y_h^+, as detailed in Section 2.1. Equation (2.8) enforces the charging due time for PHEVs. Equations (2.9) and (2.10) are capacity constraints for thermal units and wind energy, respectively. The power dispatched from a power plant at any time is constrained by its full nameplate capacity. The wind power production at each hour is confined by the total installed capacity W and availability factor for that particular hour. Finally, Equation (2.11) is the non-negativity restriction.

2.3 An Approximate Dynamic Programming Formulation

If exogenous information is stochastic, we are in a position of finding the best policy (or decision rule) for choosing decisions, since state S_h is a random variable. Let $X_h^\pi(S_h)$ denote a decision rule to make decisions depending on S_h, and let Π be a set of decision rules. The problem of finding the best policy to make a decision would be written as

$$\min_{\pi \in \Pi} \mathbf{E} \left\{ \sum_{h=1}^{H} C_h^{disp} \left(S_h, X_h^{\pi}(S_h) \right) \right\}. \tag{2.12}$$

If the state space is discrete, Bellman Equation can be used to recursively compute the value of being in state S_h, denoted as $V_h(S_h)$, thus breaking a multi-period problem into a series of smaller, more tractable problems, as discussed in Section 1.3.1. The Bellman Equation for finding the best decision rule to (2.12) can be written as

$$V_h(S_h) = \max_{x_h} \left\{ -C_h^{disp}(S_h, x_h) + \mathbf{E} \left[V_{h+1}(S_{h+1}) | S_h \right] \right\}, \quad 1 \leq h \leq H-1, \tag{2.13}$$

where $S_{h+1} = S^M \left(S_h, x_h, \omega_h \right)$. Note that finding the best decision rule using (2.13) requires enumerating all the states S_h, thus making it difficult to solve a dynamic program with a large state space.

To overcome the computational difficulties in solving the stochastic, dynamic program using Bellman Equation (2.13), we attempt to find a near-optimal policy based on approximate dynamic programming. As discussed in Section 1.3.2, the value function around a post-decision state is defined in approximate dynamic programming to avoid computing an expectation within the optimization formulation in (2.13). We use $y_h^{+,x}$ to represent the post-decision state of PHEV backlog at time h. $y_h^{+,x}$ captures the number of empty batteries in the system immediately after a charging decision z_h^+ is made, but before a particular realization of the number of new vehicles plugged in at time h, λ_h becomes known to the system. Using $y_h^{+,x}$, the original transition function for PHEV backlog, described in Equation (2.2), can be broken down into two steps: a pre-transition function and a post-transition function. The following pre-transition function is used to obtain $y_h^{+,x}$:

$$y_h^{+,x} = Y_h^+ - z_h^+ + \overline{\lambda}_h, \qquad 1 \leq h \leq H. \tag{2.14}$$

For the number of new vehicles plugged in at time h, its expected value $\overline{\lambda}_h$ is used in (2.14), since its realization will not become known until time $h+1$. Once the new information λ_h becomes known to the system, the system evolves to the next

pre-decision state of PHEV backlog in the time $h+1$, Y_{h+1}^{+}, according to the following post-transition function:

$$Y_{h+1}^{+} = \max\left\{0,\, Y_h^{+} - z_h^{+} + \lambda_h\right\}, \qquad 1 \le h \le H-1. \tag{2.15}$$

Let $V_h^x(y_h^{+,x})$ denote the value function of the post-decision PHEV backlog state $y_h^{+,x}$. Using $V_h^x(y_h^{+,x})$, Bellman Equation (2.13) can be rewritten as

$$V_h(S_h) = \max_{x_h}\left\{-C_h^{disp}(S_h, x_h) + V_h^x\left(y_h^{+,x}\right)\right\}, \qquad 1 \le h \le H. \tag{2.16}$$

This allows us to avoid computing the expectation in Bellman Equation (2.13).

Instead of calculating the exact value function around the post-decision state $V_h^x(y_h^{+,x})$, an approximation of the value function, denoted as $\bar{V}_h^x\left(y_h^{+,x}\right)$, is used to allow solving the dynamic program by stepping forward instead of working backwards. Finding a suitable approximation is problem specific. We begin with a simple linear approximation, and will show (in Section 2.5) that linear approximation is able to produce solutions highly close to the optimal solution generated by solving a deterministic linear program. For the resource planning model studied in Section 4.3, a separable, piece-wise linear approximation is used. The linear approximation of the value function around the post-decision PHEV backlog $y_h^{+,x}$ is given by

$$V_h^x\left(y_h^{+,x}\right) \approx \bar{V}_h^x\left(y_h^{+,x}\right) = \bar{V}_h^{+} \times y_h^{+,x}, \qquad 1 \le h \le H, \tag{2.17}$$

where $\bar{V}_h^{+}$ is the approximation of marginal value of increasing $y_h^{+,x}$ by one unit (in thousand). Using the linear approximation, we are only concerned about the derivative of the value function rather than the actual value.

For obtaining the value function gradient approximations $\bar{V}_h^{+}$, an iterative operation is performed. Let $n \in \{1, \ldots, N\}$ denote the iteration counter, where N is a preset, finite number. To describe the iterative operation, we add the iteration counter n to decision variables, state variables, random variables, and value function approximations. For example, the pre-decision state at time h for iteration n is referred to as S_h^n. The initial value function gradient approximations are assumed to be 0; that is, $\bar{V}_h^{+,1} = 0$, $1 \le h \le H$.

2.3.1 Making decisions approximately

Starting from iteration $n = 2$, at each time h, given a pre-decision state S_h^n, we make a decision, using the value function slope approximation computed in the previous iteration $n-1$, $\bar{V}_h^{+,n-1}$. For obtaining an optimal charging decision, we solve the hour-ahead economic dispatch problem as a linear program. Since a particular realization of random exogenous information on new vehicle arrivals and wind power production at time h will not become available until time $h+1$, their expected values $\overline{\omega}_h = \left(\overline{\lambda}_h, \overline{\beta}_h\right)$ are used to make a decision. The objective of a system operator's hour-ahead economic dispatch (in which charging decisions are assumed also made by the system operator) is to minimize the costs of meeting forecasted hourly demand, written as

$$\max_{g_{hj},\, w_h,\, q_h,\, z_h^+,\, y_h^{+,x}} \left\{ -C_h^{disp}\left(S_h^n,\, x_h\right) + \bar{V}_h^{+,n-1} \times y_h^{+,x} \right\}, \tag{2.18}$$

subject to the following constratins:

$$\sum_{j=1}^{J} g_{hj} + w_h + q_h = D_h + D_h^0 + CP \times z_h^+ + \sum_{l=1}^{L} CP \times z_{\{h-l\}>0}^{+,n}; \tag{2.19}$$

$$y_h^{+,x} = Y_h^{+,n} + \overline{\lambda}_h - z_h^+; \tag{2.20}$$

$$z_h^+ = Y_h^{+,n} + \overline{\lambda}_h, \qquad H - L + 1 \le h \le H; \tag{2.21}$$

$$0 \le g_{hj} \le G_j, \qquad 1 \le j \le J; \tag{2.22}$$

$$0 \le w_h \le \overline{\beta}_h \times W; \tag{2.23}$$

$$q_h,\, z_h^+,\, y_h^{+,x} \ge 0. \tag{2.24}$$

Although the above constraints look similar to (2.5) – (2.11) of the deterministic linear program explained in Section 2.2, there are two important differences. The first difference is that the pre-state variable at time $h+1$, Y_{h+1}^+, in (2.7), is replaced with the post-decision state variable at time h, $y_h^{+,x}$, in (2.20). Because, as discussed earlier, in the approximate dynamic programming setting, the value function is calculated around a post-decision state variable instead of a pre-decision state variable.

The second difference is that the state variables representing information available at time h, such as $z^{+,n}_{\{h-l\}_{>0}}$ in (2.19) and $Y^{+,n}_h$ in (2.20) and (2.21), are indicated by the superscript "n". In the linear program, these are all decision variables, since linear programming optimizes decisions at all time periods together. Approximate dynamic programming, however, steps forward in time and solves the economic dispatch problem for one hour at one point of time. Therefore, decisions made at and before time $h-1$, such as $z^{+,n}_{\{h-l\}_{>0}}$ in (2.19), are known to the system by the time h when the above optimization problem is solved. For example, at hour $h = 22$, the electricity demand associated with PHEV charging in power balance equation (2.19) is equal to $CP \times \left(z^{+}_{22} + z^{+,n}_{21} + z^{+,n}_{20} + z^{+,n}_{19}\right)$, where z^{+}_{22} is a decision we are solving for at the current hour; while $z^{+,n}_{21}$, $z^{+,n}_{20}$, and $z^{+,n}_{19}$ have already been determined at previous hours, and are indicated by the superscript "n".

We use $z^{+,n}_h$ to represent an optimal charging solution of (2.18) – (2.24). After $z^{+,n}_h$ is determined, and a particular realizaiton of the number of new PHEVs plugged in at time h, λ^n_h, becomes known to the system, the following post-decision transition function is used to step forward to the next pre-decision state at time $h+1$, $Y^{+,n}_{h+1}$:

$$Y^{+,n}_{h+1} = \max\left\{0,\, Y^{+,n}_h - z^{+,n}_h + \lambda^n_h\right\}. \tag{2.25}$$

λ^n_h is sampled using Monte Carlo sampling based on a Poisson distribution with the mean equal to $\overline{\lambda}_h$. In Section 2.4.4, we will present a detailed simulation model of PHEV usage based on which $\overline{\lambda}_h$ is obtained.

2.3.2 Value function approximation

In this subsection, we will discuss how to update the value function gradient approximation $\bar{V}^{+,n-1}_h$. Let $v^{+,n}_h$ denote a sample estimate of marginal value of increasing post-decision PHEV backlog at time h, $y^{+,n}_h$, by one unit. The proposed scheme to obtain $v^{+,n}_h$ involves approximating and updating wholesale electricity prices. We use $\bar{P}^n_h$ to denote the approximation of the wholesale electricity price at hour h, computed in iteration n. The initial wholesale electricity price approximation associated with

any hour is assumed to be 0; that is $\bar{P}_h^1 = 0,\ 1 \leq h \leq H$. Let p_h^n denote a new estimate of the wholesale electricity price at time h, obtained at iteration n. Starting from iteration $n = 2$, at each hour h, after a charging decision $z_h^{+,n}$ is determined from (2.18) – (2.24), and a specific realization of exogenous information at time h, ω_h^n, is known to the system, a real-time economic dispatch problem is solved to obtain p_h^n. The real-time economic dispatch is performed by a system operator to determine the after-the-fact wholesale electricity price at time h. The objective of the real-time economic dispatch is to minimize the costs of satisfying the actual electricity demand, written as

$$\min_{g_{hj}, w_h, q_h} C_h^{disp}\left(S_h^n,\ x_h\right), \tag{2.26}$$

subject to the following constraints:

$$\sum_{j=1}^{J} g_{hj} + w_h + q_h = D_h + D_h^0 + \sum_{l=1}^{L} CP \times z_{\{h-l+1\}_{>0}}^{+,n}; \tag{2.27}$$

$$0 \leq g_{hj} \leq G_j, \qquad 1 \leq j \leq J; \tag{2.28}$$

$$0 \leq w_h \leq \beta_h^n \times W; \tag{2.29}$$

$$q_h \geq 0. \tag{2.30}$$

A particular realization of wind availability factor β_h^n in (2.29) is sampled for iteration n using Monte Carlo simulation based on a time-series model. Details on the modeling of wind power production will be presented in Section 2.4.3. The dual of the power balance constraint represented by (2.27) is the ex post wholesale electricity price associated with this particular sample path, which can be used as a new estimate of wholesale electricity price.

We now use the new estimate p_h^n to update the wholesale electricity price approximation according to the following equation

$$\bar{P}_h^n = (1 - \alpha_{n-1}^P) \times \bar{P}_h^{n-1} + \alpha_{n-1}^P \times p_h^n, \qquad 2 \leq n \leq N,\ 1 \leq h \leq H; \tag{2.31}$$

where $\alpha_{n-1}^P \in (0, 1)$ is a step-size; and, the common practice is to use a constant step-size or a declining rule such as $\alpha_{n-1} = 1/(n-1)$, $2 \leq n \leq N$.

Using $\bar{P}_h^n$, $1 \leq h \leq H$, a new sample estimate of marginal value of increasing post-decision PHEV backlog $y_h^{+,n}$ (denoted as $v_h^{+,n}$) can be obtained, as illustrated in Figure 2.3. We could increase the number of empty batteries at time h, $y_h^{+,n}$, by one unit, by charging one less unit of batteries at time h. By doing this, two things will happen in the future hours till the end of a day. First, in the very next $L-1$ hours, $h+1 \leq \tau \leq h+L-1$, CP [kW] of electricity generation at a marginal cost equal to $\bar{P}_\tau^n$ will be saved. CP represents the charging power rate, and L denotes the number of hours needed to fully charge a battery. The reduction on electricity generation costs in the future hours would be given by

$$\sum_{\tau=h+1}^{h+L-1} CP \times \bar{P}_\tau^n, \tag{2.32}$$

which can be rewritten as (by letting $\tau = h+l-1$)

$$\sum_{l=2}^{L} CP \times \bar{P}_{h+l-1}^n. \tag{2.33}$$

The second thing that will occur is that we need to fully charge the one unit of batteries by the end of the day because of the charging due time constraint. The lowest cost to charge the additional unit can be estimated by solving a trivial optimization problem of finding an optimal start time of charging to minimize the associated electricity generation costs incurred during a charging cycle that lasts for L hours. The optimization problem can be written as follows

$$\min_{h+1 \leq \tau \leq H-L+1} \sum_{l=1}^{L} CP \times \bar{P}_{\tau+l-1}^n. \tag{2.34}$$

To summarize, the marginal value of increasing PHEV backlog by one unit can be estimated by the net reduction on electricity generation costs, written as

$$v_h^{+,n} = \sum_{l=2}^{L} CP \times \bar{P}_{h+l-1}^n - \min_{h+1 \leq \tau \leq H-L+1} \sum_{l=1}^{L} CP \times \bar{P}_{\tau+l-1}^n. \tag{2.35}$$

From (2.35) we can see that when future electricity prices are low, gains from increasing PHEV backlog will be relatively large, meaning that more vehicles' charging will be delayed to take advantage of low electricity prices in future hours. This

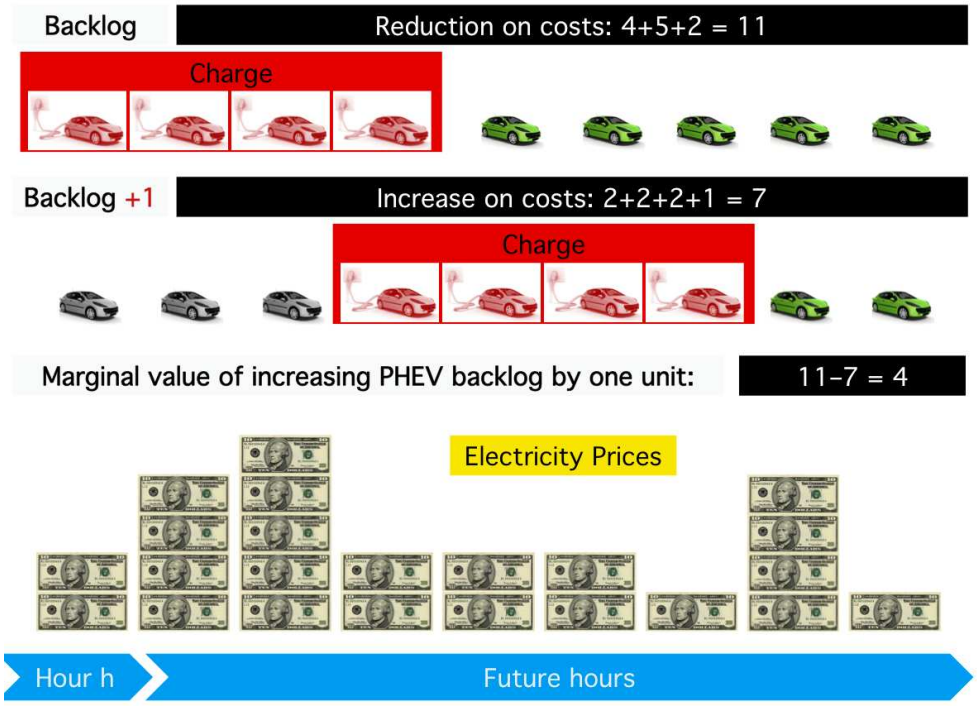

Fig. 2.3. Illustrating how to obtain a new sample estimate of the value function gradient approximation given the wholesale electricity price approximations

shows that using the designed value function approximation, combined with the iterative updating operation, a closed feedback loop is created to make better and better decisions.

We now use the new estimate $v_h^{+,n}$ to update the value function gradient approximation according to the following equation

$$\bar{V}_h^{+,n} = (1 - \alpha_{n-1}^{+}) \times \bar{V}_h^{+,n-1} + \alpha_{n-1}^{+} \times v_h^{+,n}, \qquad 2 \leq n \leq N,\ 1 \leq h \leq H; \tag{2.36}$$

where α_{n-1}^{+} is a step-size between 0 and 1; and, the common practice is to use a constant step-size or a declining rule such as $\alpha_{n-1} = 1/(n-1)$, $n = 2, \ldots, N$.

2.3.3 Complete algorithm

The complete approximate dynamic programming-based algorithm for the centralized PHEV charging scenario is presented as follows:

Step 1 Initialization. Set $\bar{V}_h^{+,1} = 0$ and $\bar{P}_h^1 = 0$, $1 \leq h \leq H$. Set iteration $n = 2$.

Step 2 Generate a sample path $\omega^n = (\lambda_h^n,\, \beta_h^n)$, $1 \leq h \leq H$.

Step 3 For $h = H - L + 2, \ldots, H$:

Step 3.1 Find the real-time PHEV charge decision at hour h:

$$z_h^{+,n} = \lambda_h^n.$$

Step 4 For $h = 1, 2, \ldots, H - L$:

Step 4.1 Solve the hour-ahead economic dispatch problem at hour h:

$$\max_{g_{hj},\, w_h,\, q_h,\, z_h^+,\, y_h^{+,x}} \left\{ -C_h^{disp}\left(S_h^n,\, x_h\right) + \bar{V}_h^{+,n-1} \times y_h^{+,x} \right\}.$$

Let $z_h^{+,n}$ be an optimal PHEV charging decision to the maximization problem.

Step 4.2 Find the pre-decision state PHEV backlog at hour $h + 1$:

$$Y_{h+1}^{+,n} = \max\{0,\, Y_h^{+,n} - z_h^{+,n} + \lambda_h^n\}.$$

Step 5 For $h = H - L + 1, \ldots, H$:

Step 5.1 Find the real-time PHEV charging decision at hour h:

$$z_h^{+,n} = \; Y_h^{+,n} + \lambda_h^n.$$

Step 5.2 If $h \leq H - 1$, find the pre-decision state PHEV backlog at hour $h+1$:

$$Y_{h+1}^{+,n} = \; 0.$$

Step 6 For $h = 1, 2, \ldots, H$:

Step 6.1 Solve the real-time economic dispatch problem at hour h:

$$\max_{g_{hj},\, w_h,\, q_h} -C_h^{disp}\left(S_h^n,\, x_h\right).$$

The dual of power balance constraint is an estimate of electricity price, p_h^n.

Step 6.2 Update the electricity price approximation:

$$\bar{P}_h^n = (1 - \alpha_{n-1}^P) \times \bar{P}_h^{n-1} + \alpha_{n-1}^P \times p_h^n.$$

Step 7 For $h = 1, 2, \ldots, H - L$:

Step 7.1 Find a new estimate of the value function gradient approximation:

$$v_h^{+,n} = \sum_{l=2}^{L} CP \times \bar{P}_{h+l-1}^n - \min_{h+1 \le \tau \le H-L+1} \sum_{l=1}^{L} CP \times \bar{P}_{\tau+l-1}^n.$$

Step 7.2 Update the value function gradient approximation:

$$\bar{V}_h^{+,n} = (1 - \alpha_{n-1}^+) \times \bar{V}_h^{+,n-1} + \alpha_{n-1}^+ \times v_h^{+,n}.$$

Step 8 Let $n = n + 1$. If $n \le N$, go to **Step 2**.

Step 9 Return value function gradient approximation $\bar{V}_h^{+,N}$, $1 \le h \le H$.

The Matlab codes associated with the above algorithm is presented in the Appendix. So far we have presented our approximate-dynamic programming based modeling and algorithm framework for solving the daily economic dispatch problem in which charging decisions are made by a system operator. The proposed framework will be tested on a realistic test case based on data available for California before it is extended to model charging schemes in which charging decisions are made by individual drivers in Chapter 3, and to solve resource investment problems in Chapter 4. The California test system will be presented in the next section of this chapter, followed by the assessment of quality of the approximate dynamic programming solutions in Section 2.5.

2.4 Test Case: the California System

The proposed approximate dynamic programming-based modeling and algorithm framework will be tested on study cases based on data available for California's electricity and transportation sectors. In this section, details of the California test system

will be provided, including the data source for system electricity demand in Section 2.4.1, the characteristics of electricity generation in Section 2.4.2, the data source and a time-series model for wind power production in Section 2.4.3, a detailed simulation model used to obtain the PHEV arrival rate in Section 2.4.4.

2.4.1 Electricity Demand

The historical system demand data for California is available on the California ISO Open Access Same-time Information System (OASIS) [82], which provides market participants and the public with reports on real-time updates of system demand, market prices, transmission outage/capacity status, and other market data.

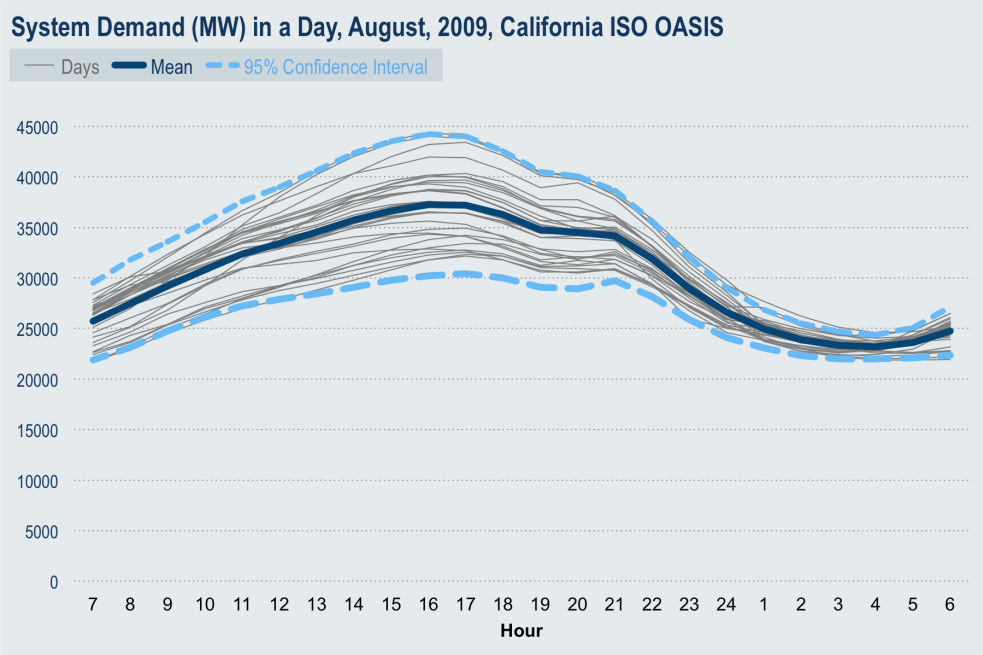

Fig. 2.4. Statistics of system demand at different hours in a day, California, August 2009

Figure 2.4 plots the dataset that we are using for system demand, which contains the actual hour-by-hour data for August 2009 (one line for each day), the estimated mean across days for each hour (bold line) and 95% confidence interval (two bold

dashed lines for upper and lower endpoints), assuming normal distributions. The system peak hours occur around 5 PM when residential consumers return home from work, turning on their air conditioner and starting household activities; while the hours from midnight to early morning are off-peak hours.

2.4.2 Electricity Generation

The characteristics of the California electric power generation sector used in this study are based on the Emissions & Generation Resource Integrated Database (eGRID) [83] of EPA, which is a comprehensive source of data on the environmental characteristics of almost all electric power generated in the United States. eGRID is unique in that it links air emissions data with electric generation data for United States power plants. The dataset that we are using is eGRID2012, which contains the complete release of year 2009 data.

Table 2.1
Statistics for the electric power generation by fuel type, California, 2009

Fuel source	**Capacity**	**# of plants**	**Emission rate**	**Heat rate**
Unit	MW		lb/MWh	MMBtu/MWh
Natural gas	38,200	214	1,143	9.7
Hydro	10,592	204	–	–
Nuclear	4,577	2	–	–
Wind	2,535	76	–	–
Geothermal	2,281	17	82	–
Biomass	1,012	80	332	13.2
Oil	494	13	2,176	12.4
Coal	415	7	1,822	8.9
Other fossil	63	2	2,281	19.5
Solar	44	18	–	–
Total	**60,212**	**633**		

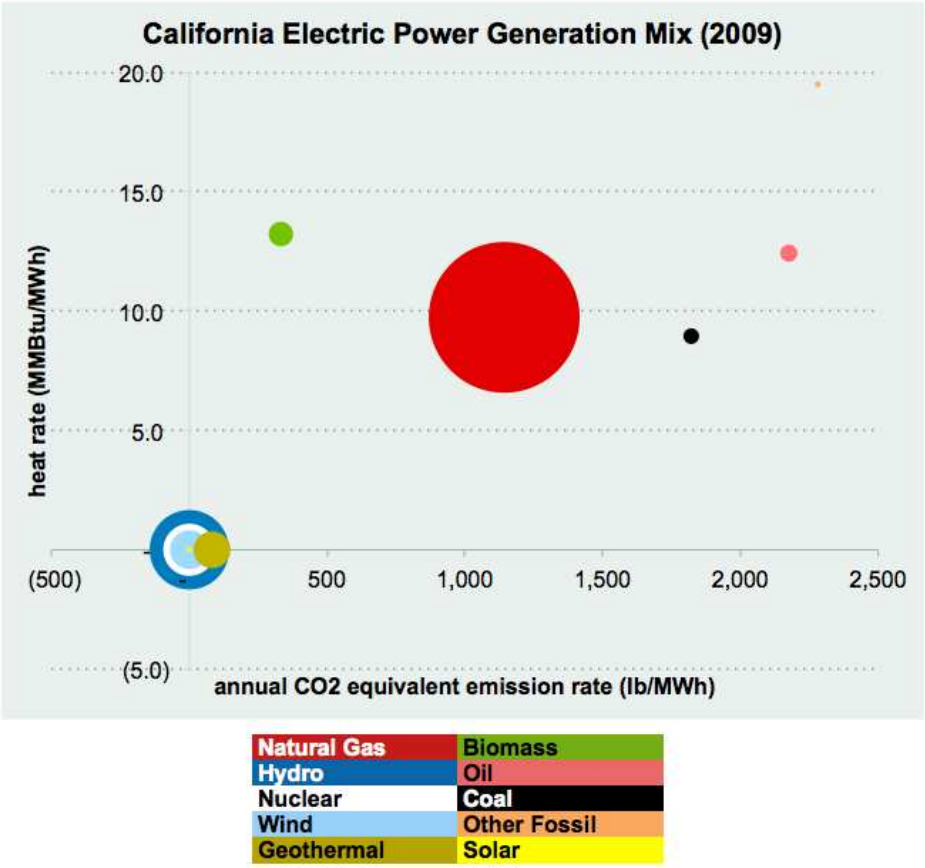

Fig. 2.5. Statistics for electric power generation mix using a bubble chart, California, 2009

We extracted the characteristics for the 633 power plants in the state of California, with a total generation capacity of about 60 GW. The characteristics that we are interested in include the fuel source, plant nameplate capacity G_j in [MW], plant annual CO2 equivalent emission rate ER_j in [lb/MWh], and plant heat rate HR_j in [MMBtu/MWh] for each power plant in California. Table 2.1 and Figure 2.5 summarize the statistics of the data that we are using. In the bubble chart, the horizontal axis represents the cleanness of the energy resource, while the vertical axis indicates how expensive to operate it (in terms of the fuel cost). In addition, the bubble size presents the percentage of each energy resource in the California generation capacity mix.

Table 2.2
Modeling the electric power generation by fuel type

Fuel source	**Capacity**	**# of plants**	**Modeling details**
Unit	MW		
Natural gas	38,200	214	Dispatch individual plants for each hour
Wind	15,000	1	Aggregated and stochastic output for each hour
Hydro	10,592	1	Aggregated and fixed output at all hours
Nuclear	4,577	1	Aggregated and fixed output at all hours
Geothermal	2,281	1	Aggregated and fixed output at all hours
Biomass	1,012	80	Dispatch individual plants for each hour
Oil	494	13	Dispatch individual plants for each hour
Coal	415	7	Dispatch individual plants for each hour
Other fossil	63	2	Dispatch individual plants for each hour
Total	**72,633**	**320**	

Table 2.2 summarizes how we actually model generation by fuel sources in the California system. Hydro, nuclear and geothermal power generators are assumed to be must-run units, which operate at its full unit capacity in all time periods since they are relatively cheap to operate (zero heat rate), and as a result we simply model it as one aggregated and fixed output for each fuel type. For fossil fuel (natural gas, oil and coal) and biomass sources, we try to optimally decide how much electricity each individual plant should generate at each time, leading to more than 300 decision variables at each hour in a day in the economic dispatch problem. Given the plant's heat rate (thermal efficiency) HR_j, the fuel cost of power plant j can be written as

$$FUEL_j \text{ [\$/MWh]} = NGP \text{ [\$/MMBtu]} \times HR_j \text{ [MMBtu/MWh]} \tag{2.37}$$

which depends on the natural gas price.

2.4.3 Modeling and Forecasting Wind Power

California's RPS is one of the most ambitious renewable energy standards in the country. Its RPS program requires investor-owned utilities, electric service providers, and community choice aggregators to increase procurement from eligible renewable energy resources to 33% of total procurement by 2020 [57]. The U.S. National Renewable Energy Laboratory (NREL) derived that the amount of new wind capacity required to meet California's RPS assuming that wind power would supply 80% of the capacity and energy required from state RPS is 12,368 MW. Therefore, we assume that the total wind capacity of the California system is 15,000 MW, which is approximately equal to the current capacity (2,535 MW) plus the required new capacity.

The wind power output data that we are using are based on the NREL Wind Integration Datasets [84], which provide a simulated set of wind profiles for the western United States. The dataset provides ten minute simulated time-series wind speed and power data for 2004, 2005, and 2006. The dataset includes over 2,800 possible onshore sites in California. Each location is assumed to contain 10 Vestas®V90 3 MW wind turbines with a hub height 100 meters above ground level. That would allow the installation of over 86 GW of capacity. Since the full amount of potential capacity is not needed in the study, sites are chosen based on their simulated capacity factors. Those sites with higher capacity factors are assumed to be chosen before lower capacity factor sites. The 500 sites with the highest average capacity factors from the dataset are used in the study. Thus, with 30 MW per site, a total of $W = 15,000$ MW is assumed to be available to the system.

Figure 2.6 plots the hour-by-hour data of the wind availability factor[1] for August 2006 (one line for each day) and the estimated mean across days for each hour $\overline{\beta}_h$ (bold line). It can be observed that the variance across days for each hour is significant, which will impose big challenge on the balance between supply and demand when

[1]The wind availability factor is defined as the actual wind power production divided by the total installed capacity at a particular hour.

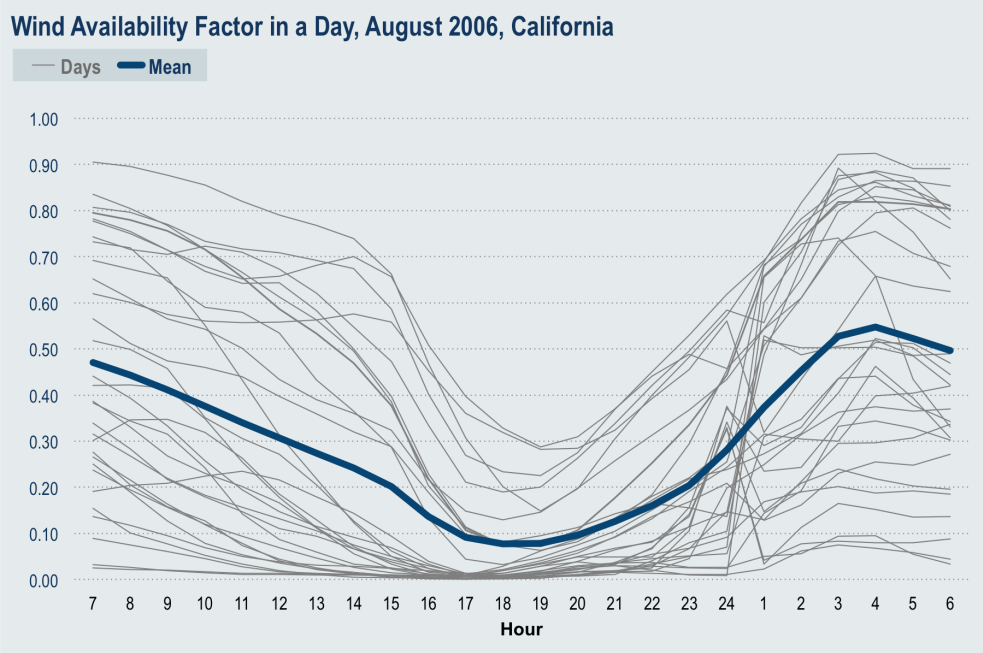

Fig. 2.6. Statistics of wind availability factor at different hour in a day, California, August 2006

the wind penetration is significant. Moreover, the comparison between daily demand profile (Figure 2.4) and wind profile (Figure 2.6) indicates that the available wind is not synchronized with the load. On the contrary, when available wind power is at its highest around early morning hours, system demand is at its lowest; while when wind power production is at its lowest around late afternoon hours, system electricity consumption is at its highest. Without solutions such as affordable storage, this asynchronous effect will greatly undermine the long-term benefits of wind energy integration.

In the approximate dynamic programming-based algorithm, we make vehicle charging decisions at any given hour h without knowing the outcome of the random events including available wind power production at time h. Therefore, we need a time-series model [85] to forecast wind power output, and a method to predict forecast errors.

There have been a number of statistical techniques developed for the forecasting of time series wind data, but none are as widely applicable and effective as the simple

persistence model [60]. While a simple approach, the persistence model is the baseline against which all other forecasting methods must be compared. The persistence model uses the value of the last time period to estimate the current time period. That is, the wind availability factor at hour h is equal to the value of the previous hour plus an error term ϵ_h, written as

$$\beta_h = \beta_{h-1} + \epsilon_h. \tag{2.38}$$

We model the wind power production forecast error using a normal distribution, justified by the the geographical dispersion of the wind power and the central limit theorem [86] written as

$$\epsilon_h \sim \mathcal{N}\left(\mu_h,\ \sigma_h\right). \tag{2.39}$$

In Ortega 2009 [64], for predictions with a horizon of 24 hour, the standard deviation of the wind forecast error can be approximated by

$$\sigma_h = 0.2 \times \beta_{h-1} + 0.02. \tag{2.40}$$

Therefore, our persistence model used for wind power productions is written as

$$\beta_h = \beta_{h-1} + \mathcal{N}\left(\mu_h,\ 0.2 \times \beta_{h-1} + 0.02\right). \tag{2.41}$$

Figure 2.7 plots the simulated hour-by-hour wind availability factor for August (one line for each day), and the mean across days for each hour (bold line). The comparison between the simulated data (Figure 2.7) and the actual wind profile (Figure 2.6) shows that there is a close match between the mean of the simulated data and that of the historical data, and the time-series model is able to capture the variation across days for each hour and the inter-temporal correlation among different hours.

2.4.4 Obtaining PHEV Arrival Rate

Hodge et al. 2011 [87, 88], and, Huang et al. 2012 [89], 2011 [40] have introduced a multi-paradigm modeling approach to examine the effects of introduction of

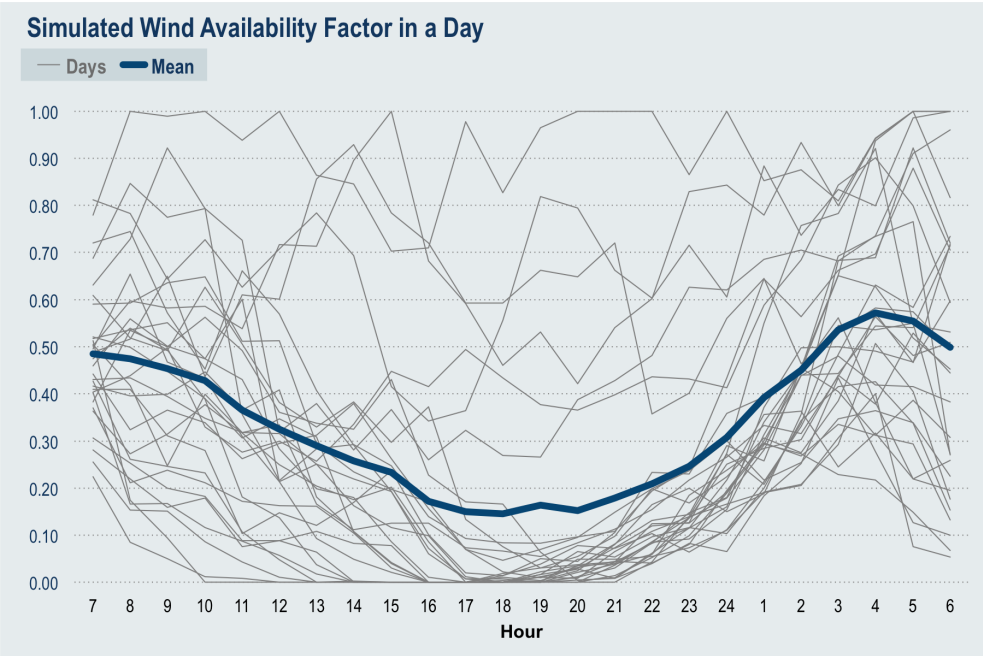

Fig. 2.7. Plot of simulated wind availability factor at different hour in a day, California, August

EVs/PHEVs on electricity demand sector. The general modeling framework is described in [87], which combines a GIS (Geographic Information System)-based transportation model and agent-based model for simulating EV/PHEV usage patterns. The same methodology is adapted here to generate the expected number of PHEVs plugged in at different hour in a day ($\overline{\lambda}_h$, $1 \leq h \leq H$). We assume that the number of PHEV arrivals at time h (λ_h) follows a Poisson distribution with mean of $\overline{\lambda}_h$.

An overview of the whole modeling process is illustrated in Figure 2.8. The transportation model is built using the transportation planning software TransCAD® [90], which combines GIS and transportation modeling capabilities in a single integrated platform. The inputs of the transportation model include zone-level socioeconomic data and GIS road networks, which can be obtained from the Metropolitan Planning Organization (MPO) of a particular city. The socioeconomic data of zones (such as population, number of households, number of automobiles, employment information, etc) are used to estimate trips between zones.

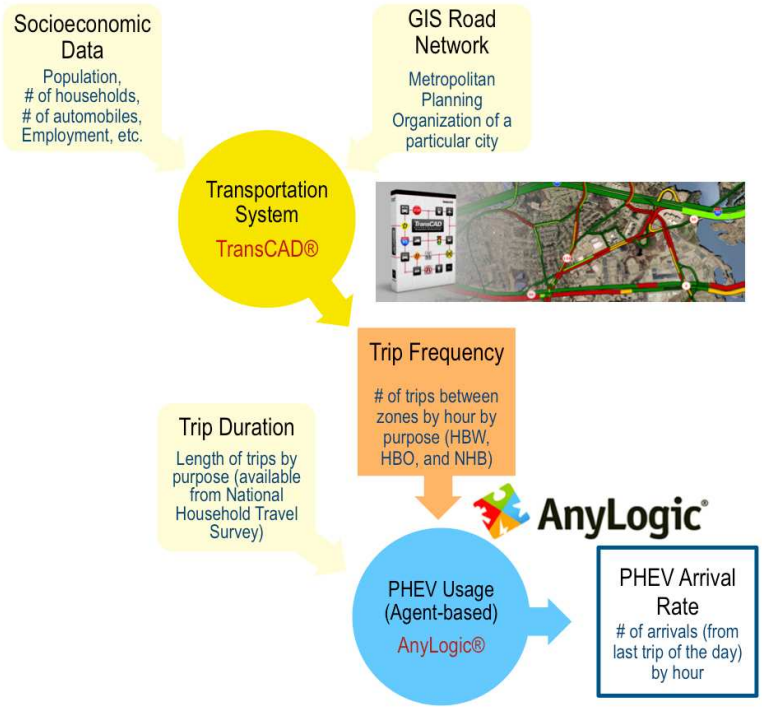

Fig. 2.8. Flowchart overview of modeling PHEV arrival at different hour in a day

The distribution of trip frequency by the three trip purposes is generated based on the simulated traffic flows, which is useful for modeling PHEV usage patterns. The other distribution needed is the distribution of trip lengths by trip purposes, which can be obtained on the National Household Travel Survey (NHTS) [91]. These two distributions of vehicle travel characteristics are used as the inputs of the agent-based model for PHEV. Agent-based modeling has been introduced and extensively implemented for simulating the actions and interactions of autonomous agents to assess their effects on the system as a whole [92–94]. The system-level behavior emerges as a result of interactions of many individual behaviors. Our agent-based model is built using the multi-method simulation software AnyLogic® [95], which brings together system dynamics, process-centric (discrete event), and agent-based methods within one modeling language and one model development environment. Detailed definition for our PHEV agents can be found in Hodge et al. 2011 [40]. A typical usage pattern for a PHEV can be described as follows.

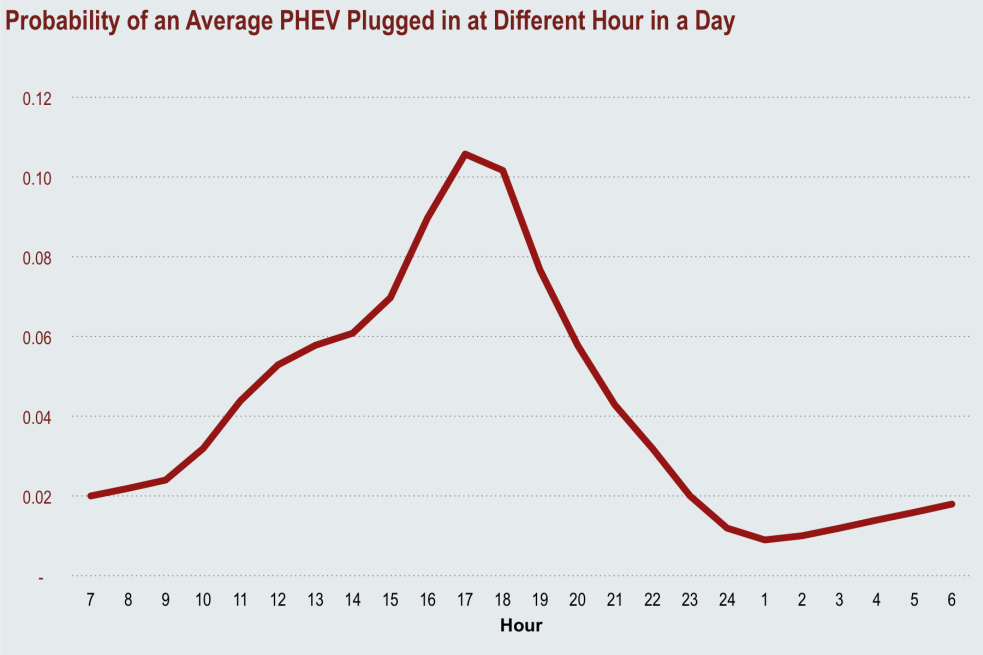

Fig. 2.9. Probability that a PHEV is plugged in at different hour in a day

Figure 2.9 summarizes the probability that a PHEV arrives at home from the last trip of a day and is plugged in at different hour in a day, obtained from our agent-based model of PHEV usage patterns. The probability gradually grows from morning, reaches its peak around 5 PM as people return home from work, and decreases after that.

To compute the expected number of PHEVs plugged in at hour h ($\overline{\lambda}_h$), we need to scale up the distribution for one PHEV (shown in Figure 2.9), according to a multiplier (denoted as θ), namely, the number of empty PHEV batteries [thousand] produced in the California transportation system in a day. The parameters used to compute the multiplier θ are defined as follows:

θ [thousand]	number of PHEVs with empty battery generated in a day,
$Cars$ [thousand]	number of passenger cars registered,
$Distance$ [mile]	daily driving distance per vehicle,
$Penetration$ [100%]	PHEV penetration rate in the California transportation system,

Range [mile]	PHEV electric range,
γ [100%]	PHEV electric driving ratio.

PHEV electric driving ratio (γ) is defined as the ratio of the daily miles driven on electricity to the total daily miles driven on average. A PHEV has a limited electric range (e.g. 35 miles for Chevy Volt), and as a result it cannot reply completely on its battery for trips longer than its electric range without charging. When its battery is depleted, a PHEV runs on its internal combustion engine which works as a backup. When we consider only home-based charging (no public charging), the PHEV electric driving ratio (γ) is less than 1. Our agent-based model of PEV usage patterns tracks each vehicle's battery level and state of charge (SOC) (from 0% for empty to 100% for full), and can be used to compute this electric driving ratio. The simulation results based on the agent-based modeling indicate that for an average Volt driver in California, about 70% of the total daily mileage can be replaced by driving on electricity. That is, $\gamma = 70\%$.

The rest of the parameters used to calculate the multiplier (θ) can be found in Table 2.3 and Table 2.4. Table 2.3 summaries the data used for the California transportation system, available from the U.S. DOE, Bureau of Transportation Statistic (BTS). Table 2.4 shows the parameters used for PHEVs, which reflect the specifications of Chevrolet Volt, extracted from the U.S. Environmental Protection Agency (EPA).

We can now calculate the average number of PHEV empty batteries produced in a day (θ) as follows

$$\begin{aligned} \theta &= Cars \times Penetration \times \frac{Distance \times \gamma}{Range} \\ &= 19,800 \text{ [thousand]} \times Penetration \text{ [100\%]} \times \frac{34 \text{ [mile]} \times 70\%}{35 \text{ [mile]}}, \end{aligned} \tag{2.42}$$

which depends on the PHEV penetration rate in the California transportation system.

The charging for PHEVs can be classified into different levels, namely level I, level II and level III, as shown in Table 2.5. Level II chargers are the preferred and

Table 2.3
Characteristics of the California transportation system (BTS)

Passenger cars registered	19,800	thousand
Daily driving distance	34	mile

Table 2.4
Characteristics of Chevrolet Volt (EPA)

Casoline range	344	mile
Electric range	35	mile
Electricity consumed for a full charge	12.9	kWh

Table 2.5
Characteristics of various charging configurations [89]

Charging level	**Voltage/Current requirement**
Level I	120 V AC/16 A
Level II	208 – 240 V AC/12 – 80 A
Level III	No specific limits; very hight voltages (e.g. 480 V DC)

recommended scheme for residential consumers who own a PHEV. For example, the Voltec®home-charging unit is a 240 V (Level II) charger with power output of 3.3 kW, and, according to General Motors, can replenish Volt's batteries in about 4 hours.

2.5 Evaluating Approximate Dynamic Programming Solutions

Jaakkola 1994 [96] provides proofs of convergence to $TD(\lambda)$ algorithm[2] (Sutton 1988 [97]) and Q-learning algorithm[3] (Watkins and Dayan 1992 [98]) used by ap-

[2] $TD(\lambda)$ algorithm addresses the problem of learning to predict in a Markov environment, using a temporal difference operator to update the predictions [97].
[3] Q-learning algorithm extended $TD(\lambda)$ algorithm to control problems.

proximate dynamic programming to update value function approximation iteratively. However, performing these two schemes requires extensive matrices calculations. Our approximate dynamic programming-based algorithm uses a linear approximation for the value functions (and separable, piece-wise linear approximation in later chapter), which avoids matrices calculations and requires less computational time. However, in general there is no guarantee that linear approximation will lead to convergence [76]. It is obvious that there is a trade-off between the computational time and quality of the solutions. To determine a good trade-off is an extension to this dissertation and will be considered for future works. We now need to know how closely our ADP solutions match the optimal solution. For this purpose, in this section, performance measures are defined to evaluate the ADP solutions.

2.5.1 Performance measures under deterministic assumption

In this subsection, we design performance measures to determine how closely the ADP solutions match the optimal solution for a deterministic problem, in which random events are replaced by their expected values. We use two types of solution methods to construct our performance measures: ADP (solution produced using approximate dynamic programming), and OPT (an optimal solution of a deterministic problem produced by solving a linear program). While updating value function approximation iteratively, an ADP algorithm generates a sequence of objective values, one for each iteration. For a deterministic problem, the ADP solution is equal to the best (lowest costs) of all the objective values generated by the ADP algorithm, since all iterations are associated with the same scenario/sample-path.

We define several terms that will be used for computing the statistics that we measure. Let C^s [Million \$] denote the objective value (costs in a day) as computed using solution method s. For example, C^{ADP} denotes the objective value computed using the ADP algorithm. Let CDE^s [Million lb] represent the carbon dioxide equivalent emissions in a day computed using solution method s, and PMT^s [Million \$]

denote the consumers' electric payment in a day computed using solution method s. PMT^s is calculated using the following equation

$$PMT^s = \sum_{h=1}^{H} d_h^s \times p_h^s, \tag{2.43}$$

where d_h^s [MW] represents the electricity demand at hour h computed using solution method s, and, p_h^s [$/MWh] denotes the wholesale electricity price at hour h computed using solution method s.

We use the terms defined above to compute the following measures. Let ΔC_{OPT}^{ADP} [100%] denote the error in the objective value computed using the ADP algorithm from the optimal objective value as a percentage of the optimal value. ΔC_{OPT}^{ADP} is computed using the following equation

$$\Delta C_{OPT}^{ADP} = \frac{C^{ADP} - C^{OPT}}{C^{OPT}} \times 100\%. \tag{2.44}$$

Similarly, we define the error associated with emissions, referred to as ΔCDE_{OPT}^{ADP} [100%], and the error for consumers' electric payment, denoted as ΔPMT_{OPT}^{ADP} [100%].

Table 2.6
Performance statistics of the ADP algorithm for deterministic cases under different PHEV penetration rates

PHEV penetration	ΔC_{OPT}^{ADP}	ΔCDE_{OPT}^{ADP}	ΔPMT_{OPT}^{ADP}
100%	0.0042%	0.0024%	0.0264%
80%	0.0000%	-0.0051%	0.1143%
60%	0.0000%	0.0014%	0.0701%
40%	0.0000%	0.0000%	0.0106%
20%	0.0000%	0.0000%	0.0105%

Figure 2.10 shows the PHEV charging decision in a day from the optimal solution (dashed line) and from the ADP algorithm (solid line). As discussed in Section 2.4.3, for the specific test case that we study, electricity demand (excluding PHEV electricity consumption) is at its highest in late afternoon; while wind power output happens

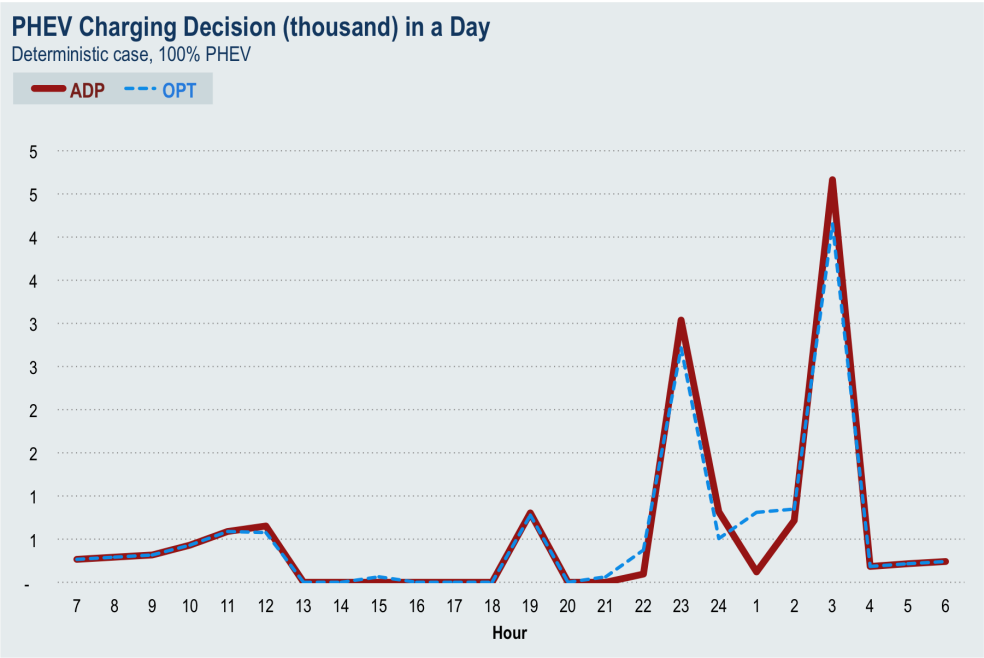

Fig. 2.10. Optimal PHEV charging decision from OPT and ADP for a deterministic case

to be at its lowest. After midnight, demand gradually falls to its lowest; meanwhile wind power production grows to its highest. With this setup, the ADP algorithm realizes that it is necessary to delay most of the PHEV charging to take advantage of lower electricity prices in late night hours. The results also show an extremely chose match between the optimal solution and that produced by the ADP algorithm.

Table 2.6 summarizes performance statistics of the ADP algorithm for different PHEV penetration levels. The negative values in the table indicate that the ADP solution performs better than the optimal solution for that particular measure. Note that the values in the ΔC_{OPT}^{ADP} column (error in the objective value computed using the ADP compared with the optimal value) are always nonnegative. We observe that the ADP algorithm is able to produce solutions that are consistently within a extremely small margin of error of the optimal for a deterministic energy model.

2.5.2 Performance measures under stochastic assumption

We now consider stochastic cases in which the number of PHEVs plugged in and wind power production at different times are random. The concept of EVPI has been first developed in decision analysis and then used in the stochastic programming setting to measure quality of stochastic programming solutions [99]. The same concept is adapted here to evaluate the ADP solutions. The expected value of perfect information (EVPI) measures the maximum amount a decision maker would be willing to pay in order to gain access to complete and accurate information about the future.

The expected value of perfect information is defined as follows. We use ω to represent randomness whose realizations correspond to a number of scenarios ω^n, $1 \leq n \leq N$. Let $C^{WS}(\omega^n)$ represent the objective value from the optimal solution for a particular scenario ω^n. The wait-and-see solution [99], a concept used in the stochastic programming setting, finds the optimal solutions for all scenarios and their optimal objective values. Let $C^{ADP}(\omega^n)$ denote the objective value for scenario ω^n produced by approximate dynamic programming. The expected value of perfect information is the difference between the expected objective value computed using the wait-and-see solution method and that from the ADP algorithm. For a minimization problem, the EVPI can be written as

$$EVPI = \mathbf{E}\left\{C^{ADP}(\omega)\right\} - \mathbf{E}\left\{C^{WS}(\omega)\right\}. \tag{2.45}$$

It is obvious that the EVPI is a nonnegative value since for any scenario ω^n, $C^{WS}(\omega^n) \leq C^{ADP}(\omega^n)$.

We use two types of solution methods to construct performance measures: ADP (solution produced using approximate dynamic programming), and WS (the wait-and-see solution assuming we have perfect information about the future). We compute the following measures to determine how closely the ADP solutions match the wait-and-see solution. Let ΔC_{WS}^{ADP} [100%] denote the difference in the objective value computed using the ADP algorithm from the objective value computed using the WS

solution method as a percentage of that associated with the WS solution method. For example, the following equation is used to compute ΔC_{WS}^{ADP}

$$\Delta C_{WS}^{ADP} = \mathbf{E}\left\{\frac{C^{ADP}(\omega) - C^{WS}(\omega)}{C^{WS}(\omega)}\right\} \times 100\%. \tag{2.46}$$

Similarly, we define the difference associated with emissions, denoted as ΔCDE_{WS}^{ADP} [100%], and difference in consumers' electric payment, referred to as ΔPMT_{WS}^{ADP} [100%].

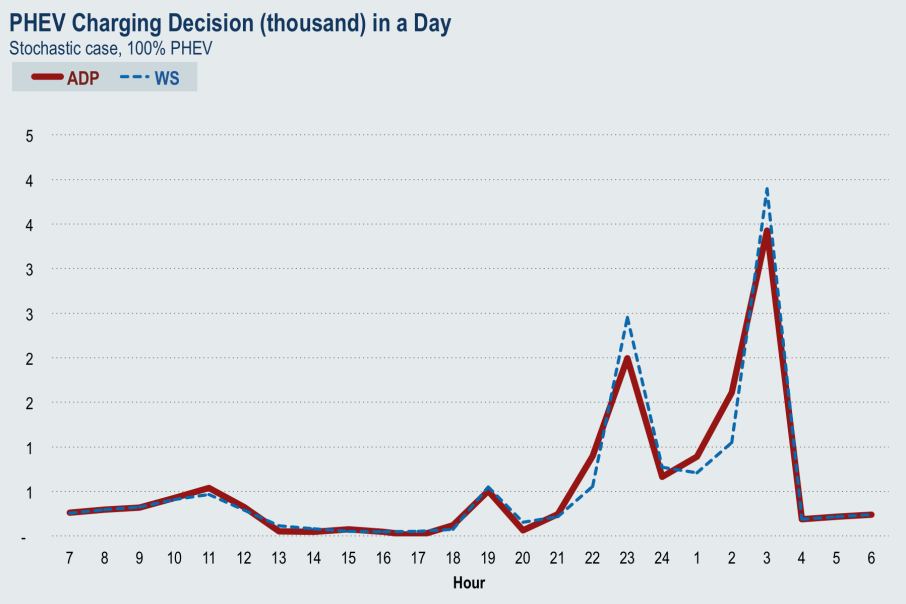

Fig. 2.11. Optimal PHEV charging decision in a day from ADP and WS for a stochastic case

Figure 2.11 shows the PHEV charging decision over the course of a day for a stochastic case from the WS solution method (dashed line) and the ADP algorithm (solid line). Figure 2.12 illustrates hourly electricity demands in a day (mean in bold line and 95% confidence interval in light lines) from the two solution methods: ADP (solid line) and WS (dashed line). Figure 2.13 summarizes wholesale electricity prices in a day from the two solution methods. We can observe a close match between the results of these two solution methods. Note that stochasticity inherent in exogenous information leads to a significant variance even in the optimal solutions associated

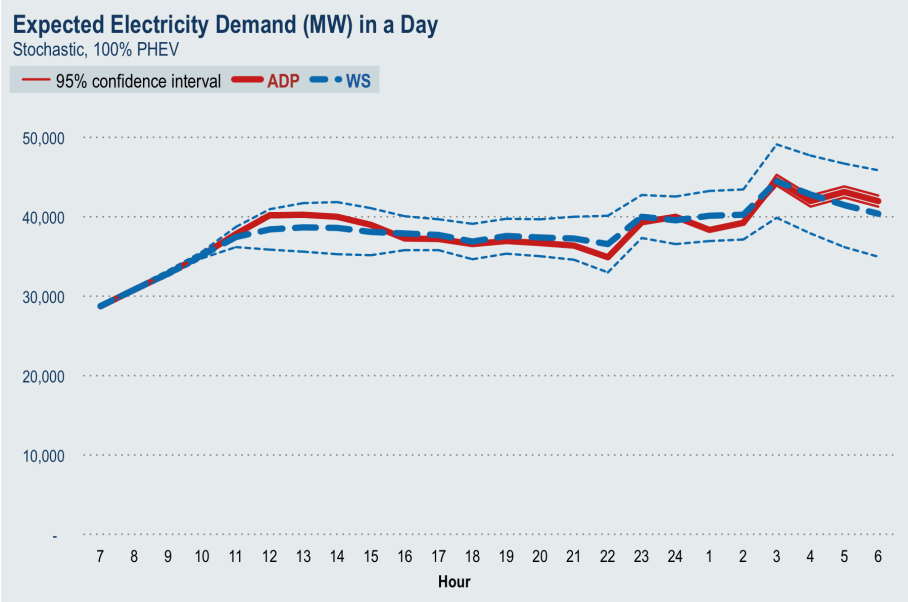

Fig. 2.12. Hourly electricity demand in a day from OPT and ADP for a stochastic case

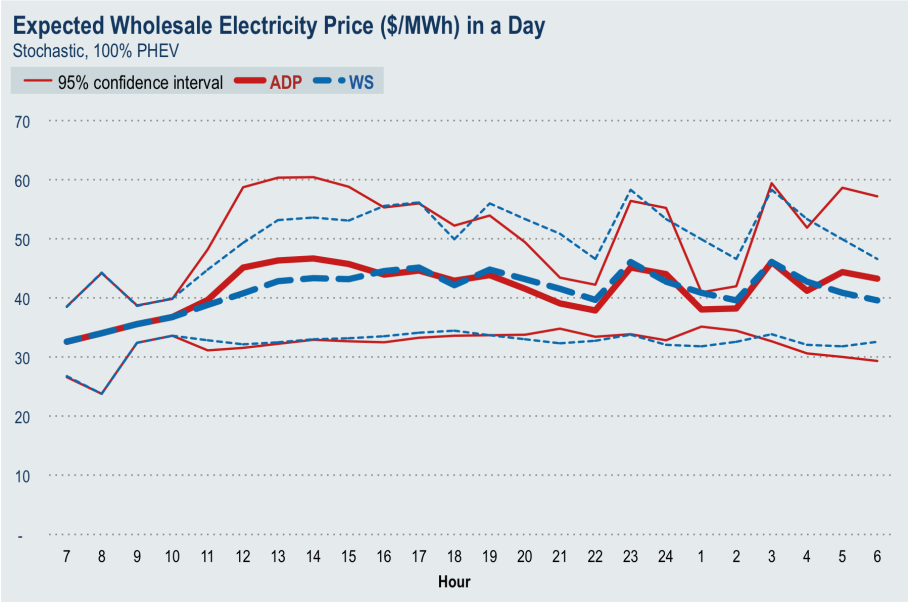

Fig. 2.13. Hourly wholesale electricity price in a day from OPT and ADP for a stochastic case

Table 2.7
Performance statistics of the ADP algorithm for stochastic cases under different PHEV penetration rates

Penetration		ΔC_{WS}^{ADP}	ΔCDE_{WS}^{ADP}	ΔPMT_{WS}^{ADP}
100%	μ	**0.5628%**	**0.6098%**	**1.2001%**
	σ	0.4290%	0.4574%	2.2012%
80%	μ	**0.1349%**	**0.1390%**	**1.1314%**
	σ	0.1301%	0.1371%	1.0881%
60%	μ	**0.0410%**	**0.0392%**	**0.1223%**
	σ	0.0562%	0.0582%	0.3013%
40%	μ	**0.0915%**	**0.0942%**	**-0.1732%**
	σ	0.1992%	0.2008%	0.5598%
20%	μ	**0.1389%**	**0.1427%**	**0.0280%**
	σ	0.3655%	0.3601%	1.5859%

Table 2.8
Performance statistics of the ADP algorithm for stochastic cases under different PHEV penetration rates (with an increased variance in wind forecast error)

Penetration		ΔC_{WS}^{ADP}	ΔCDE_{WS}^{ADP}	ΔPMT_{WS}^{ADP}
100%	μ	**1.2736%**	**1.3292%**	**1.8431%**
	σ	1.1972%	1.2472%	3.5535%
80%	μ	**0.6498%**	**0.7026%**	**2.2508%**
	σ	0.5837%	0.6051%	1.9691%
60%	μ	**0.3627%**	**0.3722%**	**0.4152%**
	σ	0.3431%	0.3640%	1.0701%
40%	μ	**0.8170%**	**0.8265%**	**-0.9937%**
	σ	1.8048%	1.8307%	2.2633%
20%	μ	**1.0947%**	**1.1112%**	**-0.8577%**
	σ	2.2516%	2.2594%	3.3853%

with various scenarios (the wait-to-see solution method in dashed lines). Nevertheless, the ADP algorithm is able to find a policy that performs well under significant uncertainty.

In Table 2.7, we summarize the performance statistics of the ADP algorithm for different PHEV penetration levels, benchmarked against the WS solution method. We observe that the ADP algorithm is able to produce solutions that are close to the wait-and-see solutions under significant randomness. Note that ΔC_{WS}^{ADP} indicates expected gains from perfect information; that is $EVPI$. Table 2.8 summarizes the results assuming that the variance of wind forecase error is increased from $0.2 \times \beta_{h-1} + 0.02$ to $0.3 \times \beta_{h-1} + 0.02$. It shows that when wind forecast error increases, a decision maker would be willing to pay more in order to have perfect information.

2.5.3 Selecting step size

Using approximate dynamic programming, we update value function approximation $\bar{V}_h^+$ and wholesale electricity price approximation $\bar{P}_h$ iteratively as the following

$$\bar{V}_h^{+,n} = (1 - \alpha_{n-1}^+) \times \bar{V}_h^{+,n-1} + \alpha_{n-1}^+ \times v_h^{+,n}, \qquad 2 \leq n \leq N,\ 1 \leq h \leq H;$$
$$\bar{P}_h^n = (1 - \alpha_{n-1}^P) \times \bar{P}_h^{n-1} + \alpha_{n-1}^P \times p_h^n, \qquad 2 \leq n \leq N,\ 1 \leq h \leq H,$$

where $\alpha_{n-1}^+ \in (0, 1)$ and $\alpha_{n-1}^P \in (0, 1)$ are step sizes for updating $\bar{V}_h^+$ and $\bar{P}_h$, respectively. The common practice for choosing a step size is to use a constant step-size or declining rule such as $\alpha_{n-1} = 1/(n-1)$, $n = 2, \ldots, N$. This leaves us the problem to choose a step size pair $\left(\alpha_{n-1}^+, \alpha_{n-1}^P\right)$. We assume both α_{n-1}^+ and α_{n-1}^P can either take on one of the five constant values $\{0.1, 0.2, 0.3, 0.4, 0.5\}$ or follow the declining rule, and as a result $(6 \times 6) = 36$ combinations are considered, among which we will choose the one that produces the best result.

The ADP algorithm generates multiple objective values, one for each iteration. For a deterministic case, the objective values produced by the ADP algorithm are benchmarked against the optimal objective values. Note that when exogenous information is deterministic, the optimal objective values for all iterations are the same

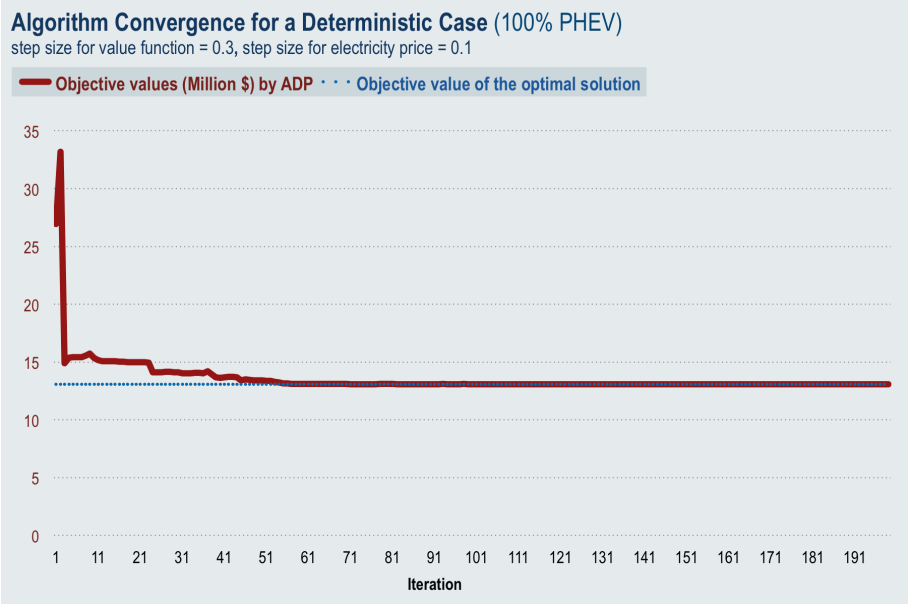

Fig. 2.14. Plot of the objective values with respect to iteration n for step size (0.3, 0.1), for a deterministic case

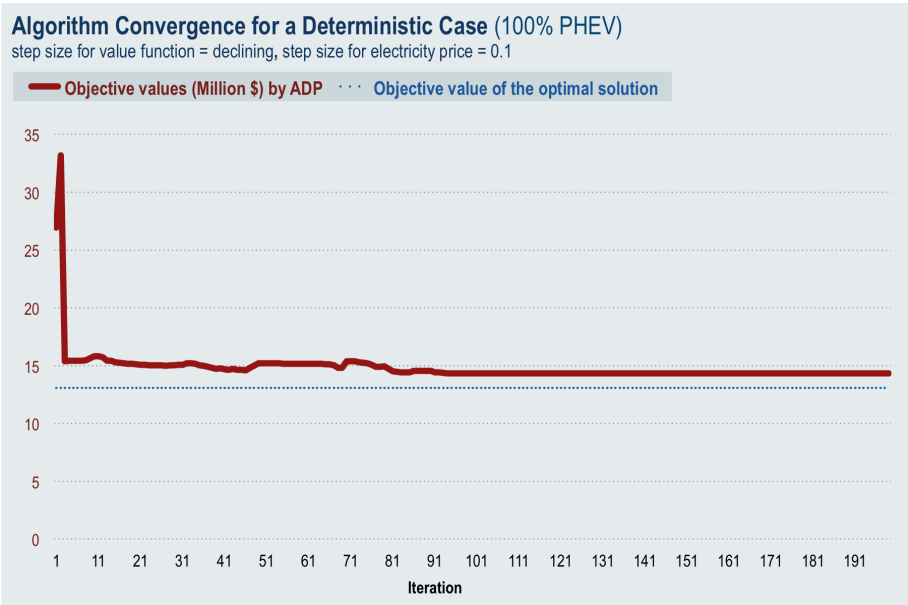

Fig. 2.15. Plot of the objective values with respect to iteration n for step size $(1/n, 0.1)$, for a deterministic case

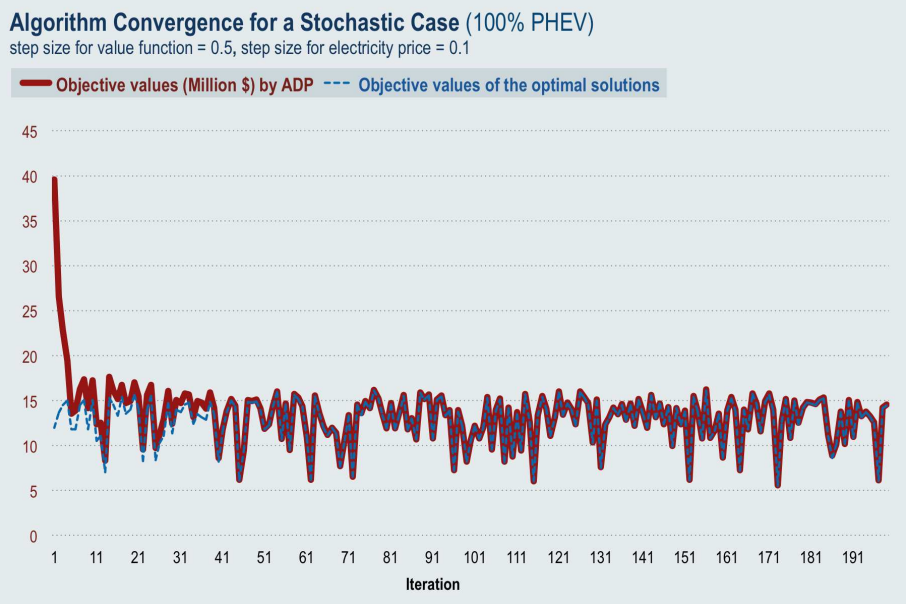

Fig. 2.16. Plot of the objective values with respect to iteration n for step size (0.5, 0.1), for a stochastic case

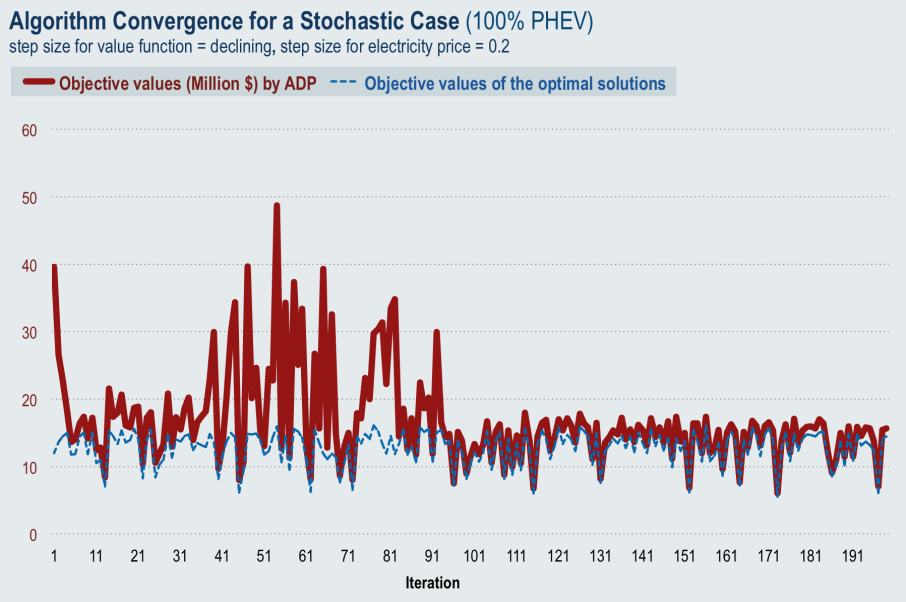

Fig. 2.17. Plot of the objective values with respect to iteration n for step size $(1/n, 0.2)$, for a stochastic case

since they are associated with the same scenario. Figure 2.14 and 2.15 plot the objective values generated by the ADP algorithm (solid line) with respect to iteration n, benchmarked against the optimal values (dashed line). It can be observed that convergence behavior is sensitive to step size. The sequence in Figure 2.14, corresponding to step size (0.3, 0.1), rapidly converges to the optimal value. After 55 iterations, the error in the ADP objective values compared with the optimal value is within 0.05%. The sequence associated with step size ($1/n$, 0.1) in Figure 2.15, however, fails to converge to the optimal value within 200 iterations. The minimum error achieved is greater than 9%.

Figure 2.16 and 2.17 represent stochastic cases. Note that for a stochastic case, a different sample path is generated for each iteration, and as a result the optimal objective values vary with respect to iteration n. The step size (0.5, 0.1), in Figure 2.16, produces fast convergence. The error after 40 iterations is less than 0.6%. The sequence associated with step size ($1/n$, 0.2), in Figure 2.17, fails to converge within a large number of iterations. The minimum error obtained is above 4%.

Mean of objective function approxiamtions [Million $]

		step size for electricity price					
		0.1	0.2	0.3	0.4	0.5	Declining
step	0.1	12.892	12.930	12.891	12.885	12.891	13.056
size	0.2	12.901	12.894	12.898	12.899	12.917	13.001
for	0.3	12.886	12.888	12.908	12.919	12.925	12.999
value	0.4	12.886	12.892	12.909	12.916	12.934	12.994
function	0.5	***12.883***	12.898	12.910	12.932	12.935	12.996
(gradient)	Declining	17.542	13.706	13.596	13.527	13.386	14.316

Standard deviation of objective function approximations [Million $]

		step size for electricity price					
		0.1	0.2	0.3	0.4	0.5	Declining
step	0.1	2.50	2.49	2.50	2.50	2.50	2.54
size	0.2	2.50	2.51	2.50	2.51	2.51	2.54
for	0.3	2.50	2.50	2.51	2.52	2.52	2.54
value	0.4	2.50	2.51	2.52	2.51	2.52	2.54
function	0.5	2.51	2.51	2.52	2.52	2.52	2.54
(gradient)	Declining	9.20	2.58	2.56	2.56	2.55	2.68

Fig. 2.18. Choosing the best step size based on the mean and standard deviation of the objective values generated by the ADP algorithm

To find the best step size among the 36 combinations, for each combination, we run the ADP algorithm for 200 iterations and calculate an estimate to which the objective values would converge, using the mean and standard deviation of the objective values generated in the last 100 iterations. Figure 2.18 shows the estimates computed for the 36 combinations, which are color scaled with red corresponding to greater (worse) values and green corresponding to smaller (better) values. Among the 36 pairs tested, $\left(\alpha_{n-1}^{+},\, \alpha_{n-1}^{P}\right) = (0.5,\, 0.1)$ is the best choice because it produces the lowest objective value.

3. EXTENSIONS OF THE SHORT-TERM ENERGY SYSTEM MODEL

In the centralized PHEV charging scenario discussed in Chapter 2, charging decisions are determined and coordinated by a system operator. As pointed out earlier, it is, however, unrealistic to implement the centralized charging scheme in the real world. A more practical scheme is to leave charging decisions to individual consumers, and design electricity tariffs to encourage PHEV owners to shift their charging to late night hours when electricity price is low. In this chapter, we will extend the ADP-based modeling and algorithm framework to examine two decentralized charging scenarios, in which real-time pricing is assumed to be deployed and set electricity prices based on wholesale electricity prices. In addition, communications and controls systems, referred to as energy management controllers (EMCs), are assumed to be universally deployed for all residential consumers to automate PHEV charging decisions in response to real-time price signals for consumers. We are also interested in effects of vehicle-to-grid (V2G) as storage resources, a case in which PHEV batteries can be discharged to send energy back to the grid when electricity demand is high.

The chapter proceeds as follows. Section 3.1 and 3.2 describe the formulations for decentralized charging without V2G and with V2G, respectively. Section 3.3 compares different charging policies and discusses their economic and environmental effects on the short-term energy system.

3.1 Decentralized PHEV Charging

At time h, the charging decision z_h^+ in the centralized charging scenario is modeled as a continuous variable because a system operator may decide to charge a subset of the empty batteries waiting to be charged and hold the charging of the rest to future

hours. When charging decisions are left to individual consumers, a PHEV owner is only responsible for their own charging decision, deciding whether to start charging their vehicle or delay its charging. Therefore, we need a set of *binary decision variables* used to represent a consumer's charging decisions at different times in a day; that is

$$k_h^+ = \begin{cases} 1 & \text{to charge their PHEV at time } h; \\ 0 & \text{to delay its charging.} \end{cases}$$

As a starting point, we assume all EMCs installed are identical. Thus, at any point of time, all EMCs will make the same charging decision for consumers facing the same electricity rates. Therefore, the total number of batteries to be charged at time h, z_h^+ can be written as:

$$z_h^+ = \begin{cases} Y_h^+ + \lambda_h & \text{if } k_h^+ = 1; \\ 0 & \text{if } k_h^+ = 0, \end{cases}$$

where λ_h represents the number of new PHEVs plugged in and waiting to be charged at time h.

3.1.1 A deterministic mixed integer linear programming formulation

If we assume that all exogenous information is deterministic, we can formulate the system operator's multi-period economic dispatch problem with charging decisions made by individual consumers as a simple mixed integer linear program (MILP). In this section, we will describe the deterministic MILP formulation in which random events are replaced by their expected values $\overline{\omega}_h = \left(\overline{\lambda}_h, \overline{\beta}_h\right)$, $1 \leq h \leq H$. The objective is to minimize the costs of generating electricity in a day, written as

$$\min_{g_{hj}, w_h, q_h, z_h^+, Y_h^+, k_h^+} \sum_{h=1}^{H} C_h^{disp}\left(S_h, x_h\right), \tag{3.1}$$

subject to the following constraints:

$$\sum_{j=1}^{J} g_{hj} + w_h + q_h = D_h + D_h^0 + \sum_{l=1}^{L} CP \times z^+_{\{h-l+1\}_{>0}}, \quad 1 \le h \le H; \tag{3.2}$$

$$Y_h^+ = 0, \qquad h = 1; \tag{3.3}$$

$$Y_{h+1}^+ = Y_h^+ + \overline{\lambda}_h - z_h^+, \qquad 1 \le h \le H-1; \tag{3.4}$$

$$z_h^+ \le bigM \times k_h^+, \qquad 1 \le h \le H-L; \tag{3.5}$$

$$Y_{h+1}^+ \le bigM \times \left(1 - k_h^+\right), \qquad 1 \le h \le H-L; \tag{3.6}$$

$$z_h^+ = Y_h^+ + \lambda_h, \qquad H-L+1 \le h \le H; \tag{3.7}$$

$$k_h^+ = 1, \qquad H-L+1 \le h \le H; \tag{3.8}$$

$$0 \le g_{hj} \le G_j, \qquad 1 \le j \le J,\ 1 \le h \le H; \tag{3.9}$$

$$0 \le w_h \le \overline{\beta} \times W, \qquad 1 \le h \le H; \tag{3.10}$$

$$k_h^+ \in \{0,1\},\ q_h,\ z_h^+,\ Y_h^+ \ge 0 \qquad 1 \le h \le H. \tag{3.11}$$

Equation (3.2) ensures system load (including electricity consumed due to PHEV charging) is exactly met at any point of time. Equation (3.3) and (3.4) define the transition functions for PHEV backlog Y_h^+. Equation (3.5) and (3.6) are unique to the decentralized charging policy as opposed to the centralized charging, stating that either all or none of the vehicles will be charged at any time. Note that $bigM$ in (3.5) and (3.6) is a large positive number. Equation (3.7) and (3.8) enforce that PHEVs whose charging cannot be finished by the end of a daily cycle will be charged without any delay. Equation (3.9) and (3.10) are capacity constraints.

3.1.2 An approximate dynamic programming formulation

If the exogenous information is stochastic, an approximate dynamic programming-based algorithm is developed to find a near-optimal policy for making decisions. As in the ADP algorithm for the centralized charging scenario, we assume a linear approximation for the value function around a post-decision state $y_h^{+,x}$, and update value function slope approximations $\bar{V}_h^+$ using an iterative updating operation. The initial

values for all value function gradient approximations are 0. Starting from iteration $n = 2$, at each time h, to obtain an optimal charging decision $k_h^{+,n}$, given a specific state[1] S_h^n, we solve the hour-ahead economic dispatch problem based on the value function gradient approximation computed in the previous iteration $n-1$, $\bar{V}_h^{+,n-1}$. The economic dispatch problem is solved as a mixed integer linear programming problem, given as follows

$$\max_{x_h} \quad \left\{-C_h^{disp}\left(S_h^n,\, x_h\right) + \bar{V}_h^{+,n-1} \times y_h^{+,x}\right\}, \tag{3.12}$$

$$\text{s.t.} \quad \sum_{j=1}^{J} g_{hj} + w_h + q_h = D_h + D_h^0$$

$$+ CP \times z_h^+ + \sum_{l=1}^{L} CP \times z_{\{h-l\}>0}^{+,n}, \qquad 1 \le h \le H; \tag{3.13}$$

$$y_h^{+,x} = Y_h^{+,n} + \overline{\lambda}_h - z_h^+, \qquad 1 \le h \le H-1; \tag{3.14}$$

$$z_h^+ \le bigM \times k_h^+, \qquad 1 \le h \le H-L; \tag{3.15}$$

$$y_h^{+,x} \le bigM \times \left(1 - k_h^+\right), \qquad 1 \le h \le H-L; \tag{3.16}$$

$$z_h^+ = Y_h^{+,n} + \lambda_h, \qquad H-L+1 \le h \le H; \tag{3.17}$$

$$k_h^+ = 1, \qquad H-L+1 \le h \le H; \tag{3.18}$$

capacity constraints: (3.9), (3.10)

$$k_h^+ \in \{0,1\},\ q_h,\ z_h^+,\ y_h^{+,x} \ge 0 \qquad 1 \le h \le H. \tag{3.19}$$

Equation (3.14) is the pre-transition function used to calculate the post-decision PHEV backlog $y_h^{+,x}$.

It is important to recognize that solving the above MILP is equivalent to solving two linear programs, by setting k_h^+ to be equal to either 0 or 1 and finding the solution which yields greater objective value. For example, when $k_h^+ = 0$ (no vehicle is to be

[1]Again, the system state captures available information on system demand, PHEV charging, generation, and wind availability.

charged, and as a result $z_h^+ = 0$ and $y_h^{+,x} = Y_h^{+,n} + \overline{\lambda}_h$), the optimization problem would be rewritten as the following linear program:

$$\max_{g_{hj},\, w_h,\, q_h} \left\{ -C_h^{disp}\left(S_h^n,\, x_h\right) + \bar{V}_h^{+,n-1} \times \left(Y_h^{+,n} + \bar{\lambda}_h\right) \right\}, \tag{3.20}$$

$$\text{s.t.} \quad \sum_{j=1}^{J} g_{hj} + w_h + q_h = D_h + D_h^0 + \sum_{l=1}^{L} CP \times z_{\{h-l\}>0}^{+,n}, \quad 1 \le h \le H; \tag{3.21}$$

$$\text{capacity constraints: (3.9), (3.10)}$$

$$q_h \ge 0, \qquad 1 \le h \le H. \tag{3.22}$$

Similarly, we can obtain the linear program associated with k_h^+ equal to 0.

After an optimal charging decision $k_h^{+,n}$ is determined from (3.12) – (3.19), and a specific realization of new information on the number of new PHEV arrivals at time h, λ_h^n, becomes known to the system, the following post-decision transition function is used to step forward to the next pre-decision state at time $h+1$, $Y_{h+1}^{+,n}$.

$$Y_{h+1}^{+,n} = \begin{cases} 0 & \text{if } k_h^{+,n} = 1; \\ Y_h^{+,n} + \lambda_h^n & \text{if } k_h^{+,n} = 0, \end{cases}$$

Our algorithm proceeds till the last hour of a day to finish iteration n. At the end of the iteration, for each time h, we solve the real-time economic dispatch (as a linear program) to obtain a new estimate of the wholesale electricity price p_h^n, and use p_h^n to update the wholesale electricity price approximation. The best estimates for wholesale electricity prices calculated so far P_h^n, $1 \le h \le H$ are then used to obtain a new estimate of marginal value of increasing the post-decision PHEV backlog by one unit, $v_h^{+,n}$. Using $v_h^{+,n}$, we can update the value function gradient approximation to obtain the best estimate so far, $\bar{V}_h^{+,n}$. The same procedure is repeated for a number of iterations to return a good policy. The details on how the new estimates are computed and how the approximations for wholesale electricity prices and value function slope approximations are updated are the same as that presented in Section 2.3.

The numerical results for various charging scenarios including the decentralized charging without V2G will be discussed in the end of this chapter, after the modeling

and algorithm details for the decentralized charging with V2G are presented in the next section.

3.2 Decentralized PHEV Charging with Vehicle-to-Grid as Storage

Lack of storage resources in the electric grid is one of the reasons why wholesale electricity prices fluctuate and price spikes occur from time to time. PHEVs could play an important role in the power system because it can be used to provide electricity storage to the electric grid through the vehicle-to-grid technology. To quantify potential benefits of a widespread adoption of V2G by PHEV owners, in this section we formulate a decentralized PHEV charging scenario, in which V2G is universally adopted by PHEV drivers, and energy management controllers are used to automatically optimize the timing for charging and discharging their PHEV battery in response to real-time pricing signals.

We assume that only a fully charged PHEV battery can be discharged to provide electricity to the grid since charging and discharging processes decrease battery life. From a modeling perspective, we would need a new set of variables to represent decisions related to discharging (indicated by the superscript "$-$"), as listed in the following

k_h^-	[0/1]	1 to discharge PHEV at time h; 0 otherwise;
z_h^-	[thousand]	number of PHEVs to be discharged at time h;
Y_h^-	[thousand]	number of fully charged PHEV batteries at time h.

The binary variable k_h^- represents a consumer's discharging decision at time h, which is whether or not to discharge their PHEV to send electricity back to the grid. Since it is assumed that all EMCs installed are identical and response to the same electricity prices, charging and discharging decisions (k_h^+ and k_h^-) made by all drivers

would be the same. Therefore, the total number of PHEVs to be discharged at time h, z_h^-, can be calculated according to the following equation

$$z_h^- = \begin{cases} Y_h^- + z_{\{h-L\}>0}^+ & \text{if } k_h^- = 1; \\ 0 & \text{if } k_h^- = 0, \end{cases}$$

where $z_{\{h-L\}>0}^+$ represents the number of PHEVs whose charging starts at time $h-L$ and become fully charged at time h; that is the number of new charging completions at time h. Similarly, the total number of PHEVs to be charged at time h, z_h^+, is written as:

$$z_h^+ = \begin{cases} Y_h^+ + \lambda_h + z_{\{h-L\}>0}^- & \text{if } k_h^+ = 1; \\ 0 & \text{if } k_h^+ = 0, \end{cases}$$

where $z_{\{h-L\}>0}^-$ is the number of PHEVs whose discharging stats at time $h-L$ and become empty at time h; that is the number of new discharging completions at time h. Note that we assume it takes L hours to charge or discharge a battery.

3.2.1 A deterministic mixed integer linear programming formulation

In this section, we will describe a deterministic MILP formulation for the decentralized charging scenario with V2G in which random events are replaced by their expected values $\overline{\omega}_h = \left(\overline{\lambda}_h, \overline{\beta}_h\right)$, $1 \le h \le H$. The objective is to minimize the costs of electricity generation in a day

$$\min_{g_{hj}, w_h, q_h, z_h^+, Y_h^+, k_h^+, z_h^-, Y_h^-, k_h^-} \sum_{h=1}^{H} C_h^{disp}\left(S_h,\, x_h\right), \tag{3.23}$$

subject to the following constraints:

$$\begin{aligned} &\sum_{j=1}^{J} g_{hj} + w_h + q_h = D_h + D_h^0 \\ &\quad + \sum_{l=1}^{L} CP \times z_{\{h-l+1\}>0}^+ - \sum_{l=1}^{L} CP \times z_{\{h-l+1\}>0}^-, \qquad 1 \le h \le H; \end{aligned} \tag{3.24}$$

$$Y_1^+ = 0; \tag{3.25}$$

$$Y_{h+1}^+ = Y_h^+ + \overline{\lambda}_h - z_h^+ + z_{\{h-L\}^+}^-, \qquad 1 \le h \le H-1; \tag{3.26}$$

$$z_h^+ \le bigM \times k_h^+, \qquad 1 \le h \le H-L; \tag{3.27}$$

$$Y_{h+1}^+ \le bigM \times \left(1 - k_h^+\right), \qquad 1 \le h \le H-L; \tag{3.28}$$

$$z_h^+ = Y_h^+ + \overline{\lambda}_h + z_{\{h-L\}^+}^-, \qquad H-L+1 \le h \le H; \tag{3.29}$$

$$k_h^+ = 1, \qquad H-L+1 \le h \le H; \tag{3.30}$$

$$Y_1^- = 0, \tag{3.31}$$

$$Y_{h+1}^- = Y_h^- - z_h^- + z_{\{h-L\}^+}^+, \qquad 1 \le h \le H-1; \tag{3.32}$$

$$z_h^- \le bigM \times k_h^-, \qquad 1 \le h \le H - 2 \times L + 1; \tag{3.33}$$

$$Y_{h+1}^- \le bigM \times \left(1 - k_h^-\right), \qquad 1 \le h \le H - 2 \times L + 1; \tag{3.34}$$

$$z_h^- = 0, \qquad H - 2 \times L + 2 \le h \le H; \tag{3.35}$$

$$k_h^- = 0, \qquad H - 2 \times L + 2 \le h \le H; \tag{3.36}$$

capacity constraints: (3.9) and (3.10);

$$k_h^+,\, k_h^- \in \{0,1\},\; q_h,\; z_h^+,\; Y_h^+,\; z_h^-,\; Y_h^- \ge 0, \qquad 1 \le h \le H. \tag{3.37}$$

Equation (3.24) is the power balance constraint, where $\sum_{l=1}^{L} CP \times z_{\{h-l+1\}^+}^-$ represents the electricity discharged from PHEVs at time h. At time h, the PHEVs whose discharging starts at time h are in the first hour of its discharging cycle; while those starting discharging at time $h - L + 1$ are in the last hour. (3.25) – (3.30) are associated with PHEV charging and similar to (3.3) – (3.8), explained in Section 3.1.1. The only difference is that with V2G, the PHEVs whose discharging starts at time $h - L$ and completes at time h (that is new discharging completions $z_{\{h-L\}^+}^-$) need to be counted towards the number of empty batteries in (3.26) and (3.29). Equation (3.31) and (3.32) define the transition functions for PHEV inventory Y_h^- (fully charged batteries ready to be discharged to send power back to the grid), where $z_{\{h-L\}^+}^+$ represents the PHEVs whose charging cycle completes at time h. Equation (3.33) and (3.34) define the decentralized discharging policy as opposed to the centralized charging, ensuring that either all or none of the vehicles will be discharged

at any time. Equation (3.35) and (3.36) enforce that at and after time $H-2\times L+2$, no PHEVs are discharged, otherwise its charging cycle cannot be finished by the end of a day.

3.2.2 An approximate dynamic programming formulation

For stochastic cases, an approximate dynamic programming-based algorithm is designed to find a near-optimal policy for making decisions. We assume linear approximation for the value function around a post-decision PHEV backlog $y_h^{+,x}$ and that around a post-decision PHEV inventory (full batteries) $y_h^{-,x}$, and update associated value function slope approximation $\bar{V}_h^+$ and $\bar{V}_h^-$ using an iterative updating operation. The initial values for all value function gradient approximations are 0. Starting from iteration $n=2$, at each time h, to obtain an optimal charging decision $k_h^{+,n}$ and discharging decision $k_h^{-,n}$, given a specific state S_h^n, we solve ISO's hour-ahead economic dispatch problem with charging and discharging decisions made by individual consumers as a mixed integer linear programming problem. Since the exact value function of being in post-decision state $y_h^{+,x}$ and $y_h^{-,x}$ is unknown, the value function slope approximation computed in the previous iteration $n-1$, $\bar{V}_h^{+,n-1}$ and $\bar{V}_h^{-,n-1}$, are used to make decisions. The objective of the MILP is given as follows

$$\max_{x_h} \quad \left\{-C_h^{disp}\left(S_h^n,\, x_h\right)+\bar{V}_h^{+,n-1}\times y_h^{+,x}+\bar{V}_h^{-,n-1}\times y_h^{-,x}\right\}, \tag{3.38}$$

subject to the following constraints:

$$\sum_{j=1}^{J} g_{hj}+w_h+q_h = D_h+D_h^0+CP\times z_h^+ + \sum_{l=1}^{L} CP\times z_{\{h-l\}_{>0}}^{+,n}-CP\times z_h^- - \sum_{l=1}^{L} CP\times z_{\{h-l\}_{>0}}^{-,n}, \quad 1\le h\le H; \tag{3.39}$$

$$y_h^{+,x} = Y_h^{+,n}+\overline{\lambda}_h+z_{\{h-L\}_{>0}}^{-,n}-z_h^+, \qquad 1\le h\le H-1; \tag{3.40}$$

$$y_h^{-,x} = Y_h^{-,n}+z_{\{h-L\}_{>0}}^{+,n}-z_h^-, \qquad 1\le h\le H-1; \tag{3.41}$$

$$z_h^+ \leq bigM \times k_h^+, \qquad 1 \leq h \leq H-L; \tag{3.42}$$

$$y_h^{+,x} \leq bigM \times \left(1 - k_h^+\right), \qquad 1 \leq h \leq H-L; \tag{3.43}$$

$$z_h^- \leq bigM \times k_h^-, \qquad 1 \leq h \leq H - 2 \times L + 1; \tag{3.44}$$

$$y_h^{-,x} \leq bigM \times \left(1 - k_h^-\right), \qquad 1 \leq h \leq H - 2 \times L + 1; \tag{3.45}$$

$$z_h^+ = Y_h^{+,n} + \overline{\lambda}_h + z_{\{h-L\}>0}^{-,n}, \qquad H-L+1 \leq h \leq H; \tag{3.46}$$

$$k_h^+ = 1, \qquad H-L+1 \leq h \leq H; \tag{3.47}$$

$$z_h^- = 0, \qquad H - 2 \times L + 2 \leq h \leq H; \tag{3.48}$$

$$k_h^- = 0, \qquad H - 2 \times L + 2 \leq h \leq H; \tag{3.49}$$

capacity constraints: (3.9) and (3.10);

$$k_h^+,\, k_h^- \in \{0,\, 1\};\; q_h,\, z_h^+,\, Y_h^+,\, z_h^-,\, Y_h^- \geq 0. \tag{3.50}$$

It is important to recognize that solving the above MILP is equivalent to solving four linear programs, by setting $\left(k_h^+,\, k_h^-\right)$ to be equal to $(0,0)$, $(0,1)$, $(1,0)$ or $(1,1)$ and finding the solution which yields the greatest objective value.

Once an optimal charging decision $k_h^{+,n}$ and an optimal discharging decision $k_h^{-,n}$ are determined, and a particular realization of new information on the number of new PHEV arrivals at time h, λ_h^n, becomes available to the system, the following post-decision transition functions are used to move forward to the next pre-decision states at time $h+1$:

1) the post-decision transition function for empty batteries plugged in and waiting to be charged $Y_{h+1}^{+,n}$, written as

$$Y_{h+1}^{+,n} = \begin{cases} Y_h^{+,n} + z_{\{h-L\}>0}^{-,n} + \lambda_h^n & \text{if } k_h^{+,n} = 0; \\ 0 & \text{if } k_h^{+,n} = 1; \end{cases}$$

2) the post-decision transition function for fully charged batteries ready to be discharged $Y_{h+1}^{-,n}$, given by

$$Y_{h+1}^{-,n} = \begin{cases} Y_h^{-,n} + z_{\{h-L\}>0}^{+,n} & \text{if } k_h^{-,n} = 0; \\ 0 & \text{if } k_h^{-,n} = 1. \end{cases}$$

where $z^{-,n}_{\{h-L\}_{>0}}$ represents the number of new discharging completions at time h, and $z^{+}_{\{h-L\}_{>0}}$ denotes the number of new charging completions at time h.

Our algorithm proceeds till the end of a day to finish iteration n. At the end of the iteration, for each time h, we solve a real-time economic dispatch to obtain a new estimate of the wholesale electricity price, p^n_h, and use it to update the wholesale electricity price approximation. The best estimates for wholesale electricity prices calculated so far, P^n_h, $1 \leq h \leq H$, are then used to obtain a new estimate of marginal value of increasing the post-decision PHEV backlog by one unit, $v^{+,n}_h$, and a new estimate of marginal value of increasing the post-decision PHEV inventory by one unit, $v^{-,n}_h$. Using $v^{+,n}_h$ and $v^{-,n}_h$, we update the post-decision states' value function gradient approximations to obtain their best estimate so far, $\bar{V}^{+,n}_h$ and $\bar{V}^{-,n}_h$. The same procedure is repeated for a number of iterations to return a good policy. The details on how to obtain $\bar{V}^{+,n}_h$ and $\bar{P}^n_h$ are the same as that presented in Section 2.3. In the rest of this section, we will explain how to generate a new estimate of marginal value of increasing the post-decision PHEV inventory at time h by one unit, $v^{-,n}_h$, and use it to update the value function slope approximation.

Figure 3.1 illustrates how we obtain a new estimate of marginal value of increasing fully charged batteries at time h, $y^{-,x}_h$, by one unit (in thousand), given wholesale electricity price approximations: $\bar{P}^n_\tau$, $1 \leq \tau \leq H$. If we discharge one more unit of batteries at time h, post-decision PHEV inventory $y^{-,x}_h$ will decrease by one unit. By doing this, two things will happen in the future hours. First, for the following $L-1$ hours, CP [kW] of electricity generation would be provided by discharging the PHEVs. CP represents the discharging power rate. The associated savings on electricity generation costs are equal to

$$\sum_{\tau=h+1}^{h+L-1} CP \times \bar{P}^n_\tau, \tag{3.51}$$

which can be rewritten as (by letting $\tau = h + l - 1$)

$$\sum_{l=2}^{L} CP \times \bar{P}^n_{h+l-1}. \tag{3.52}$$

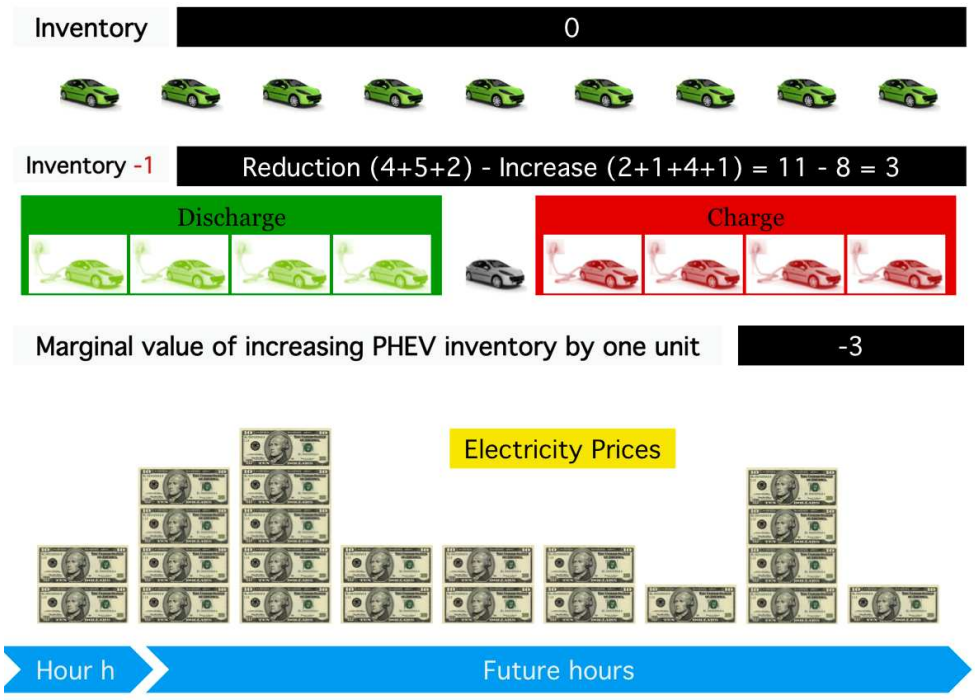

Fig. 3.1. Illustrating how to generation a new estimate of marginal value of increasing PHEV inventory by one unit, given wholesale electricity price approximations

Note that the one unit of batteries would become empty at time $h + L$. The second thing that will happen to the following hours is that we would need to recharge it to its full electricity capacity (at the lowest costs), since it is assumed that all PHEVs need to be fully charged by the end of a daily cycle. The lowest costs to recharge the one unit of batteries can be computed by solving a trivial optimization problem of finding the optimal charging start time to minimize the associated electricity costs in a full charging cycle that lasts for L hours. The optimization problem can be written as follows

$$\min_{h+L\leq\tau\leq H-L+1} \sum_{l=1}^{L} CP \times \bar{P}^{n}_{\tau+l-1}. \tag{3.53}$$

The marginal value of decreasing fully charged batteries by one unit can be estimated by the net reduction on electricity generation costs expected to make, according to

$$\sum_{l=2}^{L} CP \times \bar{P}^{n}_{h+l-1} - \min_{h+L\leq\tau\leq H-L+1} \sum_{l=1}^{L} CP \times \bar{P}^{n}_{\tau+l-1}. \tag{3.54}$$

The marginal value of increasing $y_h^{-,x}$ by one unit, $v_h^{-,n}$, can be estimated using exactly the opposite of what is calculated in (3.54), written as

$$v_h^{-,n} = \min_{h+L\leq\tau\leq H-L+1} \sum_{l=1}^{L} CP \times \bar{P}^{n}_{\tau+l-1} - \sum_{l=2}^{L} CP \times \bar{P}^{n}_{h+l-1}. \tag{3.55}$$

From (3.55) we can see that when electricity price in the immediate future is low, gains from increasing fully charged batteries (or storage resources) will be relatively large, meaning that more vehicles should be charged to store energy when electricity price is low and sell it back to the grid later when electricity price is relatively high.

By far we have presented our approximate dynamic programming-based models and algorithms for three PHEV charging scenarios. The numerical results for these three schemes will be presented and analyzed in the next section.

3.3 Comparing PHEV Charging Policies

We optimize PHEV charging under three different charging scenarios: a centralized charging scenario coordinated by the system operator, and two decentralized charging scenarios in which charging decisions are made by PHEV owners. The centralized charging scenario, referred to as the "ISO" scenario, is discussed in Chapter 2. Two decentralized charging scenarios under real-time pricing are detailed in Section 3.1 and 3.2, which are referred to as the "EMC" scenario and the "V2G" scenario, respectively, depending on whether V2G is adopted. Both decentralized charging scenarios assume that EMCs automate charging (and discharging with V2G) decisions in response to hourly-updated wholesale electricity prices. These three charging schemes will be compared with the current flat rate tariff. Under flat rate structure, we assume that PHEV owners charge their vehicle immediately after they return home from the

last trip of a day and connect their vehicle to the grid. This charging policy is referred to as the "Flat" scenario. The "Flat" scenario represents our current system (or the business-as-usual case) in which consumers have no incentive to shift their PHEV charging load. On the contrary, the "ISO" scenario is an ideal case in terms of strategically shifting charging consumption in order to minimize electricity generation costs. Although centralized charging could be unrealistic to implement (since it requires that the system operator tracks every PHEV in the system), it provides an important benchmark by which the two decentralized charging scenarios, namely "EMC" and "V2G" are evaluated. Note that all findings to be presented in the rest of the section are specific to the given input dataset that we are using.

Figure 3.2 summarizes the system demand (including electricity consumption for PHEV charging) in a day for the four charging scenarios. Excluding PHEV charging, as shown earlier, the system consumes the greatest amount of electricity in late afternoon, when wind availability happens to be in its lowest. After midnight system electricity demand gradually falls to its lowest points; meanwhile wind speed grows to its highest. Under this setup, it is clear that the "Flat" scenario (bold solid line) significantly increases peak hour demand; while the centralized charging scheme (bold dashed line) strategically shifts electricity consumption of PHEV charging and flattens the overall load profile. The figure also shows that both decentralized charging policies will be able to move PHEV charging load to late night hours to exploit lower electricity price. However, for the "EMC" charging (without V2G), charging between 5 pm and 1 am is completely delayed and released at 2 am at the same time, thereby creating a "rebound" peak (solid light line). In contrast, the "V2G" scheme (dashed light line) presents no such rebound effects and is able to closely approximate the centralized charging policy. Moreover, similar observations can be made based on the daily wholesale electricity price profiles under different charging scenarios, summarized in Figure 3.3.

The extent to which an increasing adoption of PHEVs will impact power generation costs, generator emissions, and consumers' electric payment are summarized

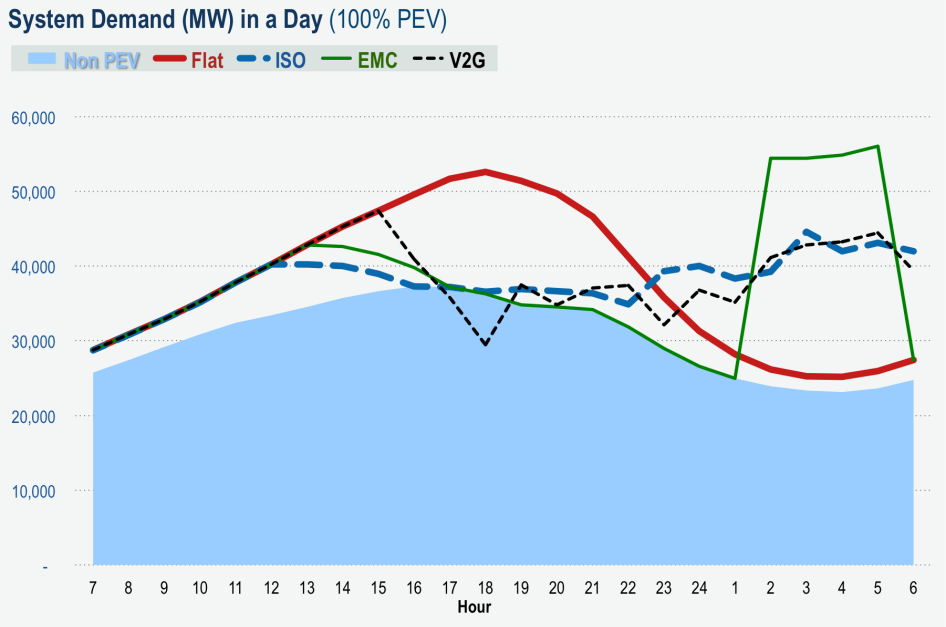

Fig. 3.2. System demand profile in a day under four charging scenarios

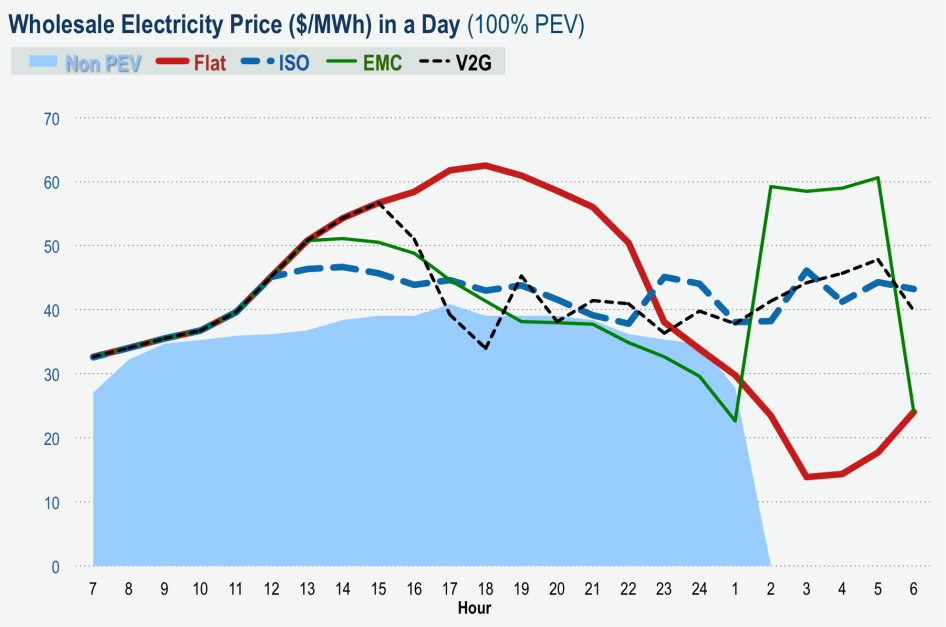

Fig. 3.3. Wholesale electricity price profile in a day under four charging scenarios

in Figure 3.4, 3.5, and 3.6, respectively. It is clear that the flat rate scheme (bold solid line) is the worst in terms of all three measures; while the centralized "ISO"

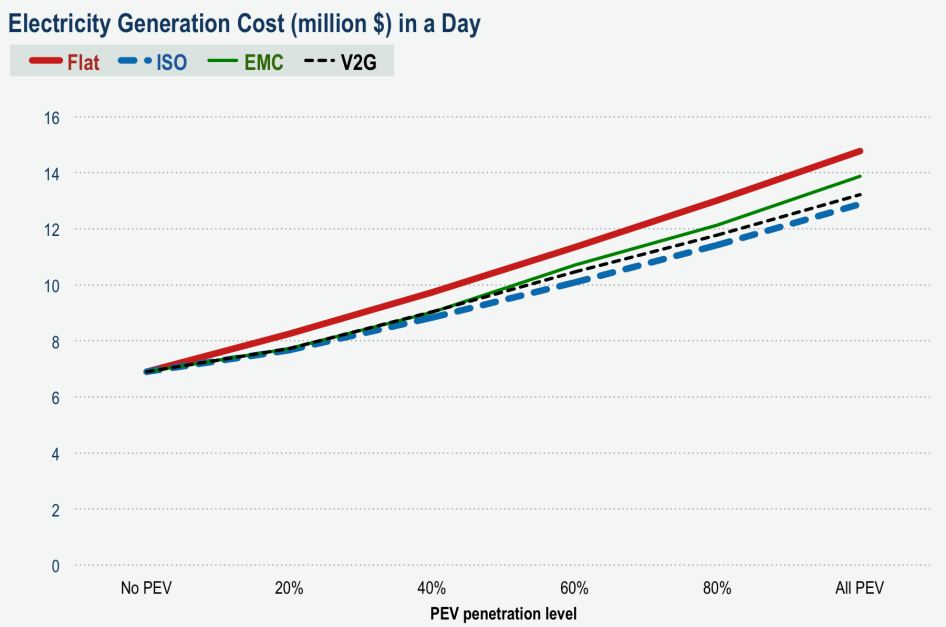

Fig. 3.4. Generation costs in a day for four charging scenarios and five PHEV penetration levels

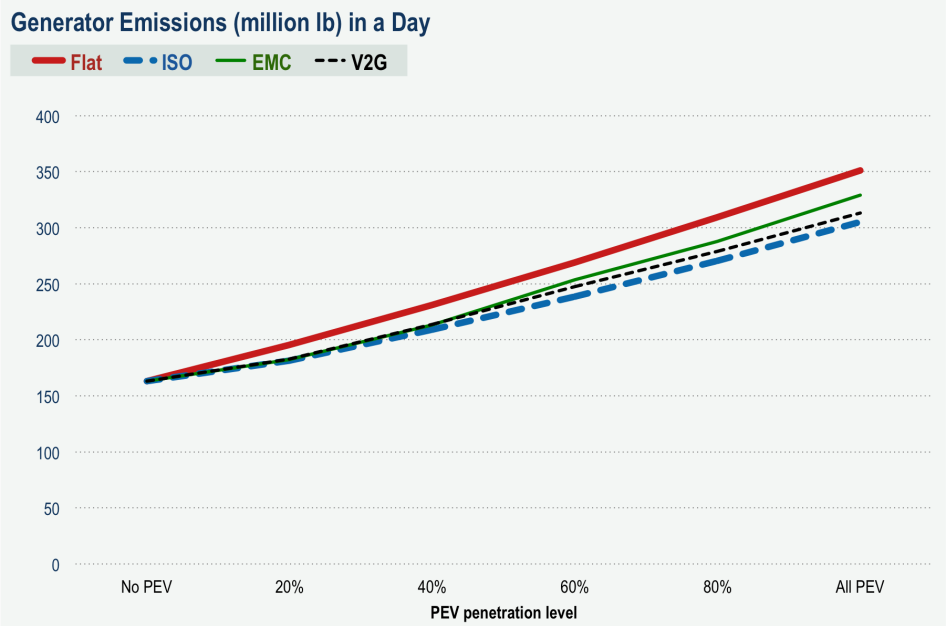

Fig. 3.5. Generator emissions in a day for four charging scenarios and five PHEV penetration levels

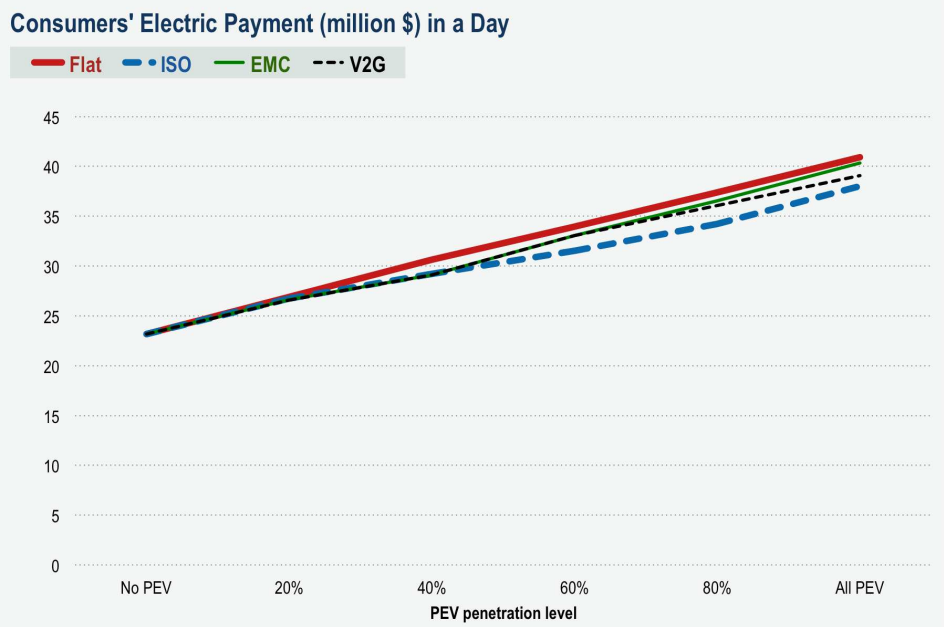

Fig. 3.6. Consumers' electric payment in a day for four charging scenarios and five PHEV penetration levels

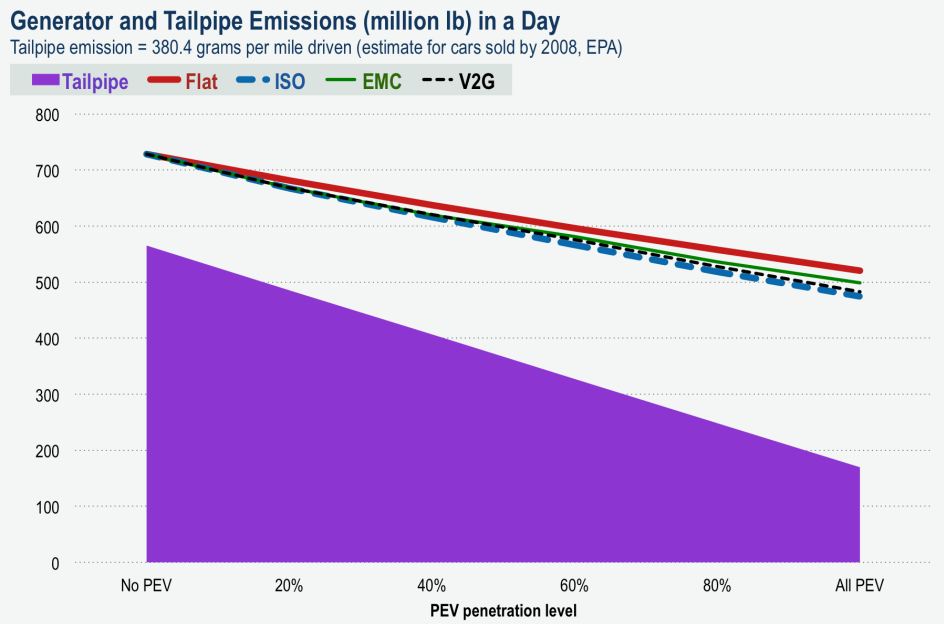

Fig. 3.7. Generator and tailpipe emissions in a day, assuming a high tailpipe emission rate

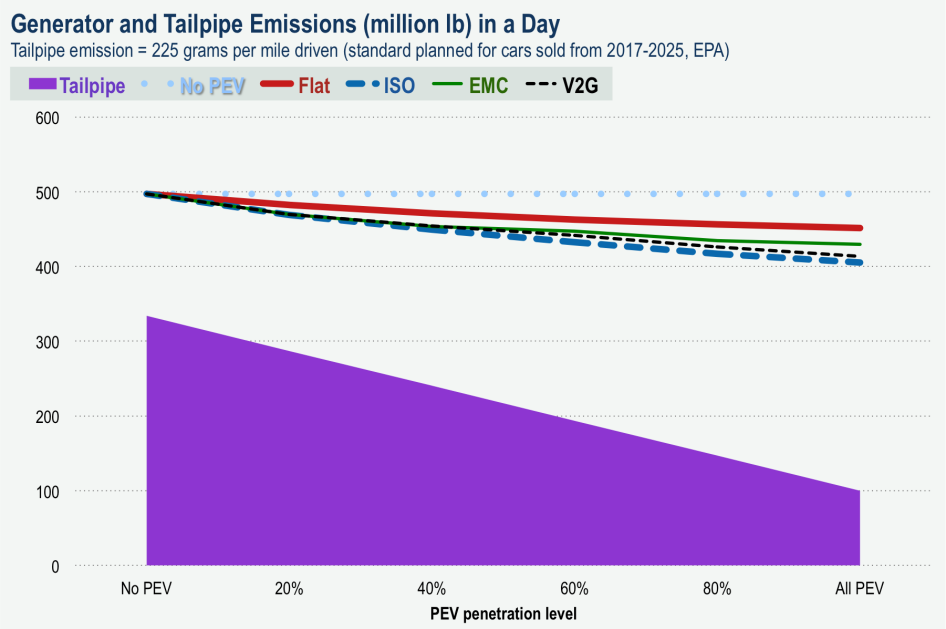

Fig. 3.8. Generator and tailpipe emissions in a day, assuming a low tailpipe emission rate

scenario (bold dashed line) is the best in those measures. The reduction in system costs would be more significant if other household appliances such as air conditioner are considered. It can be observed that the "V2G" scenario is consistently better than the "EMC" scenario in all three measures.

Figure 3.7 and 3.8 summarize environmental impacts of an increasing adoption of PHEVs under various charging schemes. We consider emission sources from both tailpipes (the dark area) and generators (difference between lines and the area). The lines represent the total emissions from both tailpipe and generator sources with respect to different PHEV penetration levels under various charging policies. Tailpipe emissions are direct vehicle emissions due to gasoline combustion. It is important to recognize that environmental competitiveness of PHEVs compared with traditional gasoline cars depends on averaged tailpipe emission of a gasoline passenger car. Considering that, we use two different rates for gasoline emission: 380.6 grams per mile driven (in which 97% comes from CO2) according to estimates for cars sold by 2008

modeled by EPA [100], and 225 grams per mile driven planned by EPA for new cars to be sold from 2017 to 2025 [101]. It shows that there is a dramatic reduction in new gasoline passenger car emissions mandated by the new EPA standard. With the current car emission standard (Figure 3.7), the reduction in tailpipe emissions would greatly outweigh the increase on generator emissions regardless of PHEV charging policy. Therefore, total emissions decrease dramatically as PHEV penetration level increases for all four charging scenarios. On the contrary, under the tightened emission standard for new cars (Figure 3.8), PHEV charging policy will play a more crucial role on increasing net emission reduction, which is equal to tailpipe emission reduction minus generator emission increase (shown as the difference between solid lines and the dotted line). The net emission reduction associated with the "ISO" charging policy consistently double that of the flat rate case.

4. RESOURCE PLANNING WITH REAL-TIME PRICING

So far we have compared various PHEV charging policies under different tariffs to quantify the benefits of real-time pricing on short-term power operations. As mentioned earlier, real-time pricing will impact the electric power system in the long run in at least two aspects. The first one is that the lack of real-time pricing in a long run will lead to wasteful investments on generating capacity in order to satisfy higher peak demand. The second one is that real-time pricing allows consumers to response to electricity market conditions including wind availability and charge their plug-in hybrid electric vehicle when wind energy is abundant, thus making wind resources more cost-efficient in the long run. To quantify the potential long-term benefits of real-time pricing, in this chapter, we will extend the scope to include generating resource investment decisions. From a modeling perspective, it is quite challenging to solve an optimization problem that involves different levels of decision granularity, handles uncertainty, and links different time periods together. To deal with the computational difficulties, the approximate dynamic programming-based modeling and algorithm framework is extended to examine the impacts of real-time pricing on capacity investments.

We begin with an outline of the long-term energy system model in Section 4.1, followed by both a deterministic optimization formulation based on linear programming in Section 4.2 and a stochastic optimization formulation based on approximate dynamic programming in Section 4.3. Finally, Section 4.4 compares different charging policies and discusses their economic and environmental effects on the long-term energy system.

4.1 Outline of the Long-Term Energy System Model

In the long-term energy model, decisions are made at two different time scales. The investment decisions on resources such as wind and natural gas are made by a system operator once every year. The acquired capacity is assumed to be effective starting from the next year. In practice, an investment may take several years before it comes online. If we wish to capture multi-year delays, an instance of a lagged asset acquisition problem is created. Information on how to address this issue in an ADP setting can be found in Powell 2011 [76]. For the remainder of the year, economic dispatch problems are solved by the system operator on an hourly basis to determine how much energy to produce from each power plant to satisfy system demand as well as how many PHEVs to charge and discharge.

The total planning horizon is assumed to be 20 years. Let $t \in \{1, \ldots, T\}$ denote years from 2011 to 2030, $m \in \{1, \ldots, M\}$ represent months within a year, $h \in \{1, \ldots, H\}$ denote hours within a day, and $i \in \{1, \ldots, I\}$ represent energy resources that can be procured over the two decades. We assume that there are two energy resources to be invested: wind and natural gas. Let $i = 1$ represent wind, and $i = 2$ denote natural gas. The decision variables at time (t, m, h), represented by x_{tmh}, include annual investment decisions and hourly energy dispatch and PHEV charge (and discharge) decisions. The annual decision variable at year t is given by

r_{ti} [MW] incremental capacity of resource i installed at year t.

The hourly energy dispatch and vehicle charging and discharging decisions are the same as those defined for the short-term energy model. To avoid repetitive presentation, we will only present the complete formulation for the resource planning model with centralized PHEV charging. The numerical results for resource planning under different charging schemes will be discussed in the end of this chapter. With cen-

tralized charging, the system operator's hourly decision variables at time (t, m, h) are defined as follows

g_{tmhj}	[MW]	power dispatched from power plant j at time (t, m, h),
e_{tmhi}	[MW]	power dispatched from resource i at time (t, m, h),
q_{tmh}	[MW]	lost load at time (t, m, h),
z^{+}_{tmh}	[thousand]	number of PHEVs to charge at time (t, m, h).

While for existing natural gas resources, we optimize power output from each individual power plant; for new natural gas resources acquired at time (t, m, h), its aggregated output is represented by one decision variable, $e_{tmh,2}$.

The state variables at time (t, m, h), denoted as S_{tmh}, represent the information available for making a decision at time (t, m, h). In this study, the state variables include information on capacity investment, system demand, PHEV charging, wind energy, and generation characteristics. The state variables at time (t, m, h) are listed as follows

R_{ti}	[MW]	accumulated capacity of resource i at year t;
CC_i	[$/MW/yr]	annualized capital cost of resource i;
RPS_t	[100%]	renewable energy mandate at year t;
D_{tmh}	[MW]	system electricity demand at time (t, m, h);
Y^{+}_{tmh}	[thousand]	number of PHEVs plugged in at time (t, m, h);
$\overline{\lambda}_{tmh}$	[thousand]	expected number of new PHEVs at time (t, m, h);
CP	[kW]	PHEV battery charge power (e.g. 3.3 kW);
$\overline{\beta}_{tmh}$	[100%]	expected wind availability factor at time (t, m, h);
NGP	[$/MMBtu]	natural gas price at year t (e.g. 5 $/MMBtu);
G_j	[MW]	maximum power output from power plant j;
HR_j	[MMBtu/MWh]	heat rate of power plant j;

$FUEL_j$	[\$/MWh]	variable fuel cost of power plant j, $FUEL_j = NGP \times HR_j$;
ER_j	[lb/MWh]	emission rate of power plant j;
$VOLL$	[\$/MWh]	value of lost load (e.g. 2000 \$/MWh).

We use ω_{tmh} to represent the vector of random information that occurs at time (t, m, h), including new PHEV arrivals and wind availability. The random exogenous information at time (t, m, h) consists of

λ_{tmh}	[thousand]	number of new PHEVs plugged in at time (t, m, h),
β_{tmh}	[100%]	wind availability factor at time (t, m, h).

The transition function governs how the system evolves with time. The system state may change in different time scales. In this study, resource investment states change once a year, when new wind and natural gas capacities are added to the system at year t and become effective starting from the next year $t+1$. The transition function used to move the accumulated capacity of resource i at year t to the next year $t+1$ would be written as

$$R_{t+1,i} = R_{ti} + r_{ti}, \qquad 1 \leq t \leq T-1,\ 1 \leq i \leq I. \tag{4.1}$$

The PHEV charging state changes on an hourly basis, as considered in the short-term energy model. The PHEV backlog at hour (t, m, h), Y^+_{tmh}, migrates to the next hour $(t, m, h+1)$ according to the following transition function

$$Y^+_{tm,h+1} = Y^+_{tmh} + \lambda_{tmh} - z^+_{tmh}, \qquad 1 \leq t \leq T,\ 1 \leq m \leq M,\ 2 \leq h \leq H. \tag{4.2}$$

Equation (4.2) states that the new backlog at hour $(t, m, h+1)$ depends on the backlog at previous hour h, Y^+_{tmh}, new vehicles plugged in at time (t, m, h), λ_{tmh}, and number of vehicles to be charged at time (t, m, h), z^+_{tmh}.

The cost function at time (t, m, h), denoted as C_{tmh}, measures system costs incurred at time h. In the long-term energy model, system costs at time (t, m, h) consist of capacity investment costs incurred annually and electricity generation costs

incurred on an hourly basis. The equation used to compute capacity investment costs at year t, denoted as C_t^{cap}, is given as follows:

$$C_t^{cap} = \sum_{i=1}^{I} \left(CC_i \times \sum_{\tau=1}^{t-1} r_{\tau,i} \right), \qquad 1 \leq t \leq T, \tag{4.3}$$

where CC_i is the annualized capital cost[1] [\$/MW/yr] for resource i. Note that the incremental capacity procured at year t, r_{ti}, is assumed to be effective at and after year $t+1$. The equation used to calculate electricity generation costs at hour (t, m, h), referred to as C_{tmh}^{disp}, is written as

$$C_{tmh}^{disp} = \sum_{j=1}^{J} FUEL_j \times g_{tmhj} + FUEL^{ng} \times e_{tmh,2} + VOLL \times q_{tmh}, \tag{4.4}$$

where $FUEL^{ng}$ represents variable fuel cost[2] [\$/MWh] for new natural gas energy. Fuel cost for wind energy is zero.

4.2 A Deterministic Linear Programming Formulation

Assuming that exogenous information is deterministic, we can formulate ISO's long-term resource planning model with centralized charging as a single (albeit very large) deterministic linear program. The objective is to minimize the costs of procuing new capacities and generating electricity to meed system demand over the entire planning horizon, written as

$$\min \quad \sum_{t=1}^{T} C_t^{cap} + \sum_{t=1}^{T} \sum_{m=1}^{M} \left(ND_m \times \sum_{h=1}^{H} C_{tmh}^{disp} \right), \tag{4.5}$$

where ND_m represents the number of days in the mth month of a year. Note that we consider one representive day[3] for every month of each year. In total, $(T \times M \times H) =$

[1]The annualized capital cost for wind or natural gas is defined as its overnight capital costs [\$/MW] divided by its average plant lifetime. For example, overnight capital costs for wind (onshore) is 2,000,000 \$/MW, and, average wind plant lifetime is 20 years [102]. Therefore, the annualized capital cost for wind energy is equal to 100,000 \$/MW/yr. Similarly, the annualized capacity cost for combustion turbine natural gas is equal to $\frac{600{,}000 \text{ \$/MW}}{30 \text{ yr}} = 20,000$ \$/MW/yr

[2]The fuel cost for combustion turbine is assumed to be 50 \$/MWh [102].

[3]Using approximate dyamic programming, variations in exogenous information such as new vehicle arrivals and wind power production across days in a month are captured by multiple sample pathes generated for different iteration.

5760 different hours are modeled in the long-term model. The objective is subject to the following constraints:

$$\sum_{j=1}^{J} g_{tmhj} + \sum_{i=1}^{I} e_{tmhi} + q_{tmh} = D_{tmh} + D^0_{tmh}$$
$$+ \sum_{l=1}^{L} CP \times z^+_{\{tm,h-l+1\}_{h-l+1>0}}, \quad 1 \le t \le T,\ 1 \le m \le M,\ 1 \le h \le H; \tag{4.6}$$

$$\sum_{m=1}^{M} \left(ND_m \times \sum_{h=1}^{H} e_{tmh,wind} \right) \ge RPS_t \times$$
$$\left\{ \sum_{m=1}^{M} \left[ND_m \times \sum_{h=1}^{H} \left(\sum_{j=1}^{J} g_{tmhj} + \sum_{i=1}^{I} e_{tmhi} + q_{tmh} \right) \right] \right\}, \qquad t = T; \tag{4.7}$$

$$R_{ti} = 0, \qquad t = 1,\ 1 \le i \le I; \tag{4.8}$$

$$R_{t+1,i} = R_{ti} + r_{ti}, \qquad 1 \le t \le T-1,\ 1 \le i \le I; \tag{4.9}$$

$$r_{ti} = 0, \qquad t = T,\ 1 \le i \le I; \tag{4.10}$$

$$Y^+_{tmh} = 0, \qquad 1 \le t \le T,\ 1 \le m \le M,\ h = 1; \tag{4.11}$$

$$Y^+_{tm,h+1} = Y^+_{tmh} + \overline{\lambda}_{tmh} - z^+_{tmh}, \quad 1 \le t \le T,\ 1 \le m \le M,\ 1 \le h \le H-1; \tag{4.12}$$

$$z^+_{tmh} = Y^+_{tmh} + \overline{\lambda}_{tmh}, \qquad 1 \le t \le T,\ 1 \le m \le M,\ H-L+1 \le h \le H; \tag{4.13}$$

$$0 \le g_{tmhj} \le G_j, \qquad 1 \le t \le T,\ 1 \le m \le M,\ 1 \le h \le H,\ 1 \le j \le J; \tag{4.14}$$

$$0 \le e_{tmh,1} \le \overline{\beta}_{tmh} \times R_{t,1}, \qquad 1 \le t \le T,\ 1 \le m \le M,\ 1 \le h \le H; \tag{4.15}$$

$$0 \le e_{tmh,2} \le R_{t,2}, \qquad 1 \le t \le T,\ 1 \le m \le M,\ 1 \le h \le H; \tag{4.16}$$

$$r_{ti} \ge 0, \qquad 1 \le t \le T,\ 1 \le i \le I; \tag{4.17}$$

$$z^+_{tmh},\ Y^+_{tmh} \ge 0, \qquad 1 \le t \le T,\ 1 \le m \le M,\ 1 \le h \le H. \tag{4.18}$$

Equation (4.6) is the power balance constraint for time (t, m, h). Equation (4.7) is the renewable mandate constraint used to ensure that environmental requirement is met at the end of the planning horizon. For example, California's Renewable Portfolio Standard requires that 33% of electricity will be provided by renewables such as wind by year 2030. That is, $RPS_T = 33\%$. Equation (4.8) - (4.10) are transition functions for resource investments. Equation (4.13) is the PHEV charging due time constraint.

Equation (4.14) - (4.16) are capacity constraints for existing power plants, wind, and new natural gas resources, respectively. In (4.15) and (4.16), power dispatched from wind or new natural gas resources at time (t, m, h) is constrained by available capacity for the corresponding resource at year t.

Finding a solution to the above deterministic problem requires solving a linear program with approximately $T \times M \times H \times J$ decision variables, where T, M, H, and J represent the number of years within the planning horizon, months within a year, hours within a day, and individual power plants, respectively. It is difficult to handle stochasticity using linear programming, since it tries to optimize all decisions variables together, and, the computational time required grows exponentially with the number of decision variables. Suppose we model uncertainty using a number of scenarios/sample-pathes, and use N to represent the total number of scenarios. The linear programming version of the long-term resource planning problem would have approximately $T \times M \times H \times J \times N$ decision variables and easily becomes too large to solve. To deal with the computational challenge, in the next section, we present an approximate dynamic programming-based framework for the large-scale, multi-scale, dynamic, and stochastic resource planning problem.

4.3 An Approximate Dynamic Programming Formulation

The ADP algorithm for the long-term energy model with centralized charging is different from the one for the short-term energy model in two important aspects. The first difference is that energy dispatch is solved at each hour h of a day in every month m and every year t since the optimization horizon is T years instead of one day. The other difference is that at the beginning of year t, a capacity expansion problem is solved to make resource investment decisions. For the value function of the investment state at year $t+1$, referred to as V_{t+1}, a separable, piece-wise linear approximation is used. Let $\bar{V}_{t+1,i}\left(R_{t+1,i}\right)$ denote a piece-wise linear approximation

of the value function for state $R_{t+1,i}$. V_{t+1} is defined as the sum of value function approximations for all resources, given by

$$V_{t+1} \approx \sum_{i=1}^{I} \bar{V}_{t+1,i}\left(R_{t+1,i}\right), \qquad 1 \leq t \leq T-1. \tag{4.19}$$

We assume that $\bar{V}_{t+1,i}$ is piece-wise linear in $R_{t+1,i}$. Let $b \in \{1, \ldots, B\}$ denote the indexes for segments of a value function approximation, and $Q_{t+1,ib}$ and $Q_{t+1,i,b+1}$ represent the lower and upper bound of $R_{t+1,i}$ for segment b, respectively. Hence, $Q_{t+1,i1} < Q_{t+1,i2} < \cdots < Q_{t+1,i,B+1}$. Let $\bar{V}_{t+1,ib}$ denote approximation of marginal value of increasing $R_{t+1,i}$ by one unit, when $Q_{t+1,ib} \leq R_{t+1,i} < Q_{t+1,i,b+1}$, $1 \leq b \leq B$. It is assumed that the slopes of a piece-wise value function are monotonically decreasing in $R_{t+1,i}$ because of law of diminishing marginal returns. That is, $\bar{V}_{t+1,i1} \geq \bar{V}_{t+1,i2} \geq \cdots \geq \bar{V}_{t+1,iB}$, $1 \leq b \leq B$. Given that $R_{t+1,i}$ falls in segment $b^\star$, the piece-wise linear approximation of being in state $R_{t+1,i}$, would be written as

$$\bar{V}_{t+1,i}\left(R_{t+1,i}\right) = \sum_{b=1}^{B} \bar{V}_{t+1,ib} \times q_{t+1,ib}; \tag{4.20}$$

$$q_{t+1,ib} = Q_{t+1,i,b+1} - Q_{t+1,ib}, \qquad b < b^\star; \tag{4.21}$$

$$q_{t+1,ib} = R_{t+1,i} - Q_{t+1,ib}, \qquad b = b^\star; \tag{4.22}$$

$$q_{t+1,ib} = 0, \qquad b > b^\star. \tag{4.23}$$

In the rest of this section, we will discuss how to make resource investment decisions using value function slope approximations, and how to update these approximations iteratively.

Starting from iteration $n = 2$, at year t, in a specific state of resource investment R^n_{ti}, it is to be decided how much new wind and natural gas capacity to install at year t, r^n_{ti}. Since the exact value for being in state $R_{t+1,i}$ is unknown, value function slope approximations calculated in iteration $n-1$, $\bar{V}^{n-1}_{t+1,ib}$, $b \in B$ are used. We solve the annual capacity expansion problem as the following linear program

$$\max_{x_t} \left\{ -C_t^{cap} + \sum_{i=1}^{I} \sum_{b=1}^{B} \bar{V}_{t+1,ib}^{n-1} \times q_{t+1,ib} \right\}, \tag{4.24}$$

$$\text{s.t. } \bar{\beta}_{t+1,mh} \times R_{t+1,1} + R_{t+1,2} = PEAK_{t+1}^{n-1} \quad 1 \le t \le T-1; \tag{4.25}$$

$$R_{ti} = 0, \qquad t = 1,\ 1 \le i \le I; \tag{4.26}$$

$$R_{t+1,i} = R_{ti}^{n} + r_{ti}, \qquad 1 \le t \le T-1,\ 1 \le i \le I; \tag{4.27}$$

$$r_{ti} = 0, \qquad t = T,\ 1 \le i \le I; \tag{4.28}$$

$$\sum_{b=1}^{B} q_{t+1,ib} = R_{t+1,i}, \qquad 1 \le t \le T-1,\ 1 \le i \le I; \tag{4.29}$$

$$0 \le q_{t+1,ib} \le Q_{t+1,i,b+1}^{n-1} - Q_{t+1,ib}^{n-1}, \qquad 1 \le t \le T-1,\ 1 \le i \le I,\ 1 \le b \le B; \tag{4.30}$$

$$r_{ti},\ R_{t+1,i} \ge 0, \qquad 1 \le t \le T-1,\ 1 \le i \le I. \tag{4.31}$$

Equation (4.25) enforce that peak demand of the following year is satisfied by generation including the new added capacity, where $PEAK_{t+1}^{n-1}$ represents the peak demand net the generation from existing power plants at year $t+1$, computed in the previous iteration $n-1$. Equation (4.26) – (4.28) are transition functions for available resources. Equation (4.29) and (4.30) define segments of piece-wise linear value function approximation.

We need a method to update value function slope approximations $\bar{V}_{t+1,ib}^{n-1}$. Let $v_{t+1,i}^{n}$ denote a new estimate of marginal value of increasing $R_{t+1,i}^{n}$ by one unit. Consider any hour in year at and after $t+1$, (τ, m, h), $t+1 \le \tau \le T$, $1 \le m \le M$, $1 \le h \le H$. Let $\bar{P}_{\tau mh}^{n-1}$ denote the approximation for wholesale electricity price at time (τ, m, h), computed in iteration $n-1$. By increasing accumulated wind capacity at and after year $t+1$, $R_{t+1,1}$, by one unit, $\bar{\beta}_{\tau mh}$ of generation from a marginal power unit at a marginal cost of $\bar{P}_{\tau mh}^{n-1}$ would be saved and provided by wind energy at zero fuel cost. $\bar{P}_{\tau mh}^{n-1}$ represents wind availability at time (τ, m, h). Therefore, the marginal value of

increasing $R_{t+1,1}$ by one unit can be estimated by the sum of savings on electricity generation cost at all future hours together, written as

$$v^n_{t+1,1} = \sum_{\tau=t+1}^{T} \sum_{m=1}^{M} ND_m \times \left(\sum_{h=1}^{H} \bar{\beta}_{\tau mh} \times \bar{P}^{n-1}_{\tau mh} \right), \tag{4.32}$$

where ND_m represents number of days within month m. The same method is used to obtain an estimate of marginal value of increasing accumulated natural gas capacity at and after year $t+1$, $R_{t+1,2}$, by one unit. For hours whose marginal electricity price (approximated by $\bar{P}^{n-1}_{\tau mh}$) is higher than fuel cost of natural gas $FUEL^{ng}$, one unit of generation from a marginal unit will be substituted by natural gas. Therefore, net reduction on electricity generation costs for this particular hour would be equal to $\left(\bar{P}^{n-1}_{\tau mh} - FUEL^{ng}\right)$. For hours with lower marginal electricity price than natural gas fuel cost, an additional unit of natural gas will not bring any cost reduction since it is too expensive to be dispatched to provide electricity. Therefore, marginal value of increasing natural gas capacity by one unit is equal to zero. To summarize, v^n_{t2} would be written as

$$v^n_{t+1,2} = \sum_{\tau=t+1}^{T} \sum_{m=1}^{M} ND_m \times \left[\sum_{h=1}^{H} \max\left(0,\, \bar{P}^{n-1}_{\tau mh} - FUEL^{ng}\right) \right]. \tag{4.33}$$

The standard updating algorithm to update value function slope approximation $\bar{V}^{n-1}_{t+1,i}$ using new estimate $v^n_{t+1,i}$, is written as follows

$$\bar{V}^n_{t+1,i} = (1 - \alpha_{n-1}) \times \bar{V}^{n-1}_{t+1,i} + \alpha_{n-1} \times v^n_{t+1,i}, \tag{4.34}$$

where α_{n-1} represents the step size. After the update, it is quite possible that the updated approximation no longer satisfies the monotonicity property. We implement the leveling algorithm [76] to make sure the slopes are declining in available resource $R_{t+1,i}$. The leveling algorithm can be described as follows

$$\bar{V}^n_{t+1,i}\left(R_{t+1,i}\right) = \begin{cases} (1-\alpha_{n-1}) \times \bar{V}^{n-1}_{t+1,i}\left(R^n_{t+1,i}\right) + \alpha_{n-1} \times v^n_{t+1i}, \\ \quad \text{if } R_{t+1,i} = R^n_{t+1,i}; \\ \max\left\{\bar{V}^{n-1}_{t+1,i}\left(R^n_{t+1,i}\right),\ (1-\alpha_{n-1}) \times \bar{V}^{n-1}_{t+1,i}\left(R^n_{t+1,i}\right) + \alpha_{n-1} \times v^n_{t+1,i}\right\}, \\ \quad \text{if } R_{t+1,i} < R^n_{t+1,i}; \\ \min\left\{\bar{V}^{n-1}_{t+1,i}\left(R^n_{t+1,i}\right),\ (1-\alpha_{n-1}) \times \bar{V}^{n-1}_{t+1,i}\left(R^n_{t+1,i}\right) + \alpha_{n-1} \times v^n_{t+1,i}\right\}, \\ \quad \text{if } R_{t+1,i} > R^n_{t+1,i}. \end{cases}$$

Once a resource investment decision is made at the beginning of a year, we step forward and solve economic dispatch problems on an hourly basis to make power operation and vehicle charging decisions till the last hour of the year to complete iteration n. The algorithm repeats the same procedure for a number of iterations to obtain a good policy (in the form of value function slope approximations) for making decisions.

The same modeling and algorithm framework is adapted to solve the long-term resource planning model with decentralized charging with and without vehicle-to-grid. The only difference in models and algorithms for decentrailized charging compared with centralized charging lies in the details for hourly economic dispatch problems, which are already presented in Section 3.1 and Section 3.2.

4.4 Numerical Results

To examine effects of various PHEV charging policies on long-term resource planning, the proposed approximate dynamic programming-based modeling and algorithm framework is tested on cases based on data available for California. Details on the test system are described in Section 2.4. The algorithm optimizes resource investment decisions once every year over a 20-year horizon (from year 2011 to 2030). Some important assumptions are explained as follows. First, system demand excluding electricity comsumed for PHEV charging is assumed to increase at an annual rate of 2% [14]. Second, we assume that the PHEV penetration rate increases by 5% every

year, and all passenger cars are PHEVs at 2030. Finally, at 2030, 33% of electricity generation is provided by wind energy.

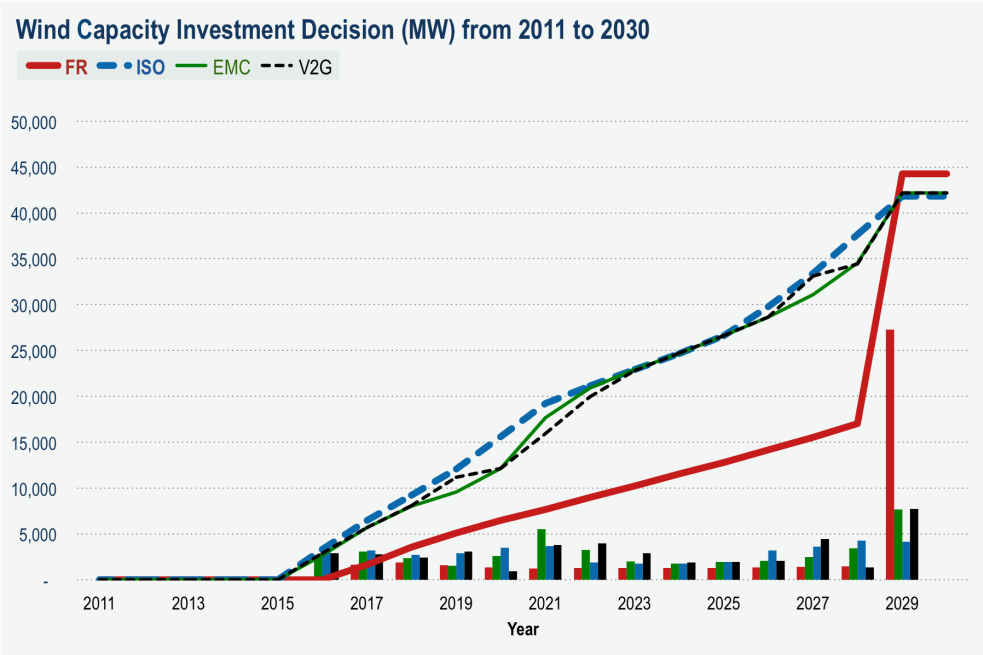

Fig. 4.1. Wind capacity investment decision under different pricing and charging schemes

Figure 4.1 summarizes the optimal resource investment decision over the planning horizon for wind resources, and 4.2 shows that for natural gas resources. The lines represent accumulative capacity at each year under various charging policies ("Flat" in bold solid line, "ISO" in bold dashed line, "EMC" in light solid line, and "V2G" in light dashed line). The bars show incremental capacity installed at each year. There are two important insights that can be drawn based on these two figures. First, charging policy has a great impact on long-term resource investment decision. It is clear that the flat rate structure (the business-as-usual case) will lead to very different resource investment mix than the other three charging scenarios. Under flat rate pricing, majority of wind capacity is added at year 2029 solely to meet the 33% Renewable Portfolio Standards at 2030, and, significant amount of natural gas is needed to meet the increasing demand. With the other three policies, wind energy is more

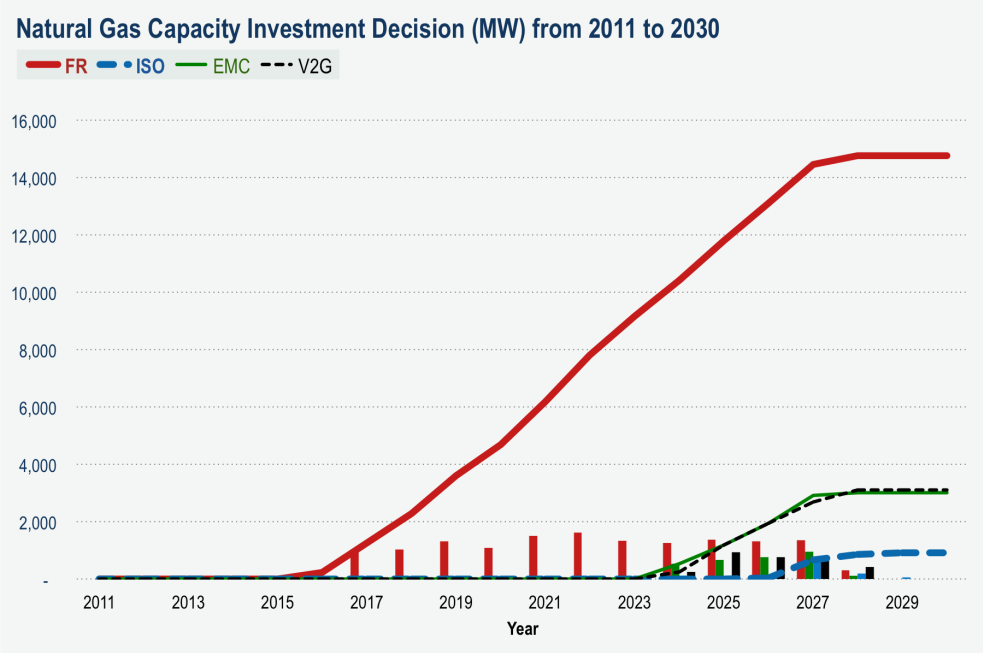

Fig. 4.2. Natural gas capacity investment decision under different pricing and charging schemes

cost-effective than natural gas, and gradually integrated to the system throughtout the planning horizon, although wind energy has much higher capital costs. Under the centralized charging scheme, almost no natural gas is added to the system. To summarize, coordinated PHEV charging is able to significantly increase wind economic effectiveness and help integrate more wind resources into the electric grid, despite of asynchronous effect between wind and demand profiles. The second insight is that there is a close match between the ISO-controlled scheme and decentralized charging (both with and without V2G).

Table 4.1 summarize effects of charging policies on electricity generation costs, consisting of capital costs and power dispatch costs. Note that time value of money is not considered in the calculations for this table. Table 4.2 includes carbon tax costs in the comparison. Carbon tax is considered at a rate of \$15[4] per metric ton of carbon dioxide [104], or \$0.006804 \$/lb. It is obvious that the flat rate structure is the

[4]Multiply by 0.0004536 to convert CO2 in lb to metric tons [103].

Table 4.1
Costs comparison for various charging policies

Item	**Unit**	**Flat**	**ISO**	**EMC**	**V2G**
Capital costs	Billion $	18.2	30.4	29.0	29.1
Dispatch costs	Billion $	113.0	89.1	92.5	92.3
Total costs	Billion $	*131.2*	*119.5*	*121.5*	*121.4*
Reduction compared with flat rate	%		-8.9%	-7.4%	-7.5%
Cost savings per household	$		958	799	803

Table 4.2
Costs comparison for various charging policies (with carbon tax)

Item	**Unit**	**Flat**	**ISO**	**EMC**	**V2G**
Total costs	Billion $	*131.2*	*119.5*	*121.5*	*121.4*
Carbon tax costs	Billion $	17.7	14.4	14.8	14.8
Total costs with carbon tax	Billion $	*148.9*	*133.9*	*136.3*	*136.2*
Reduction compared with flat rate	%		-10.1%	-8.5%	-8.5%
Cost savings per household	$		1,234	1,037	1,041

worst in terms of total electricity generation costs (both with and without carbon tax consideration). The flat rate policy will leads to the lowest capital costs because the system delays the installation of wind resources with high capital costs and replies on operating expensive existing and new natural gas units. Therefore, power dispatch costs and carbon tax costs for the flat rate structure are significantly higher than the rest three charging policies. Benchmarked against the centralized charging scenario, both two decentralized charging cases are able to achieve, to a great extent, what the ISO-controlled policy is capable of.

5. CONCLUSIONS AND FUTURE WORK

In this study, we present an approximate dynamic programming-based modeling and algorithm framework to implement real-time pricing, with smart meters, household energy management devices and controllable appliances such as plug-in hybrid electric vehicles. We show how this framework captures the feedback loop between wholesale electricity prices and consumer electricity usages. By solving the system operator's economic dispatch problem on an hourly basis (even in the long-term resource planning model), wholesale electricity prices are endogenously determined. The computational results based on the data for California demonstrate economic and environmental benefits of real-time pricing as opposed to the current flat rates of electricity, in terms of accommodating plug-in hybrid electric vehicles in the electric grid, and increasing wind energy economic competitiveness in the long run.

This work can be improved in several ways. First, one important aspect of the power system that is neglected in our study is transmission. There are at least two reasons why transmission is relevant in this context. First, one potential benefit of demand participation is to reduce transmission congestions [20]. For example, Parvania and Fotuhi-Firuzabad 2010 [22] integrate incentive-based demand response into the wholesale electricity markets, and argue that demand response alleviates transmission line congestions caused by outage of system components. This alleviation effect could be even more significant when V2G is present in the system to provide storage resources. The second reason is that transmission costs could have great impact on wind investment decisions. One of the challenges in integrating wind resources is that wind resources are usually located far away from large electricity demand centers. To connect these wind resources to the electric grid, the system operator must ensure that existing transmission lines are updated, and new transmission lines are built, if needed. The high capital costs for the required transmission investment will be

reflected in consumers' electricity bill eventually, and thus raising electricity rates. Xiao et al. 2011 [105] determine long-term decisions for wind farm locations and sizes, and observe that transmission constraints affect investment decisions of wind resources. Our model needs to be modified to incorporate transmission networks. Including transmission modeling will expand the decision variable space and add extra transmission related constraints, thus increasing the computational time needed.

The second possible extension is to model the non-convexities of a power generation system. For illustrative purposes, we neglect integer variables such as the on and off status of individual power units, and only consider continuous power generations. However, real-time pricing is believed to be inefficient to properly capture the non-convex startup costs of the power system operations [106]. For example, Sioshansi 2012 [48] examines PHEV charging under various tariffs with the non-convexity modeling, and finds out that RTP performs worse than other electricity tariffs because its generator startup costs are higher. The non-convex startup costs may not have significant impact on the California system studied in this dissertation, since the capacity of coal plants (usually with high startup costs) is less than 1% of the total system capacity. Nevertheless, it is of great interests to include the non-convex nature of the power operations when studying real-time pricing in general, especially for regions where coal generation makes up a significant portion of the total generation, such as ERCOT (33.8% in 2012). From the modeling perspective, adding the non-convexities gives us a unit commitment model [66, 107, 108]. Binary variables are required to model the on and off status of each power plant. Additional constraints for ramping up and down, and minimum on and off times, linking multiple time periods together, will further complicate the calculations. Adding these non-convexity components will naturally impose great burdens on algorithm computations.

Thirdly, either of the above two possible improvements in modeling would require for a faster and more efficient algorithm, especially for the resource planning model. One possible approach is to modify our algorithm to allow for the use of recent advances high performance computing [109]. Our framework has the potential to

implement parallel computing and improve algorithm efficiency. For example, in our algorithm for the long-term planning model, the annual capacity expansion problems are sequential (since the investment decisions at previous years affect the decisions in the upcoming years). However, within every year, representative days for different months are assumed to be independent of each other, and as a result, can be computed in parallel. By doing so, the computational time will be greatly reduced. Note that the hourly economic dispatch problems are sequential.

Finally, in addition to algorithm efficiency, another concern raised when we extend our framework to model a more complex system using approximate dynamic programming is the quality of the solution. We use linear and separable piece-wise linear approximations to update value function approximation in this study. Although we evaluate the approximate dynamic programming solutions benchmarked against the optimal solutions and demonstrate a close match, in general there is no guarantee that linear value function approximation will converge [76]. Jaakkola 1994 [96] provide proofs of convergence to $TD(\lambda)$ algorithm[1] (Sutton 1988 [97]) and Q-learning algorithm[2] (Watkins and Dayan 1992 [98]) used to update value function approximation iteratively. However, implementing these algorithms require extensive matrices calculations. Thus, a tradeoff needs to be found between the quality of the ADP solutions and the computational time.

[1] $TD(\lambda)$ algorithm addresses the problem of learning to predict in a Markov environment, using a temporal difference operator to update the predictions [97].

[2] Q-learning algorithm extended $TD(\lambda)$ algorithm to control problems.

LIST OF REFERENCES

LIST OF REFERENCES

[1] H. Allcott, "Rethinking real-time electricity pricing," *Resource and Energy Economics*, vol. 33, no. 4, pp. 820–842, 2011.

[2] H. Allcott, "Real time pricing and electricity market design," *Working Paper, New York University*, 2012.

[3] S. Borenstein, M. Jaske, and A. Rosenfeld, "Dynamic pricing, advanced metering, and demand response in electricity markets," *University of California Energy Institute*, 2002.

[4] J. Bushnell, B. Hobbs, and F. Wolak, "When it comes to demand response, is FERC its own worst enemy?," *The Electricity Journal*, vol. 22, no. 8, pp. 9–18, 2009.

[5] W. Hogan, "Demand response pricing in organized wholesale markets," *ISO/RTO Council Comments on Demand Response Compensation in Organized Wholesale Energy Markets*, vol. 13, 2010.

[6] Y. Oum, S. Oren, and S. Deng, "Hedging quantity risks with standard power options in a competitive wholesale electricity market," *Naval Research Logistics*, vol. 53, no. 7, pp. 697–712, 2006.

[7] A. Rose, G. Oladosu, and S. Liao, "Business interruption impacts of a terrorist attack on the electric power system of Los Angeles: customer resilience to a total blackout," *Risk Analysis*, vol. 27, no. 3, pp. 513–531, 2007.

[8] Y. Xue, "The was from a simple contingency to system-wide disaster – Lessons from the Eastern Interconnection blackout in 2003," *Automation of Electric Power Systems*, vol. 18, 2003.

[9] S. Chen, S. Song, L. Li, and J. Shen, "Survey on smart grid technology," *Power System Technology*, vol. 33, no. 8, pp. 1–7, 2009.

[10] X. Fang, S. Misra, G. Xue, and D. Yang, "Smart grid – the new and improved power grid: A survey," 2011.

[11] H. Farhangi, "The path of the smart grid," *IEEE Power and Energy Magazine*, vol. 8, no. 1, pp. 18–28, 2010.

[12] J. Kassakian and R. Schmalensee, "The future of the electric grid," *An Interdisciplinary MIT Study*, 2011.

[13] S. Massoud and B. Wollenberg, "Toward a smart grid: Power delivery for the 21st century," *IEEE Power and Energy Magazine*, vol. 3, no. 5, pp. 34–41, 2005.

[14] Federal Energy Regulatory Commission, "A national assessment of demand response potential," 2009.

[15] M. Albadi and E. El-Saadany, "Demand response in electricity markets: An overview," pp. 1–5, 2007.

[16] M. Albadi and E. El-Saadany, "A summary of demand response in electricity markets," *Electric Power Systems Research*, vol. 78, no. 11, pp. 1989–1996, 2008.

[17] P. Cappers, C. Goldman, and D. Kathan, "Demand response in US electricity markets: Empirical evidence," *Energy*, vol. 35, no. 4, pp. 1526–1535, 2010.

[18] J. Torriti, M. Hassan, and M. Leach, "Demand response experience in Europe: Policies, programs and implementation," *Energy*, vol. 35, no. 4, pp. 1575–1583, 2010.

[19] A. Faruqui, R. Hledik, and J. Palmer, "Time-varying and dynamic rate design," *Regulatory Assistance Project*, 2012.

[20] H. Aalami, M. Moghaddam, and G. Yousefi, "Demand response modeling considering interruptible/curtailable loads and capacity market programs," *Applied Energy*, vol. 87, no. 1, pp. 243–250, 2010.

[21] S. Caron and G. Kesidis, "Incentive-based energy consumption scheduling algorithms for the smart grid," *First IEEE International Conference on Smart Grid Communications*, pp. 391–396, 2010.

[22] M. Parvania and M. Fotuhi-Firuzabad, "Demand response scheduling by stochastic SCUC," *IEEE Transactions on Smart Grid*, vol. 1, no. 1, pp. 89–98, 2010.

[23] M. El-Hawary, *Introduction to electrical power systems*, vol. 50. John Wiley & Sons, 2008.

[24] Federal Energy Regulatory Commission, "National action plan on demand response," 2010.

[25] D. Hart, "Using AMI to realize the Smart Grid," *IEEE Power and Energy Society General Meeting-Conversion and Delivery of Electrical Energy in the 21st Century*, pp. 1–2, 2008.

[26] S. Andersen, "Saving the smart grid – Hype, hysteria, and strategic planning," *Public Utilities Fortnightly*, pp. 33–39, January 2011.

[27] C. Ibars, M. Navarro, and L. Giupponi, "Distributed demand management in smart grid with a congestion game," *First IEEE International Conference on Smart Grid Communications*, pp. 495–500, 2010.

[28] A. Mohsenian-Rad, V. Wong, J. Jatskevich, R. Schober, and A. Leon-Garcia, "Autonomous demand-side management based on game-theoretic energy consumption scheduling for the future smart grid," *IEEE Transactions on Smart Grid*, vol. 1, no. 3, pp. 320–331, 2010.

[29] C. Stephan and J. Sullivan, "Environmental and energy implications of plug-in hybrid-electric vehicles," *Environmental Science & Technology*, vol. 42, no. 4, pp. 1185–1190, 2008.

[30] C. Giffi, R. Hill, M. Gardner, and M. Hasegawa, "Gaining traction: A customer view of electric vehicle mass adoption in the US automotive market," *Deloitte Development LLC*, 2010.

[31] S. Hadley and A. Tsvetkova, "Potential impacts of plug-in hybrid electric vehicles on regional power generation," *The Electricity Journal*, vol. 22, no. 10, pp. 56–68, 2009.

[32] K. Clement, E. Haesen, and J. Driesen, "The impact of charging plug-in hybrid electric vehicles on the distribution grid," 2008.

[33] C. Roe, J. Meisel, A. Meliopoulos, F. Evangelos, and T. Overbye, "Power system level impacts of PHEVs," *IEEE International Conference on System Sciences*, pp. 1–10, 2009.

[34] K. Clement, E. Haesen, and J. Driesen, "Coordinated charging of multiple plug-in hybrid electric vehicles in residential distribution grids," pp. 1–7, 2009.

[35] K. Clement, E. Haesen, and J. Driesen, "The impact of charging plug-in hybrid electric vehicles on a residential distribution grid," *IEEE Transactions on Power Systems*, vol. 25, no. 1, pp. 371–380, 2010.

[36] P. Denholm and W. Short, "An evaluation of utility system impacts and benefits of optimally dispatched plug-in hybrid electric vehicles," *National Renewable Energy Laboratory*, 2006.

[37] E. Sortomme, M. Hindi, S. Mac Pherson, and S. Venkata, "Coordinated charging of plug-in hybrid electric vehicles to minimize distribution system losses," *IEEE Transactions on Smart Grid*, vol. 2, no. 1, pp. 198–205, 2011.

[38] G. Kalogridis, C. Efthymiou, S. Denic, T. Lewis, and R. Cepeda, "Privacy for smart meters: Towards undetectable appliance load signatures," pp. 232–237, 2010.

[39] J. Axsen, K. Kurani, R. McCarthy, and C. Yang, "Plug-in hybrid vehicle GHG impacts in California: Integrating consumer-informed recharge profiles with an electricity-dispatch model," *Energy Policy*, vol. 39, no. 3, pp. 1617–1629, 2011.

[40] S. Huang, B. Hodge, F. Taheripour, J. Pekny, G. Reklaitis, and W. Tyner, "The effects of electricity pricing on PHEV competitiveness," *Energy Policy*, vol. 39, no. 3, pp. 1552–1561, 2011.

[41] K. Parks, P. Denholm, and A. Markel, "Costs and emissions associated with plug-in hybrid electric vehicle charging in the Xcel Energy Colorado service territory," *National Renewable Energy Laboratory*, 2007.

[42] A. Conejo, J. Morales, and L. Baringo, "Real-time demand response model," *IEEE Transactions on Smart Grid*, vol. 1, no. 3, pp. 236–242, 2010.

[43] S. Han, S. Han, and K. Sezaki, "Development of an optimal vehicle-to-grid aggregator for frequency regulation," *IEEE Transactions on Smart Grid*, vol. 1, no. 1, pp. 65–72, 2010.

[44] S. Kishore and L. Snyder, "Control mechanisms for residential electricity demand in smart grids," *First IEEE International Conference on Smart Grid Communications*, pp. 443–448, 2010.

[45] K. Valentine, W. Temple, and K. Zhang, "Intelligent electric vehicle charging: Rethinking the valley-fill," *Journal of Power Sources*, vol. 196, no. 24, pp. 10717–10726, 2011.

[46] A. Mohsenian-Rad and A. Leon-Garcia, "Optimal residential load control with price prediction in real-time electricity pricing environments," *IEEE Transactions on Smart Grid*, vol. 1, no. 2, pp. 120–133, 2010.

[47] P. Samadi, A. Mohsenian, R. Schober, V. Wong, and J. Jatskevich, "Optimal real-time pricing algorithm based on utility maximization for smart grid," *First IEEE International Conference on Smart Grid Communications*, pp. 415–420, 2010.

[48] R. Sioshansi, "Modeling the impacts of electricity tariffs on plug-in hybrid electric vehicle charging, costs, and emissions," *Operations Research*, vol. 60, no. 3, pp. 506–516, 2012.

[49] D. Livengood and R. Larson, "The energy box: Locally automated optimal control of residential electricity usage," *INFORMS Service Science*, vol. 1, no. 1, pp. 1–16, 2009.

[50] D. O'Neill, M. Levorato, A. Goldsmith, and U. Mitra, "Residential demand response using reinforcement learning," *First IEEE International Conference on Smart Grid Communications*, pp. 409–414, 2010.

[51] C. Chen, S. Kishore, and L. Snyder, "An innovative RTP-based residential power scheduling scheme for smart grids," *IEEE International Conference on Acoustics, Speech and Signal Processing*, pp. 5956–5959, 2011.

[52] W. Kempton and J. Tomić, "Vehicle-to-grid power fundamentals: Calculating capacity and net revenue," *Journal of Power Sources*, vol. 144, no. 1, pp. 268–279, 2005.

[53] W. Kempton and J. Tomić, "Vehicle-to-grid power implementation: From stabilizing the grid to supporting large-scale renewable energy," *Journal of Power Sources*, vol. 144, no. 1, pp. 280–294, 2005.

[54] A. Saber and G. Venayagamoorthy, "Intelligent unit commitment with vehicle-to-gridA cost-emission optimization," *Journal of Power Sources*, vol. 195, no. 3, pp. 898–911, 2010.

[55] R. Sioshansi and P. Denholm, "Emissions impacts and benefits of plug-in hybrid electric vehicles and vehicle-to-grid services," *Environmental science & technology*, vol. 43, no. 4, pp. 1199–1204, 2009.

[56] E. Sortomme and M. El-Sharkawi, "Optimal charging strategies for unidirectional vehicle-to-grid," *IEEE Transactions on Smart Grid*, vol. 2, no. 1, pp. 131–138, 2011.

[57] California Public Utilities Commission, "33% renewables portfolio standard: Implementation analysis preliminary results," *Technical Analysis by E3 and Aspen Environmental Group*, 2009.

[58] M. Blanco, "The economics of wind energy," *Renewable and Sustainable Energy Reviews*, vol. 13, no. 6, pp. 1372–1382, 2009.

[59] A. Fabbri, T. Romn, J. Abbad, and V. Quezada, "Assessment of the cost associated with wind generation prediction errors in a liberalized electricity market," *IEEE Transactions on Power Systems*, vol. 20, no. 3, pp. 1440–1446, 2005.

[60] B. Hodge and M. Milligan, "Wind power forecasting error distributions over multiple timescales," pp. 1–8, 2011.

[61] F. Bouffard and F. Galiana, "Stochastic security for operations planning with significant wind power generation," pp. 1–11, 2008.

[62] R. Doherty and M. O'Malley, "A new approach to quantify reserve demand in systems with significant installed wind capacity," *IEEE Transactions on Power Systems*, vol. 20, no. 2, pp. 587–595, 2005.

[63] J. Morales, A. Conejo, and J. Pérez-Ruiz, "Economic valuation of reserves in power systems with high penetration of wind power," *IEEE Transactions on Power Systems*, vol. 24, no. 2, pp. 900–910, 2009.

[64] M. Ortega-Vazquez and D. Kirschen, "Estimating the spinning reserve requirements in systems with significant wind power generation penetration," *IEEE Transactions on Power Systems*, vol. 24, no. 1, pp. 114–124, 2009.

[65] J. Wang, M. Shahidehpour, and Z. Li, "Security-constrained unit commitment with volatile wind power generation," *IEEE Transactions on Power Systems*, vol. 23, no. 3, pp. 1319–1327, 2008.

[66] J. Xiao, B. Hodge, J. Pekny, and G. Reklaitis, "Operating reserve policies with high wind power penetration," *Computers & Chemical Engineering*, vol. 35, no. 9, pp. 1876–1885, 2011.

[67] S. Borenstein, "The long-run efficiency of real-time electricity pricing," *Energy Journal*, vol. 26, no. 3, 2005.

[68] C. De Jonghe, B. Hobbs, and R. Belmans, "Integrating short-term demand response into long-term investment planning," 2011.

[69] S. Gabriel, A. Kydes, and P. Whitman, "The National Energy Modeling System: a large-scale energy-economic equilibrium model," *Operations Research*, vol. 49, no. 1, pp. 14–25, 2001.

[70] L. Fishbone and H. Abilock, "Markal, a linear-programming model for energy systems analysis: Technical description of the bnl version," *International journal of Energy research*, vol. 5, no. 4, pp. 353–375, 1981.

[71] S. Stoft, *Power system economics*. IEEE press Piscataway, 2002.

[72] A. Mazer, *Electric power planning for regulated and deregulated markets*. Wiley, 2007.

[73] A. Keane, M. Milligan, C. Dent, B. Hasche, C. D'Annunzio, K. Dragoon, H. Holttinen, N. Samaan, L. Soder, and M. O'Malley, "Capacity value of wind power," *IEEE Transactions on Power Systems*, vol. 26, no. 2, pp. 564–572, 2011.

[74] W. Powell, A. George, H. Simão, W. Scott, A. Lamont, and J. Stewart, "SMART: A stochastic multiscale model for the analysis of energy resources, technology, and policy," *INFORMS Journal on Computing*, vol. 24, no. 4, pp. 665–682, 2012.

[75] R. Bellman, "Dynamic programming and the smoothing problem," *Management Science*, vol. 3, no. 1, pp. 111–113, 1956.

[76] W. B. Powell, *Approximate dynamic programming: Solving the curses of dimensionality*. WILEY, 2nd ed., 2011.

[77] D. Zhang and D. Adelman, "An approximate dynamic programming approach to network revenue management with customer choice," *Transportation Science*, vol. 43, no. 3, pp. 381–394, 2009.

[78] H. P. Simão, J. Day, A. P. George, T. Gifford, J. Nienow, and W. Powell, "An approximate dynamic programming algorithm for large-scale fleet management: A case application," *Transportation Science*, vol. 43, no. 2, pp. 178–197, 2009.

[79] K. Kariuki and R. Allan, "Evaluation of reliability worth and value of lost load," *IEE proceedings-Generation, transmission and distribution*, vol. 143, no. 2, pp. 171–180, 1996.

[80] R. Rosenthal, "GAMS–a user's guide," *ALS-NSCORT*, 2004.

[81] Cplex, ILOG, "11.0 Users manual," *ILOG SA*, 2007.

[82] California ISO, "California ISO Open Access Same-time Information System, http://oasis.caiso.com/."

[83] U.S. Environmental Protection Agency, "Emissions & Generation Resource Integrated Database, http://www.epa.gov/cleanenergy/energy-resources/egrid/index.html."

[84] National Renewable Energy Laboratory, "NREL Wind Integration Datasets, http://www.nrel.gov/electricity/transmission/wind_integration_dataset.html."

[85] J. Hamilton, *Time series analysis*, vol. 2. Cambridge University Press, 1994.

[86] W. Hoeffding and H. Robbins, "The central limit theorem for dependent random variables," *Duke Mathematical Journal*, vol. 15, no. 3, pp. 773–780, 1948.

[87] B. Hodge, S. Huang, J. Siirola, J. Pekny, and G. V. Reklaitis, "A multi-paradigm modeling framework for energy systems simulation and analysis," *Computers & Chemical Engineering*, vol. 35, no. 9, pp. 1725–1737, 2011.

[88] B. Hodge, A. Shukla, S. Huang, G. Reklaitis, V. Venkatasubramanian, and J. Pekny, "Multi-paradigm modeling of the effects of PHEV adoption on electric utility usage levels and emissions," *Industrial & Engineering Chemistry Research*, vol. 50, no. 9, pp. 5191–5203, 2011.

[89] S. Huang, H. Safiullah, J. Xiao, B. Hodge, R. Hoffman, J. Soller, D. Jones, D. Dininger, W. Tyner, and A. Liu, "The effects of electric vehicles on residential households in the city of Indianapolis," *Energy Policy*, 2012.

[90] J. Ma and Y. Pei, "Development and application of TransCAD for urban traffic planning," *Journal of Harbin University of Civil Engineering and Architecture*, 2002.

[91] U.S. Department of Transportation Federal Highway Administration, "2009 national household travel survey user's guide," 2011.

[92] R. Axelrod, *The complexity of cooperation: Agent-based models of competition and collaboration*. Princeton University Press, 1997.

[93] M. Batty, *Cities and complexity: understanding cities with cellular automata, agent-based models, and fractals*. The MIT press, 2007.

[94] E. Bonabeau, "Agent-based modeling: Methods and techniques for simulating human systems," *Proceedings of the National Academy of Sciences of the United States of America*, vol. 99, no. Suppl 3, pp. 7280–7287, 2002.

[95] AnyLogic, *The big book of AnyLogic, http://www.anylogic.com/the-big-book-of-anylogic/*.

[96] T. Jaakkola, M. Jordan, and S. Singh, "On the convergence of stochastic iterative dynamic programming algorithms," *Neural Computation*, vol. 6, no. 6, pp. 1185–1201, 1994.

[97] R. Sutton, "Learning to predict by the methods of temporal differences," *Machine learning*, vol. 3, no. 1, pp. 9–44, 1988.

[98] C. Watkins and P. Dayan, "Q-learning," *Machine learning*, vol. 8, no. 3-4, pp. 279–292, 1992.

[99] J. Birge and F. Louveaux, *Introduction to stochastic programming*. Springer, 2nd ed., 2011.

[100] Office of Transportation and Air Quality, U.S. Environmental Protection Agency, "Average annual emissions and fuel consumption for gasoline-fueled passenger cars and light trucks," 2008.

[101] "EPA and NHTSA set standards to reduce greenhouse gases and improve fuel economy for model years 2017-2025 cars and light trucks," 2012.

[102] R. Tidball, J. Bluestein, N. Rodriguez, and S. Knoke, "Cost and performance assumptions for modeling electricity generation technologies," *Contract*, vol. 303, pp. 275–300, 2010.

[103] U.S. Environmental Protection Agency, "Unit conversions, emissions factors, and other reference data," 2004.

[104] K. Hassett, A. Mathur, and G. Metcalf, "The incidence of a US carbon tax: A lifetime and regional analysis," *National Bureau of Economic Research*, 2007.

[105] J. Xiao, B. Hodge, A. L., J. Pekny, and G. Reklaitis, "Long-term planning of wind farm siting in the electricity grid," *Proceeding for 21st European Symposium on Computer Aided Process Engineering*, 2011.

[106] R. O'Neill, P. Sotkiewicz, B. Hobbs, M. Rothkopf, and J. Stewart, "Efficient market-clearing prices in markets with nonconvexities," *European Journal of Operational Research*, vol. 164, no. 1, pp. 269–285, 2005.

[107] M. Carrión and J. Arroyo, "A computationally efficient mixed-integer linear formulation for the thermal unit commitment problem," *IEEE Transactions on Power Systems*, vol. 21, no. 3, pp. 1371–1378, 2006.

[108] P. Ruiz, C. Philbrick, E. Zak, K. Cheung, and P. Sauer, "Uncertainty management in the unit commitment problem," *IEEE Transactions on Power Systems*, vol. 24, no. 2, pp. 642–651, 2009.

[109] V. Kumar, A. Grama, A. Gupta, and G. Karypis, *Introduction to parallel computing*, vol. 110. Benjamin/Cummings Redwood City, 1994.

APPENDIX

A. MATLAB CODES

The following Matlab codes are associated with the ADP-based algorithm for a system operator's daily economic dispatch problem with centralized charging, which is described in Section 2.3. To avoid repetitive presentation, the Matlab codes of the algorithms for solving the two decentralized charging schemes presented in Section 3.1.2 and 3.2.2, and for solving the long-term resource planning problem described in Section 4.3 are not presented here.

```
clear
load('CADayInput')

N = 200;

Cost_ADP(1:N) = 0;
CDE_ADP(1:N) = 0;
PMT_ADP(1:N) = 0;

D_ADP(1:H, 1:N) = 0;
g_ADP(1:H, 1:N) = 0;
p_ADP(1:H, 1:N) = 0;
zPlus_ADP(1:H, 1:N) = 0;
YPlus_ADP(1:H, 1:N) = 0;

P_ADP(1:H, 1:N) = 0;
vPlus_ADP(1:H, 1:N) = 0;
VPlus_ADP(1:H, 1:N) = 0;

NCol = J + 4;
NRowEq = 2;
NRow = 1;
f(1:NCol) = 0;
lb(1:NCol, 1) = 0;
ub(1:NCol, 1) = 0;
Aeq(1:NRowEq, 1:NCol) = 0;
beq(1:NRowEq, 1) = 0;
A(1:NRow, 1:NCol) = 0;
b(1:NRow, 1) = 0;

g(1,1:J) = 0;
sumCharge(1:H) = 0;

for n = 2:N
    for h = H-L+2:H
        zPlus_ADP(h,n) = U(h,n);
    end
```

```
    for h = 1:H-L
        %% Solve the hour-ahead dispatch problem
        NCol = J + 4; % # of decision variables j) g(h,j), 1) w(h), 2) q(h),
% 3) zPlus(h), 4) yPlusx(h)
        NRowEq = 2; % # of equality constraints
        NRow = 1; % # of inequality constraints
        f(1:NCol) = 0;
        lb(1:NCol, 1) = 0;
        ub(1:NCol, 1) = 0;
        Aeq(1:NRowEq, 1:NCol) = 0;
        beq(1:NRowEq, 1) = 0;
        A(1:NRow, 1:NCol) = 0;
        b(1:NRow, 1) = 0;

        for j = 1:J
            f(j) = FUEL(j); % g(h,j)
            ub(j) = G(j); % g(h,j)
        end

        f(J+2) = VOLL; % q(h)
        f(J+4) = -VPlus_ADP(h,n-1); % yPlusx(h)
        ub(J+1) = WCFMean(h)*W; % w(h)
        ub(J+2) = D(h); % q(h)
        ub(J+3) = sum(UMean); % zPlus(h)
        ub(J+4) = sum(UMean); % yPlusx(h)

        % power balance - 1 rows
        for j = 1:J
            Aeq(1,j) = 1; % g(h,j)
        end
        Aeq(1,J+1) = 1; % w(h)
        Aeq(1,J+2) = 1; % q(h)
        Aeq(1,J+3) = -RHO; % zPlus(h)
        beq(1) = D(h)-Hydro; % D(h)

        for l = 2:L
            if h-l+1 > 0
                beq(1) = beq(1)+ RHO*zPlus_ADP(h-l+1,n);
            else
                beq(1) = beq(1)+ RHO*zPlus_ADP(h-l+1+24,n);
            end
        end

        % transition equation - 1 rows
        Aeq(2, J+4) = 1; % yPlusx(h)
        Aeq(2, J+3) = 1; % zPlus(h)
        beq(2) = UMean(h) + YPlus_ADP(h,n);

        [x,fval,exitflag,~,lambda] = linprog(f,A,b,Aeq,beq,lb,ub);
        if exitflag ~= 1
            ERROR_ADP_DHLP = n;
```

```
        break
    end

    %% Find the hour-ahead charge decision
    zPlus_ADP(h,n) = x(J+3);
    if zPlus_ADP(h,n) < ZERO
        zPlus_ADP(h,n) = 0;
    end

    %% Find the real-time charge decision
    zPlus_ADP(h,n) = min(YPlus_ADP(h,n) + U(h,n), zPlus_ADP(h,n));

    %% Find the next pre-decision state
    YPlus_ADP(h+1,n) = YPlus_ADP(h,n) + U(h,n) - zPlus_ADP(h,n);
end

for h = H-L+1:H
    zPlus_ADP(h,n) = YPlus_ADP(h,n) + U(h,n);
    if h <= H-1
        YPlus_ADP(h+1,n) = 0;
    end
end

if abs(sum(U(:,n)) - sum(zPlus_ADP(:,n))) > 1
    ERROR_ADP_ChargeBalance = n;
end

for h = 1:H
    %% Solve the real-time dispatch problem
    NCol = J + 4; % # of decision variables j) g(h,j), 1) w(h), 2) q(h)
    NRowEq = 2; % # of equality constraints
    NRow = 1; % # of inequality constraints
    f(1:NCol) = 0;
    lb(1:NCol, 1) = 0;
    ub(1:NCol, 1) = 0;
    Aeq(1:NRowEq, 1:NCol) = 0;
    beq(1:NRowEq, 1) = 0;
    A(1:NRow, 1:NCol) = 0;
    b(1:NRow, 1) = 0;

    g(1,1:J) = 0;

    for j = 1:J
        f(j) = FUEL(j); % g(h,j)
        ub(j) = G(j); % g(h,j)
    end

    f(J+2) = VOLL; % q(h)
    ub(J+1) = WCF(h,n)*W; % w(h)
    ub(J+2) = D(h); % q(h)

    % power balance - 1 rows
```

```
for j = 1:J
    Aeq(1,j) = 1; % g(h,j)
end
Aeq(1,J+1) = 1; % w(h)
Aeq(1,J+2) = 1; % q(h)
beq(1) = D(h)-Hydro; % D(h)

for l = 1:L
    if h-l+1 > 0
        beq(1) = beq(1)+ RHO*zPlus_ADP(h-l+1,n);
    else
        beq(1) = beq(1)+ RHO*zPlus_ADP(h-l+1+24,n);
    end
end

[x,fval,exitflag,~,lambda] = linprog(f,A,b,Aeq,beq,lb,ub);
if exitflag ~= 1
    ERROR_ADP_RTLP = n;
    break
end

D_ADP(h,n) = D(h);
for l = 1:L
    if h-l+1 > 0
        D_ADP(h,n) = D_ADP(h,n) + zPlus_ADP(h-l+1,n)*RHO;
    else
        D_ADP(h,n) = D_ADP(h,n) + zPlus_ADP(h-l+1+24,n)*RHO;
    end
end

for j = 1:J
    g(j) = x(j);
    if g(j) < ZERO
        g(j) = 0;
    end
end
g_ADP(h,n) = sum(g);

Cost_ADP(n) = Cost_ADP(n) + fval;

%% Compute a sample estimate of electricity price
p_ADP(h,n) = abs(lambda.eqlin(1));

%% Update electricity price approximation
if stepSizeP == 0
    P_ADP(h,n) = (1-1/(n-1))*P_ADP(h,n-1) + 1/(n-1)*p_ADP(h,n);
else
    if n == 2
        P_ADP(h,n) = 1*p_ADP(h,n);
    else
        P_ADP(h,n) = (1-stepSizeP)*P_ADP(h,n-1) + stepSizeP*p_ADP(h,n);
    end
```

```
        end
    end

    for h = 1:H-L
        %% Compute a sample estimate of value function gradient
        vPlus_ADP(h,n) = sum(P_ADP(h+1:h+L-1,n));
        sumCharge(1:H) = 0;
        for h1 = h+1:H-L+1
            sumCharge(h1) = sum(P_ADP(h1:h1+L-1,n));
        end
        vPlus_ADP(h,n) = RHO*(vPlus_ADP(h,n)-min(sumCharge(h+1:H-L+1)));

        %% Update value function (gradient) approximation
        if stepSizePlus == 0
             VPlus_ADP(h,n) = (1-1/(n-1))*VPlus_ADP(h,n-1) + 1/(n-1)*vPlus_ADP(h,n);
        else
            if n == 2
                VPlus_ADP(h,n) = 1*vPlus_ADP(h,n);
            else
                VPlus_ADP(h,n) = (1-stepSizePlus)*VPlus_ADP(h,n-1)
+ stepSizePlus*vPlus_ADP(h,n);
            end
        end
    end
end
```

VITA

VITA

Jingjie Xiao
315 N. Grant Street
West Lafayette, IN 47907-2023

765.237.1639 (phone)
jingjie.xiao@gmail.com
xiaoj@purdue.edu

Education

Purdue University — West Lafayette, IN, USA
Ph.D. in Operations Research, School of Industrial Engineering (GPA: 4.0/4.0) — *Aug 2009 - Dec 2013*
- *Teaching Assistantship for 4 Grad Courses – Risk Management, Power Systems and Smart Grid, Smart Grid Seminar, Entrepreneurship and Teamwork*

The University of Texas at Austin — Austin, TX, USA
Ph.D. in OR and IE at ME Dept. (GPA: 4.0/4.0) — *Aug 2008 - May 2009*
- *Teaching Assistantship for Course Engineering Finance (2 semesters)*
- Transferred to Purdue University after the first year of the program

Tsinghua University — Beijing, China
M.S. in System Engineering, School of Info. Science and Tech. (GPA: 88/100) — *Aug 2005 - May 2007*

Tsinghua University — Beijing, China
B.E. in Automation, School of Info. Science and Tech. (GPA: 88/100) — *Aug 2001 - May 2005*
- *Excellent Graduate Award (2005), Dongfeng Motor Scholarship (2002), Boke Scholarship (2003)*

Research Experience

Purdue University — West Lafayette, IN, USA
Research Assistantship — *Aug 2009 - Aug 2013*
- Developed a stochastic unit commitment model for the two-settlement day-ahead electricity market where the power generation and operating reserve for wind energy are co-optimized[1] (GAMS)
- Proposed a stochastic generating capacity expansion model to optimize the long-term planning for wind farm locations and sizes[2] (GAMS)
- Partnered with IPL – an Indianapolis utility company to examine the electric vehicle competitiveness and charging infrastructure allocation for the city of Indianapolis[3] (GAMS, AngLogic)
- (Working Papers) Presented an approximate dynamic programming model to quantify economic and environmental benefits from dynamic retail electricity rates and demand-side management (Matlab)

Tsinghua University — Beijing, China
Research Assistant — *Aug 2005 - May 2007*
- (Master Thesis) Developed a heuristic algorithm for large-scale scheduling problem[5] (Matlab)
- (Senior Thesis) Presented a genetic algorithm for single-machine scheduling *(Excellent Thesis Award)*

Publications

[1] **Operating Reserve Policies with High Wind Power Penetration** *Computers & Chemical Eng.*
J. Xiao, B.-M. Hodge, J. F. Pekny, G. V. Reklaitis — *In Press, 2011*

[2] **Long-Term Planning of Wind Farm Siting in Electricity Grid** *Proceedings of 21st ESCAPE*
J. Xiao, B.-M. Hodge, A. L. Liu, J. F. Pekny, G. V. Reklaitis — *2011*

Quantify System Level Benefits from Distributed Solar and Storage *Journal of Energy Eng.*
S. Huang, J. Xiao, J. F. Pekny, G. V. Reklaitis, A. L. Liu *In Press, 2011*

[3] **Effects of Electric Vehicles in the City of Indianapolis** *Energy Policy*
S. Huang, H. Safiullah, J. Xiao, B. Hodge, R. Hoffman, J. Soller, D. Jones, D. Dininger, W. Tyner, A. Liu, J. Pekny *In Press, 2011*

[5] **Performance-Enhancing Approach for Single-Machine Sched.** *J Tsinghua Univ (Sci & Tech)*
J. Xiao, X. Huang, S. Wang *In Press, 2008*

Work Experience

Baidu.com, Inc. Beijing, China
Assistant Product Manager at Online Advertising Business Services Group *June 2007 - June 2008*

- Performed data-driven analysis and delivered internal revenue reports to Vice President and senior managers on driving forces behind the revenue growth, and predictions of future trends (SQL, Excel)
- Interacted with third-party distributor managers to identify opportunities to boost sales and increase advertisers' ROI, improving Baidu's online advertising services and products to meet customers' needs

Electric Reliability Council of Texas, Inc. Taylor, Texas, USA
Summer Intern at Network Modeling Group *June 2012 - Aug 2012*

- Evaluated and improved the business process of new generation resource interconnection, identifying coordination weakness through studying documents and interviewing 10+ internal working groups
- Developed a swimlane diagram to visualize the entire business process, which captures 100+ identified key activities and 400+ elements over coordination timeline for 18 (external or internal) entities, interdependency and interaction among them, data migration path for critical processes, etc.

Skills

MATLAB, GAMS/CPLEX, C/C++, Linux, AnyLogic, AutoMod, SQL, SAS, Crystal Ball
MS Office Word/Excel/PowerPoint/Visio/Access, LaTeX, PowerWorld, PSSE, Photoshop, Premiere
Language: Mandarin Chinese and English

Conference Presentations/Posters or Workshop Certificates

USAEE/IAEE North American Conference Austin, TX, USA, *2012*
Institute for OR & Management Sciences (INFORMS) Annual Meeting Phoenix, *2012*, Charlotte, *2011*
IEEE Power & Energy Society (PES) General Meeting San Diego, CA, USA, *2012*
Institute of Industrial Engineers (IIE) Annual IE Conference Orlando, FL, USA, *2012*
European Symposium on Computer Aided Process Engineering (ESCAPE) Chalkidiki, Greece, *2011*
Workshop of Process Modeling & Optimization for Energy & Sustainability Angra dos Reis, RJ, Brazil
the Pan-American Advanced Studies Institute (PASI) *July 2011*
Workshop of AnyLogic In-Depth by *AnyLogic North America, LLC* Arlington, VA, USA, *2012*
Groups and Associations: INFORMS, IIE, IEEE, USAEE/IAEE

Other Achievements

An Approach to Extract Key Segments of Popular Songs **Patent** CN 2004 1 0009537.0, China
J. Zhou, Y. Zhang, S. Feng, Z. Li, H. Yuan, J. Xiao *2004*

A Multifunctional Seeding Machine **Patent** CN 2002 2 0014870.1, China
J. Qu, H. Xiao, J. Xiao, X. Jiao *2002*

Best Actress Award the 2nd DV Festival at Tsinghua University, China
Tsinghua Story (A 110-min DV film) *2005*

11th in National Higher Education Entrance Examination (2001) Shandong Province, China

Top 50 in Physics (2000) and Math (1997) Olympiad Shandong Province, China